NASA Research Grant NAG-1-797

Photonuclear Absorption Cross Sections

Final Report

(October 1, 1987 - August 15, 1989)

by

John W. Norbury
Physics Department
Washington State University
Pullman, WA 99164-2814

Publications List

The following articles have been published or are under consideration for publication. They have all been supported in whole, or in part, by NASA Grant NAG-1-797 and this grant has been acknowledged in these articles. Copies are enclosed.

1) "Comment on Electromagnetic Dissociation of ^{59}Co and ^{197}Au Targets by Relativistic ^{139}La Projectiles" (J. W. Norbury) Physical Review C. 39 2472 (1989).

2) "Nucleon Emission Via Electromagnetic Excitation in Relativistic Nucleus-Nucleus Collisions: Re-Analysis of the Weizsacker-Williams Method" (J. W. Norbury) submitted to Physical Review C.

3) "Electric Quadrupole Excitations in the Interactions of ^{89}Y with Relativistic Nuclei" (J. W. Norbury) Submitted to Physical Review C.

4) "Electric Quadrupole Excitations in Relativistic Nucleus-Nucleus Collisions" (J. W. Norbury) to be submitted to Physical Review C.

5) "Electromagnetic Interactions of Cosmic Rays with Nuclei" (J. W. Norbury) to be submitted to Astrophysical Journal.

6) "An Optical Model Description of Momentum Transfer in Heavy Ion Collisions" (F. Khan, G. S. Khandelwal, L. W. Townsend, J. W. Wilson, and J. W. Norbury) submitted to Modern Physics Letters A.

7) "The Invariance of Classical Electromagnetism under Charge Conjugation, Parity and Time-Reversal (CPT) Transformations" (J. W. Norbury) submitted to European Journal of Physics.

Conference Proceedings and NASA Papers

The following papers were presented at conferences. Copies are enclosed.

7) "Excitation Decay Contribution of Projectile and Projectile Fragments to (^{12}C, ^{11}B + p) Cross Section at 2.1 A GeV with ^{12}C Targets" (F. Khan, G. S. Khandelwal, J. W. Wilson, L. W. Townsend, and J. W. Norbury) Proc. Eighth High Energy Heavy Ion Study, Lawrence Berkeley Laboratory, University of California, Berkeley, California, November 16-20 (1988).

8) "Excitation Decay Contribution of Projectile and Projectile Fragments to (^{12}C, ^{11}B + p) and (^{16}O, ^{15}N + p) Cross Section at 1.05 A GeV and 2.1 A GeV with ^{12}C Targets" (F. Khan, G. S. Khandelwal, J. W. Wilson, L. W. Townsend, and J. W. Norbury) presented at the Spring 1988 Meeting of the American Physical Society, Baltimore, Maryland, April 18-21 (1988). Bull. Am. Phys. Soc. 33 963 (1988).

9) "Electromagnetic Excitation of Nuclei with Heavy Ions" (J. W. Norbury) presented to the 1988 CEBAF Summer Workshop, Christopher Newport College, Newport News, Virginia, June 20-24.

10) "Momentum Downshifts of Projectile Fragments in ^{12}C Fragmentation at 2.1 A GeV on Be, C, Al, Cu, Ag, and Pb Targets" (F. Khan, G. S. Khandelwal, J. W. Wilson, L. W. Townsend, and J. W. Norbury) presented at the 1988 Annual Meeting of the Southeastern Section of the American Physical Society, Raleigh, North Carolina, November 10-12 (1988). Bull. Am. Phys. Soc. 33 2193 (1988).

11) "Corrections to Pole Diagrams in ^{4}He Fragmentation at 1 GeV/N" (F. A. Cucinotta, L. W. Townsend, and J. W. Norbury) presented at the Spring 1988 Meeting of the American Physical Society, Baltimore, Maryland, May 1-4 (1989). Bull. Am. Phys. Soc. 34 1138 (1989).

12) "Multiple Nucleon Knockout by Coulomb Dissociation in Relativistic Heavy Ion Collisions" (F. A. Cucinotta, J. W. Norbury, and L. W. Townsend) NASA Technical Memorandum 4070 November (1988).

13) "Calculation of Two-Neutron Multiplicity in Photonuclear Reactions" (J. W. Norbury, and L. W. Townsend) NASA Technical Paper (in press).

Seminars and Colloquia

The following talks were presented at various institutions.

1) ***"The Protection of Astronauts from Cosmic Rays,"*** Washington State University, Physics Colloquium, 19 January 1988.

2) ***"Electromagnetic Dissociation in Nucleus-Nucleus Collisions,"*** Washington State University, Electrical Engineering Department, Electromagnetic Seminar, 1 March 1988.

3) ***"Cosmic Rays and the NASA Space Program,"*** (1) Washington State University, Society of Physics Students (SPS) Seminar, 15 September 1988; (2) Washington College (Chestertown, Maryland), Seminar, 20 January 1989.

4) ***"Electromagnetic Processes in Nucleus-Nucleus Collisions,"*** (1) Tennessee Technological University, Physics Colloquium, 2 March 1989, (2) University of Toledo, Physics Colloquium, 3 April 1989.

Introduction

As the United States' space program heads toward the era of permanent occupation of the near Earth environment via the habitation of a permanent Space Station, the problem of protection of astronauts from the harmful effects of cosmic radiation assumes greater and greater importance. Of special concern are the effects of galactic cosmic rays in the form of relativistic nuclei.[1] When a relativistic nucleus impinges upon a spacecraft wall, it undergoes several reactions, an important one of which is fragmentation, whereby the nucleus breaks up into smaller pieces which subsequently decay. It is these secondary particles which contribute to the radiation environment inside a spacecraft. The problem of fragmentation of relativistic nuclei is the subject of a continuing research effort by the present author and others.[2] An alternative mechanism, which can produce the same sort of radiation environment as the fragmentation mechanism, is that of electromagnetic dissociation by which the electromagnetic field of one nucleus excites states in another nucleus which subsequently decay. The present author has led a study[3] of the significance of this mechanism to the galactic heavy ion breakup and has concluded that it is of major importance (i.e. large cross section) for the removal of a few nucleons when a relativistic nucleus impinges upon a spacecraft wall. Consequently, the mechanism of the electromagnetic dissociation must be included when one is trying to predict the radiation environment in the interior of a spacecraft when the exterior environment is composed of galactic heavy ions.

Analysis of Weizsacker-Williams Theory

The Weizsacker-Williams (WW) method of virtual quanta has been used extensively in the literature (see reference 4) to analyze the electromagnetic (EM) interactions of nuclei. The prevailing opinion seemed to be that WW theory worked quite well with a few exceptions. However, I believed that it was quite difficult to judge the validity of WW theory because authors generally used different input values of the minimum impact parameter, b_{min}, below which the reaction proceeds via the Strong Force. I decided that a better way to proceed would be to fit the calculated WW cross section to experiment treating b_{min} as an adjustable parameter. Thus if b_{min} turned out to have a ridiculous value, then it was absolutely clear that WW theory failed. Based on this work[5] it is clear that WW theory does not work for nucleon emission from ^{197}Au. Furthermore, there are problems with some other reactions as well. A possible explanation[5] for the ^{197}Au discrepancy is the use of the one-photon exchange approximation inherent in WW theory. Future studies of these discrepancies are strongly recommended.

Also, in the course of this study I found that some rather serious wrong calculations had been presented in the literature by a group of authors. I have subsequently corrected the mistakes of those authors [6,7].

Electric Quadrupole Interactions

WW theory is also based completely on electric dipole (E1) interactions[4], whereas it has been known for some time that electric quadrupole (E2) effects could perhaps contribute a substantial fraction to the cross section[4]. However, calculations were not performed in detail because it was not known exactly how to break up photonuclear cross sections into their separate E1 and E2 components.

I subsequently developed a calculational method which primarily uses experimental photonuclear cross sections as input. The E1 contribution is then defined as

$$\sigma_{E1} = \sigma_{expt} - \sigma_{E2} \qquad (1)$$

where σ_{E2} is calculated theoretically. The advantage of this procedure is that even if the E2 parameters are not very well known, the total cross section will still be very accurate. This is because an underestimate in σ_{E2} will cause an overestimate in σ_{E1} and the effects tend to cancel.

It was found[9] that electric quadrupole effects are not significant for proton and neutron emission from ^{12}C, ^{16}O or ^{18}O. However, E2 contributions[8,9] are substantial for neutron emission from ^{59}Co, ^{89}Y and ^{197}Au, generally leading to improved agreement between theory and experiment. Notable disagreements occur for ^{139}La projectiles (1.26 GeV/N) where the theoretical cross sections are too big. Quadrupole effects improve the theoretical results for ^{16}O projectiles at 60 and 200 GeV/N, although the theoretical cross sections are still too small.

In general it was found that electric quadrupole effects are an important component in nucleus-nucleus collisions and that these effects can be calculated accurately[8,9].

Parameterization of the Cross Sections

A parameterization of nucleus-nucleus EM cross sections has been presented previously[10,11]. However, since then a much more accurate theory which includes E2 effects has been developed[8,9]. In addition a much more extensive experimental data set is now available, including very heavy projectiles such as ^{139}La and energies as high as 200 GeV/N for ^{16}O projectiles.

I therefore decided to re-examine this problem and try to come up with a more accurate and simpler parameterization[12]. In this I succeeded. The new parameterization now includes E2 effects, and, in addition does not require the numerical integration over energy that the old parameterization[10,11] required.

Actually I have worked out three new parameterizations with accuracy varying inversely with simplicity[12]. The first parameterization[12] (which includes E2 effects) is the most accurate and requires numerical integration over energy. The second parameterization[12] (which again includes E2) is based on photonuclear sum rules[4] and does not require numerical integration and is almost as accurate as the first parameterization. The third parameterization[12] (which does not include E2) involves a very simple formula which can be evaluated on a pocket calculator, and it no longer involves evaluation of complicated Bessel functions.

These parameterizations will be extremely useful in calculating the radiation environment inside a spacecraft. What needs to be done now is to implement them into the NASA Langly Research Center's computer transport codes.

Other Work

I was also involved in several other projects such as multiple nucleon knockout, two-neutron multiplicity, excitation energy calculations and alpha break-up. Details can be found in the articles in the publication list and the conference proceedings and NASA papers listed at the beginning of this report.

References

1) P. Todd, Adv. Space Res. 3, 187 (1983).

2) L. W. Townsend, J. W. Wilson and J. W. Norbury, Can. J. Phys. 63, 135 (1985).

3) J. W. Norbury and L. W. Townsend, NASA TP-2527 (1986).

4) C. A. Bertulani and G. Baur, Phys. Rep. 163, 299 (1988).

5) J. W. Norbury, "Nucleon Emission Via Electromagnetic Excitation in Relativistic Nucleus-Nucleus Collisions: Re-Analysis of the Weizsacker-Williams Method" submitted to Physical Review C.

6) J. W. Norbury, Phys. Rev. C. 39, 2472 (1989).

7) J. C. Hill and F. K. Wohn, Phys. Rev. C. 39, 2474 (1989).

8) J. W. Norbury, "Electric Quadrupole Excitations in the Interactions of ^{89}Y with Relativistic Nuclei" submitted to Physical Review C.

9) J. W. Norbury, "Electric Quadrupole Excitations in Relativistic Nucleus-Nucleus Collisions" to be submitted to Physical Review C.

10) J. W. Norbury, F. A. Cucinotta, L. W. Townsend and F. F. Badavi, Nucl. Inst. Meth. in Phys. Res. B 31, 535 (1988).

11) J. W. Norbury L. W. Townsend and F. F. Badavi, NASA TM 4038 June (1988).

12) J. W. Norbury, "Electromagnetic Interactions of Cosmic Rays with Nuclei" to be submitted to Astrophysical Journal.

CALCULATION OF TWO-NEUTRON MULTIPLICITY IN PHOTONUCLEAR REACTIONS

John W. Norbury

Department of Mathematics and Physics
Rider College
Lawrenceville, NJ 08648

Lawrence W. Townsend

NASA Langley Research Center
Hampton, VA 23665

ABSTRACT

The most important particle emission processes for electromagnetic excitations in nucleus-nucleus collisions are the ejection of single neutrons and protons and also pairs of neutrons and protons. Methods are presented for calculating two-neutron emission cross sections in photonuclear reactions. The results are in a form suitable for application to nucleus-nucleus reactions.

INTRODUCTION

When cosmic rays in the form of heavy nuclei pass through spacecraft walls and astronauts' bodies, they undergo an interaction with the atomic nuclei in the spacecraft or astronauts. Of the four forces that we currently know about (strong, weak, electromagnetic and gravitational), the cosmic ray interaction occurs via both the strong and electromagnetic forces. The strong and electromagnetic (EM) cross sections are of comparable magnitude in some situations. Previous work (refs. 1-5) has concentrated on studying this electromagnetic aspect of nucleus-nucleus collisions. This study has so far considered only single-nucleon emission processes. A preliminary study has been made of multiple-nucleon emission (ref. 5) . However, the results of this study are unable to be utilized in heavy-ion transport codes because experimental photonuclear cross sections are used as inputs into the calculation of nucleus-nucleus EM cross sections.

The aim of the present work is to show how to calculate these photonuclear cross sections for multiple-nucleon emission. Given analytic expressions for these cross sections, it will then be possible to add multiple-nucleon emission due to the EM effect into heavy-ion transport codes. Calculating multiple-nucleon emission effects for the EM interaction is much more difficult than the calculation for single-nucleon emission. Thus the present work will consider only the most important multiple-nucleon emission process-that of two-neutron emission. Other multiple-nucleon effects such as emission of two protons, a neutron and a proton, or an alpha particle are more strongly suppressed than two-neutron emission primarily due to the Coulomb barrier. This is especially true for heavy nuclei. In fact even single-proton emission is completely Coulomb-suppressed for heavy nuclei (ref. 1).

MULTIPLE NUCLEON EMISSION AND ARBITRARY ELECTROMAGNETIC MULTIPOLES

Before proceeding to the study of two-neutron emission, we shall first place it in the broad context of arbitrary EM multipoles and multiple-nucleon emission.

The total nucleus-nucleus EM absorption cross section σ_{EM} is given by

$$\sigma_{EM} = \sum_{x} \sigma_{EM}(x) \qquad (1)$$

where the sum is over all possible species emitted in the heavy ion collision and $\sigma_{EM}(x)$ is the nucleus-nucleus EM reaction cross section for producing a particular species x. The cross section $\sigma_{EM}(x)$ was given as equation (1) in ref. 1, but we now generalize it as (see also equation 2.1 of ref. 6 and equation 4.11 of ref. 7)

$$\sigma_{EM}(x) = \sum_{\pi\ell} \int_{E_o(x)} \sigma_{\nu}^{\pi\ell}(E, x)\, N^{\pi\ell}(E)\, dE \qquad (2)$$

where π can be either electric ($\mathcal{E}$) or magnetic ($\mathcal{M}$) and ℓ is the order of multipolarity. Each term in the summation of equation (2) represents nuclear excitation by a particular EM multipole. Each different EM multipole $\pi\ell$ causes a particular type of nuclear excitation. For example, the $\mathcal{E}1$ photon field causes the nucleus to go into the giant electric dipole resonance (GDR) mode of oscillation parameterized as

$$\sigma_{abs}^{\mathcal{E}1}(E) = \frac{\sigma_m}{1 + [(E^2 - E_{GDR}^2)/E^2\Gamma^2]}, \qquad (3)$$

(see equation 8 of ref. 1 and equation 6 below) which would subsequently decay into various channels x, with a probability $g_x^{\mathcal{E}1}$, sometimes called the branching ratio. However, an $\mathcal{E}2$ multipole (ref. 8) would cause the nucleus to go into a giant electric quadrupole resonance (GQR), the cross section of which would have a <u>different</u> parameterization from equation (3), and where various decay probabilities $g_x^{\mathcal{E}2}$ (e.g., neutron versus proton decay) <u>may</u> also be different from $g_x^{\mathcal{E}1}$. Thus the photonuclear

reaction cross section for production of species x is some fraction of the total photonuclear absorption cross section

$$\sigma_{\nu}^{\pi\prime}(E, x) = g_{x}^{\pi\prime}(E)\, \sigma_{abs}^{\pi\prime}(E) \qquad (4)$$

for a particular multipole. Equation (4) is a generalization of equation (7) of ref. 1, and means physically that a particular EM multipole $\pi\ell$, causes a collective nuclear vibration $\sigma_{abs}^{\pi\prime}(E)$ which can then decay into various channels via $g_{x}^{\pi\prime}(E)$. Note that

$$\sum_{x} g_{x}^{\pi\prime}(E) = 1 \qquad (5)$$

By combining equations (2) and (4) and assuming an energy independent branching ratio (replacing $g_{x}^{\pi\prime}(E)$ with $g_{x}^{\pi\prime}$), the nucleus-nucleus EM reaction cross section becomes

$$\sigma_{EM}(x) \approx \sum_{\pi\prime} g_{x}^{\pi\prime} \int_{E_o(x)} \sigma_{abs}^{\pi\prime}(E)\, N^{\pi\prime}(E) dE = \sum_{\pi\prime} g_{x}^{\pi\prime}\, \sigma_{EM\text{ - }abs}^{\pi\prime} \qquad (6)$$

where the nucleus-nucleus EM total absorption cross section is

$$\sigma_{EM\text{ - }abs}^{\pi\prime} \equiv \int_{E_O(x)} \sigma_{abs}^{\pi\prime}(E)\, N^{\pi\prime}(E)\, dE. \qquad (7)$$

The above three equations are generalizations of the three equations on page 7 of ref. 1. (Note that in ref. 1 the absorption cross section was written as $\sigma_{EM\text{ - }abs}(x)$ in equation (15) of ref. 1. The dependence on x came out because the threshold $E_o(x)$ is the lower limit of integration. We prefer here simply to write $\sigma_{EM\text{ - }abs}$ because a true absorption cross section should not depend on x.) In the above equations, it is the photonuclear total absorption cross section $\sigma_{abs}{}^{\pi\prime}(E)$ which gets parameterized according to the particular nuclear multipole excitation. For example the nuclear $E1$ GDR excitation is parameterized in equation (3).

If one assumes that the branching ratios are independent of multipolarity (which may receive some justification from the Bohr independence hypothesis (ref. 9)), then, replacing $g_x^{\pi\ell}$ with g_x, equation (6) becomes

$$\sigma_{EM}(E) \approx g_x \sum_{\pi l} \sigma_{EM\text{-}abs}^{\pi\ell} = g_x \, \sigma_{EM\text{-}abs} \qquad (8)$$

where the nucleus-nucleus EM total absorption cross section summed over all EM multipoles is

$$\sigma_{EM\text{ - }abs} = \sum_{\pi\ell} \sigma_{EM\text{ - }abs}^{\pi\ell} \qquad (9)$$

Equation (8) is interpreted physically as meaning that a nucleus-nucleus EM reaction has occurred exciting a nucleus into a superposition of multipolarities $\sum_{\pi\ell} \sigma_{EM\text{ - }abs}^{\pi\ell}$ (such as a linear combination of GDR and GQR). This superposition can be likened to the Compound Nucleus concept of Blatt and Weisskopf (ref. 9). This compound nucleus superposition then decays via multipole-independent branching ratios g_x as in equation (8).

Although equation (6) is probably more correct, it will be impossible to implement in practice due to the difficulty of calculating multipole-dependent branching ratios. Therefore in practical calculations, equation (8) will be used. This equation is entirely consistent with the concept of compound nucleus formation (ref. 9) and decay independent of the mode of formation (Bohr independence hypothesis). This is identical in spirit to the Abrasion-Ablation model (ref. 10). In fact, attempts (ref. 11) have been made to understand the Abrasion-Ablation model in terms of compound nucleus formation and decay using a T-matrix approach. Thus our basic equation (8) can be thought of as an Electromagnetic Abrasion-Ablation model.

Finally, we put our previous studies (refs. 1-5) in the context of equations (1) and (8). First of all, equation (8) tells us that in order to calculate the nucleus-nucleus EM

reaction cross section, we should sum over all possible EM multipolarities ($\mathcal{E}0, \mathcal{E}1, \mathcal{E}2$ ..., $\mathcal{M}0, \mathcal{M}1, \mathcal{M}2$ ...). The only multipolarity that has been studied so far is $\mathcal{E}1$ (ref. 1-5) leading to the Giant Electric Dipole Resonance. Clearly the effects of other multipolarities must be considered. Bertulani and Baur have concluded (ref. 6) that the electric quadrupole ($\mathcal{E}2$) contribution to the total nucleus-nucleus EM cross section can be as much as 50 percent of the $\mathcal{E}1$ contribution at 100 MeV/N and about 20 percent at 1 GeV/N dropping to about 10 percent at higher energies. Note that all the EM data (see ref. 1) are at high energy and so in comparing our theory (ref. 1) with experiment, the $\mathcal{E}2$ contribution has not been large. Nevertheless we require the nucleus-nucleus (fragmentation and EM) theory to include all energies in the cosmic ray spectrum, and thus it is very important to consider other EM multipoles as well. Apart from multipoles other than $\mathcal{E}1$, equation (1) tells us that we need also consider not only single-ucleon emission but multiple-nucleon emission as well, such as emission of np, 2n, 2p, α, nnp, npp and 3n. However, references 1-4 have considered only the $\mathcal{E}1$ multipole and only single-nucleon emission. Thus there still remains much territory to explore, namely multiple-nucleon emission with $\mathcal{E}1$ excitation and then single-nucleon and multiple-nucleon emission for all other multipoles. The present paper is concerned only with two-neutron (2n) emission from $\mathcal{E}1$ excitation.

THEORY OF TWO-NEUTRON EMISSION

Cucinotta et al. (ref. 5) have in fact studied the problem of multiple-nucleon emission (2n, 2p, p3n, 3n) with $\mathcal{E}1$ excitations only. However, the photonuclear reaction cross section $\sigma_V(E,x)$ was obtained from experimental data, and so even though useful conclusions were drawn, the work of ref. 5 was incomplete and cannot be used in a transport code, which requires analytical expressions for $\sigma_V^{\pi\prime}(E, x)$. The aim of the present work therefore is to begin the study of multiple nucleon emission in nucleus-nucleus electric dipole ($\mathcal{E}1$) excitation reactions using an analytic approach. The motivation for such an approach is to implement analytic cross section expressions into cosmic ray transport codes. There is no cosmic ray transport code in existence which includes anything other than single-nucleon emission for EM reactions. Because a full theory for multiple-nucleon emission is much more complicated than for single-nucleon emission, the present work will be limited to a study of two-neutron emission, which is the dominant multiple-nucleon contribution.

TWO-NEUTRON MULTIPLICITY

Fuller et al. (ref. 12, pp. 190; ref. 13, pp. 4; ref. 14, pp. 143-145) have defined the total photoneutron yield cross section as

$$\sigma(\gamma, xn) \equiv \sigma(\gamma,n) + 2\sigma(\gamma, 2n) + 3\sigma(\gamma, 3n) + ... \quad (10)$$

and the photoneutron cross section (i.e., the sum of cross sections in which at least one neutron is emitted)

$$\sigma(\gamma, sn) \equiv \sigma(\gamma, n) + \sigma(\gamma, np) + \sigma(\gamma, 2n) + \sigma(\gamma, n\alpha) + \sigma(\gamma, 3n) + ... \quad (11)$$

The neutron multiplicity is defined (ref. 15) as

$$M(E) \equiv \frac{\sigma(\gamma, xn)}{\sigma(\gamma, sn)} \quad (12)$$

which for n and 2n emission only becomes (ref. 16)

$$M(E) \approx \frac{\sigma(\gamma, n) + 2\sigma(\gamma, 2n)}{\sigma(\gamma, n) + \sigma(\gamma, 2n)} \tag{13}$$

This expression for the multiplicity has been implicitly assumed also in Thies and Spicer (ref. 17, equation 5). Note the reason for writing the neutron multiplicity this way: for $\sigma(\gamma, 2n)$ equal to zero (meaning that only single neutrons (n) are emitted), the multiplicity is 1 as expected, and for $\sigma(\gamma, n)$ being zero (meaning only two-neutron pairs (2n) are emitted), the multiplicity is 2 as expected. Often instead of using multiplicity, one works with the quantity

$$\frac{\sigma(\gamma, 2n)}{\sigma(\gamma, n) + \sigma(\gamma, 2n)} = M(E) - 1 \tag{14}$$

Blatt and Weisskopf (ref. 9, chapter VIII, section 6B) have worked out the general theory of multiple-nucleon emission, which they call secondary nuclear reactions. They write the cross section for production of particle b (see ref. 9, equation on pp. 375), which we specialize to photoproduction as

$$\sigma(\gamma, sb) = \sigma(\gamma, b) + \sum_{c} \sigma(\gamma, bc) \tag{15}$$

This is made up of a primary, single-step cross section $\sigma(\gamma, b)$ in which particle b is emitted directly from decay of the compound nucleus and a secondary, multiple-step cross section $\sigma(\gamma, bc)$ is which either particle b or c is emitted from the compound nucleus which decays to a lower excited state which again decays via emission of particle c or b. Blatt and Weisskopf (ref. 9, pp. 376-379) then go on to calculate $\sigma(\gamma, b)$ and $\sigma(\gamma, bc)$ in terms of $\sigma(\gamma, sb)$; however, one generally needs to work the integrals out numerically. We shall eventually do this when working out the general expression for multiple-nucleon emission. However, for the case of two-neutron emission, certain simplifying assumptions concerning the integrals can be made so that analytic expressions can be obtained. These are (ref. 9, eqn. 6.14, pp. 377)

$$\sigma(\gamma, n) \approx \sigma(\gamma, sn)\,(1 + \varepsilon_{sec}/\Theta)\exp(-\varepsilon_{sec}/\Theta) \tag{16}$$

and (ref. 9, eqn 6.18, pp.379)

$$\sigma(\gamma, 2n) \approx \sigma(\gamma, sn) [1 - (1 + \varepsilon_{sec}/\Theta)\exp(-\varepsilon_{sec}/\Theta)] \quad (17)$$

where Θ is the nuclear temperature and

$$\varepsilon_{sec} \equiv E\gamma - E_o(\gamma, 2n) \quad (18)$$

The above equations are also discussed in references 15, 16, 17, 18. Equation (17) is derived on the assumption that the photoneutrons are produced via statistical decay of the compound nucleus (ref. 9). However this is not always necessarily true. It can sometimes happen that the incident photon, rather than exciting a compound nucleus which subsequently decays via neutron emission, will rather knock a neutron out directly. (Note that this direct emission violates the abrasion-ablation concept.) We therefore introduce a fraction of direct emission f_d, which typically has values (ref. 15, and G. O'Keefe and R. Rassool, private communication) in the range 0.1 - 0.2 although it can be as large as 0.4 (ref. 17). This direct fraction is incorporated into our theory (ref. 15, 17) by generalizing equation (17) as

$$\sigma(\gamma, 2n) \approx \sigma(\gamma, sn) (1 - f_d) [1 - (1 + \varepsilon_{sec}/\Theta) \exp (-\varepsilon_{sec}/\Theta)] \quad (19)$$

This equation is our main result for 2n emission. The quantities f_d, ε_{sec}, and Θ are easily calculated so that the only input required is $\sigma(\gamma, sn)$. Blatt and Weisskopf (ref. 9, pp. 379) claim that $\sigma(\gamma, sn)$ can usually be closely approximated by the compound nucleus formation cross section, i.e., the total absorption cross section. (This is done in reference 18.) However, this is only true when compound nucleus decay proceeds predominantly by neutron emission which is the case for heavy nuclei. For light nuclei, where proton emission is just as important (ref. 1), the above approximation is not valid. Thus we now neglect all contributions to $\sigma(\gamma, sn)$ other than $\sigma(\gamma, n)$ and $\sigma(\gamma, 2n)$ so that

$$\frac{\sigma(\gamma, 2n)}{\sigma(\gamma, n) + \sigma(\gamma, 2n)} \approx (1 - f_d) [1 - (1 + \varepsilon_{sec}/\Theta) \exp(-\varepsilon_{sec}/\Theta)] \quad (20)$$

which is the result written in reference 16 and 18 for $f_d = 0$. Defining

$$Xfrac \equiv (1 - f_d) [1 - (1 + \varepsilon_{sec}/\Theta)\exp(-\varepsilon_{sec}/\Theta)] \quad (21)$$

we rearrange (20) to obtain

$$\sigma(\gamma, 2n) = \frac{\text{Xfrac}}{1 - \text{Xfrac}}\,\sigma(\gamma, n). \qquad (22)$$

Although equation (19) is our fundamental equation for 2n emission, we shall in fact use equation (22) to test the general theory. This is because several authors have reported both $\sigma(\gamma, n)$ and $\sigma(\gamma, 2n)$. We shall use experimental input for $\sigma(\gamma, n)$ and then calculate $\sigma(\gamma, 2n)$ using (22) and see how well our calculations agree with experimental measurements. If we obtain good results, we can be confident that the theory outlined above can be used to calculate 2n emission in EM nucleus-nucleus collisions.

Finally, we note that the above equations can be used for an approximate calculation of the neutron multiplicity given in equation (13) as

$$M(E) = 1 + (1 - f_d)[1 - (1 + \varepsilon_{sec}/\Theta)\exp(-\varepsilon_{sec}/\Theta)] \qquad (23)$$

which is the result reported in references 15 and 17. (Note however the error in equation (3.12) of reference 15, which is that $\sigma(\gamma, np)$ should not appear in the numerator).

NUCLEAR TEMPERATURE

In the above expressions, the nuclear temperature Θ plays a central role. For a Maxwell-Boltzmann (classical) gas (ref. 19, pp. 117), the relation between energy and temperature is linear

$$E = \frac{3}{2} N_o \, k \, \Theta \tag{24}$$

whereas for a Fermi gas, the relation is quadratic

$$E = (\text{const.}) \, k^2 \, \Theta^2 \tag{25}$$

The theory developed by Blatt and Weisskopf (ref. 9, pp. 372) uses a Fermi gas nuclear temperature given by

$$\Theta = \left(\frac{E}{A}\right)^{1/2} \tag{26}$$

where the constant A depends on the total nucleon number A. We shall not use the Blatt and Weisskopf theory for nuclear temperature, but rather use a more sophisticated version developed by Bohr and Mottelson where (ref. 20, eqn. 2-50, pp. 154)

$$\Theta^{-1} = \frac{1}{\rho} \frac{\partial \rho}{\partial E} \tag{27}$$

with the Fermi gas energy level density (ref. 20, eqn. 2-47, pp. 153)

$$\rho(N, Z, E) = \frac{6^{1/4}}{12} \frac{g_o}{(g_o E)^{5/4}} \exp\left[2\left(\frac{\pi^2}{6} \, g_o E\right)^{1/2}\right] \qquad N \approx Z \tag{28}$$

being of similar form to that of Blatt and Weisskopf (ref. 9, eqn. 2-50, pp. 154). The symbol E is the excitation energy, and g_o is the "one-particle level density at the Fermi energy, representing the sum of neutron and proton level densities" (ref. 20, pp. 153). Thus the nuclear temperature becomes (ref. 20, eqn. 2-50, pp. 154)

$$\Theta^{-1} = \left(\frac{\pi^2}{6} \frac{g_o}{E}\right)^{1/2} - \frac{5}{4E} \tag{29}$$

which is the same form as used in reference 15. It is very important to realize that the energy E in the above expressions is, in fact

$$E = E_\gamma - E_0(\gamma, n) \tag{30}$$

given by the single-neutron emission threshold $E_0(\gamma, n)$. This is emphasized in references 18 (pp.304) and by G. O'Keefe and R. Rassool (private communication). The one-particle level density g_0 is related to the level density parameter a via (ref. 20, eqn. 2-123, pp. 187)

$$a = \frac{\pi^2}{6} g_o, \tag{31}$$

which is plotted in Figures 2-12 of reference 20 (pp. 187). It is seen that a very much depends on shell structure, and therefore whenever possible, a should be obtained directly from Figures 2-12 (ref. 20). However, a rough approximation is

$$a \approx \frac{A}{8} (MeV^{-1}) \tag{32}$$

but note that this fails badly for A between 190 and 210, (ref. 20).

Rewriting the nuclear temperature as

$$\Theta^{-1} = \left(\frac{a}{E}\right)^{1/2} - \frac{5}{4E} \tag{33}$$

with the first term corresponding to the form used by Blatt and Weisskopf (ref. 9), we approximate a to obtain

$$\Theta^{-1} = \left(\frac{A}{8E}\right)^{1/2} - \frac{5}{4E} \tag{34}.$$

TEST OF TWO-NEUTRON MULTIPLICITY THEORY

A computer code was written to implement the theory described above. Necessary inputs are the energy level density parameter a which was taken directly from Figs. 2-12 (ref. 20, pp. 187) rather than from equation (32). The two-neutron cross section was then calculated from the single-neutron cross section with a best-fit value of f_d, the fraction of direct emission. The results are listed in Tables 1-8. As can be seen, the agreement between theory and experiment is good, except for a few notable exceptions. It is disturbing, however, that the direct emission fractions are so high.

DISCUSSION

We have demonstrated that the theory of two-neutron emission described herein is able to predict most two-neutron multiplicities with a high degree of accuracy. One therefore wishes to implement this theory into the calculation of nucleus-nucleus cross sections and eventually into a transport code. A parameterization of the energy level density parameter a can be very easily worked out (ref. 20). Thus the only unknowns are f_d and $\sigma(\gamma, n)$.

The values of f_d were obtained from an overall best fit to $\sigma(\gamma, 2n)$ data. (In practice, a single $\sigma(\gamma, 2n)$ value at a single energy determines f_d.) Clearly some new work remains to be done here. One can either work out a parameterization by determining f_d from best fits to a whole range of data, or better still, one should determine f_d theoretically. Our initial effort will undoubtedly be a parameterization, so that the theory can be used within transport codes.

The most serious unknown is $\sigma(\gamma, n)$ which is used as input for the $\sigma(\gamma, 2n)$ calculation at each energy. One might think that the liquid drop model calculations for $\sigma(\gamma, n)$, described extensively in reference 1, would be adequate for this purpose, especially as these same model calculations gave such good results for nucleus-nucleus cross sections. Unfortunately, this is not the case. Even though the liquid drop model calculations of $\sigma(\gamma, n)$ are quite accurate at most photon energies, they are unfortunately not very accurate for high photon energies. The reason that this did not matter for the calculations of reference 1 was that the virtual photon spectrum N(E) predominated at low photon energies, and so energy integrated nucleus-nucleus cross sections were quite accurate. However, obviously $(\gamma, 2n)$ processes only occur in the high energy (γ, n) region. The $\sigma(\gamma, 2n)$ calculations require $\sigma(\gamma, n)$ as input, and thus we now need very accurate calculations for $\sigma(\gamma, n)$ at high energy. (Calculations described in the present paper used experimental numbers.)

Thus, the most pressing need for inclusion of the effects of multiple-nucleon emission in heavy ion transport codes is the accurate calculation of $\sigma(\gamma, n)$ at high energy. The first such step will require the study of deformation splitting (ref. 14, 17, 18, 24, 25) and isospin splitting of the giant dipole resonance (ref. 24, 25).

Finally, even though only two-neutron emission has been considered herein, it is now clear how to proceed with the general multiple-nucleon emission problem. One can simply numerically integrate the expressions of Blatt and Weisskopf (ref. 9) to obtain any multiple-nucleon final state. (These expressions simplified in the two-neutron case considered herein, so that numerical integration was not necessary.) This method has previously been applied to $^{32}S(\gamma, d)$ by Norbury (ref. 26).

As an alternative to the whole approach taken in the present work (and even for the single-nucleon work of ref. 1), it may be feasible to instead do calculations using some of the modern nuclear evaporation codes (e.g., EVAP-4 and EVA-3). The advantage of these codes is that they fully incorporate both statistical and direct emission. The excitation energy in these codes is simply the photon energy considered above.

CONCLUSIONS

Electromagnetic excitations is nucleus-nucleus collisions can often involve the ejection of pairs of nucleons. Methods have been presented for calculating two-neutron emission cross sections in photonuclear reactions. These cross sections are now in a form suitable for use in nucleus-nucleus reaction theory.

References

1. Norbury, J.W.; and Townsend, L.W.: *Electromagnetic Dissociation Effects in Galactic Heavy-Ion Fragmentation.* NASA TP-2527. 1986.

2. Norbury, J.W.; Townsend, L.W.; and Badavi, F.F.: *Parameterization of Nucleus-Nucleus Electromagnetic Dissociation Cross Sections: A Computer Program.* NASA TM (submitted).

3. Norbury, J.W.; Cucinotta, F.A.,: Townsend, L.W.; and Badavi, F.F.: *Parameterized Cross Sections for Coulomb Dissociation in Heavy Ion Collisions.* Nuclear Instruments and Methods in Physics Research, ser. B (in press).

4. Badavi, F.F.; Townsend, L.W.; Wilson, J.W.; and Norbury, J.W.: *An Algorithm for a Semiempirical Nuclear Fragmentation Model.* Computer Physics Communications,vol. 47, 1987, pp.281.

5. Cucinotta, F.A., Norbury, J.W.; and Townsend, L.W.: *Multiple Knockout by Coulomb Dissociation in Relativistic Heavy Ion Collisions.* NASA TM (submitted).

6. Bertulani, C.A.; and Baur, G.: *Electromagnetic Processes in Relativistic Heavy Ion Collisions.* Nuclear Physics, ser. A, vol. 458, 1986, pp. 725-744.

7. Jäckle, R.; and Pilkuhn, H.: *Profile Functions for Coulomb Excitation at High Energies.* Nuclear Physics, ser. A, vol. 247, 1975, pp. 521-528.

8. Überall, Herbert: *Electron Scattering from Complex Nuclei*, Part B, Academic Press, Inc., 1971.

9. Blatt, John M.; and Weisskopf, Victor F.: *Theoretical Nuclear Physics.* Springer-Verlag, c. 1979.

10. Bowman, J.D.; Swiatecki, W.J.; and Tsang, C.F.: *Abrasion and Ablation of Heavy Ions.* LBL-2908, Univ. of California, July 1973.

11. Norbury, J.W.; Townsend, L.W.; and Deutchman, P.A.: *A T-Matrix Theory of Galactic Heavy-Ion Fragmentation.* NASA TP-2363, January 1985.

12. Fuller, E.G.: *Photonuclear Reaction Cross Sections for ^{12}C, ^{14}N and ^{16}O.* Physics Reports, vol. 127, no. 3, 1985, pp. 185-231.

13. Fuller, E.G.; Gerstenberg, H.M.; Van der Molen, H.; and Dunn, T.C.: *Photonuclear Reaction Data*, 1973. NBS SP-380, March 1973.

14. Fuller, E.G.; and Gerstenberg, H.: Photonuclear Data Index, 1973-1981. NBSIR 82-2543-1, August, 1983.

15. Assafiri, Y.I.: *The Giant Dipole Resonance in "Closed Shell ±2 Nucleons" Nuclei.* Ph.D. Thesis, Univ. of Melbourne, 1984.

16. Veyssiere, A.; Beil, H.; Bergere, R.; Carlos, P.; and Lepretre, A.: *Photoneutron Cross Sections of ^{208}Pb and ^{197}Au*. Nuclear Physics, ser. A, vol. 159, 1970, pp. 561-576.

17. Thies, H.H.; and Spicer , B.M.: *The Photodisintegration of Rare Earth Elements.* Australian J. Phys., vol. 13, 1960, pp.505-521.

18. Spicer, B.M.; Thies., H.H.; Baglin, J.E.; and Allum, F.R.: *The Giant Resonance of Photodisintegration of Tantalum.* Australian J. Phys., vol. 11, 1958, pp.298-309.

19. Cohen, B.L.: *Concepts of Nuclear Physics* , McGraw-Hill Book Co., c. 1971.

20. Bohr, Aage; and Mottelson, Ben R. *Nuclear Structure*, vol. 1, W. A. Benjamin, Inc., 1969.

21. Kayser, K.; Collin, W.; Filss, P.; Guldbakke, S.; Nolte, G.; Reich, H.; Trier, J.O.; and Witschel, W.: *Untersuchung der Kernphotoreaktion $^{12}C(\gamma, n)$, $^{12}C(\gamma, 2n)$, $^{39}K(\gamma, n)$ und $^{40}Ca(\gamma, np)$ bis zur Mesonenschwelle.* Z. Physik, vol. 239, 1970, pp. 447-460.

22. Penfold, A.S.; and Garwin, E.L.: *Photonuclear Cross Sections for ^{40}A.* Phys. Rev., vol. 114, no. 4, 1959, pp. 1139-1142.

23. Sund, R.E.; Baker, M.P.; Kull, L.A.; and Walton, R.B.: *Measurements of the $^{63}Cu(\gamma, n)$ and $(\gamma, 2n)$ Cross Sections.* Phys. Rev., vol. 176, no. 4, 1968, pp. 1366-1376.

24. Berman, B.L.; and Fultz, S.C.: *Measurements of the Giant Dipole Resonance with Monenergetic Photons.* Rev. Mod. Phys., vol. 47, no. 3, 1975, pp. 713-761.

25. Spicer, B.M.: *The Giant Dipole Resonance.* Adv. Nucl, Phys., vol. 1, 1969, pp. 1-78.

26 Norbury, J.W.: *The $^{54}Fe(\gamma, n)$ and $^{32}S(\gamma, d)$ Cross Sections* M.S. Thesis, Univ. of Melbourne, Nov. 1978.

27. Woodworth, J. G.; McNeill, K. G.; Jury, J. W.; Alvarez, R. A.; Berman, B. L.; Faul, D. D.; and Meyer, P.: Photonuclear Cross Sections for ^{18}O. Phys. Rev., ser. C, vol. 19, 1979, pp. 1667-1683.

28. Alvarez, R. A.; Berman, B. L.; Faul D. D.; Lewis, F. H.; and Meyer, P.: Photoneutron Cross Sections for ^{55}Mn and ^{59}Co. Phys. Rev. ser. C, vol. 20, 1979, pp. 128-138.

29. Berman, B.L.; Caldwell, J. T.; Harvey, R. R.; Kelly, M. A.; Bramblett, R. L.; and Fultz, S. C.: Photoneutron Cross Sections for ^{90}Zr, ^{91}Zr, ^{92}Zr, ^{94}Zr and ^{89}Y. Phys. Rev. vol. 162, 1967, pp. 1098-1111.

30. Berman, B. L.; Pywell, R. E.; Dietrich, S. S.; Thompson, M. N.; McNeill, K. G.; and Jury, J. W.; Absolute Photoneutron Cross Sections for Zr, I, Pr, Au and Pb. Phys. Rev. ser. C, vol. 36, 1987, pp. 1286-1292.

Table 1 ^{12}C photoneutron cross sections. Data are from ref. 21

Eγ, MeV	σ(γ, n), mb	σ(γ, 2n), mb	
		Experimental	Theoretical $f_d = 0.9$ $a = 2\ MeV^{-1}$
35	2	0.004	0.043
40	0.8	0.012	0.051
50	0.2	0.015	0.020
60	0.1	0.014	0.011
80	0.1	0.095	0.011

Table 2 ^{18}O photoneutron cross sections. Data are from ref. 27

Eγ, MeV	σ(γ, n), mb	σ(γ, 2n), mb	
		Experimental	Theoretical $f_d = 0.5$ $a = 3\ MeV^{-1}$
14	4	1	0.5
18	2.4	3	1.3
22	4	3	3.1
26	7	3	6
30	5	3	5
34	2	3	1.9
38	2	2	1.9
42	1	3	1.2

Table 3 ^{40}Ar photoneutron cross sections. Data are from ref. 22

Eγ, MeV	σ(γ, n), mb	σ(γ, 2n), mb	
		Experimental	Theoretical $f_d = 0.05$ $a = 6\ MeV^{-1}$
18	16	5	6
20	7	14	12
21	5	13	14
22	3	11	12
23	2	10	11

Table 4 ^{59}Co photoneutron cross sections. Data are from ref. 28

Eγ, MeV	σ(γ, n), mb	σ(γ, 2n), mb	
		Experimental	Theoretical $f_d = 0.6$ $a = 8\ MeV^{-1}$
18	65	0.3	27
20	47	9	4
22	21	17	7
24	17	12	9
26	14	11	8
28	19	9	12
30	20	5	13
32	9	6	6
34	1	6	1
36	4	3	3

Table 5 ^{63}Cu photoneutron cross sections. Data are from ref. 23

Eγ, MeV	σ(γ, n), mb	σ(γ, 2n), mb	
		Experimental	Theoretical $f_d = 0.3$ $a = 8\ MeV^{-1}$
20	44	2	0.6
21	26	4	5
22	20	8	11
23	13	12	12
24	11	13	13
25	10	13	15

Table 6 ^{89}Y photoneutron cross sections. Data are from ref. 29

Eγ, MeV	σ(γ, n), mb	σ(γ, 2n), mb	
		Experimental	Theoretical $f_d = 0.5$ $a = 12\ MeV^{-1}$
20	70	0	36
22	35	7	6
24	10	10	6
26	2	16	2
28	0.5	16	0.5

Table 7 ^{197}Au photoneutron cross sections. Data are from ref. 16 but have been multiplied by 0.93 following the suggestion of ref. 30

Eγ, MeV	σ(γ, n), mb	σ(γ, 2n), mb	
		Experimental	Theoretical $f_d = 0.4$ $a = 24$ MeV^{-1}
15	391	9	20
16	214	73	121
17	93	98	98
18	56	93	74
19	37	65	53
20	27	58	40
21	17	42	25
22	11	47	16
23	7	40	11
24	2	37	3

Table 8 ^{208}Pb photoneutron cross sections. Data are from ref. 16

Eγ, MeV	σ(γ, n), mb	σ(γ, 2n), mb	
		Experimental	Theoretical $f_d = 0.2$ $a = 8\ MeV^{-1}$
16	180	80	104
18	30	80	51
20	20	50	55

LIST OF SYMBOLS

A	nuclear temperature constant, MeV^{-1}
a	energy level density parameter, MeV^{-1}
E	energy, MeV
EM	abbreviation for "electromagnetic"
E_{GDR}	giant dipole resonance central energy, MeV
$E_o(x)$	photonuclear reaction threshold for a particular species x, MeV
E_γ	photon energy, MeV
El	electric multipole of multipolarity l
f_d	fraction of direct, non-statistical emission
g_o	one particle level density at the Fermi energy, MeV^{-1}
$g_x^{\pi l}$	energy independent branching ratio for species x due to a πl nuclear excitation
$g_x^{\pi l}(E)$	energy dependent branching ratio for species x due to a πl nuclear excitation
k	Boltzmann constant 1.3805×10^{-23} J/K
l	multipolarity
Ml	magnetic multipole of multipolarity l
mb	millibarn
N_o	number of particles
$N^{\pi l}(E)$	virtual photon number spectrum of a particular multipole, MeV^{-1}
n	neutron
p	proton
x	particular particle species emitted in a heavy ion collision
α	alpha particle
Γ	giant dipole resonance width, MeV
ε_{sec}	maximum energy available for emission of secondary particles, MeV

$\pi\ell$	particular electromagnetic multipole (e.g., $E1, M0$)
ρ	energy level density, MeV^{-1}
σ	cross section, mb
$\sigma(\gamma, sb)$	sum of cross sections in which at least one particle b is emitted
$\sigma(\gamma, sn)$	photoneutron cross section, mb
$\sigma(\gamma, xn)$	total photoneutron yield cross section, mb
$\sigma_{abs}^{\pi\ell}(E)$	photonuclear total absorption cross section, mb
σ_{EM}	total nucleus-nucleus EM absorption cross section, mb
$\sigma_{EM}(x)$	nucleus-nucleus EM reaction cross section for production of a particular species x, mb
$\sigma_{EM\text{-}abs}$	nucleus-nucleus EM total absorption cross section summed over all EM multipoles, mb
$\sigma_{EM\text{ - }abs}^{\pi\ell}$	nucleus-nucleus EM total absorption cross section for a particular multipole, mb
σ_m	giant dipole resonance cross section peak value, mb
$\sigma_\nu^{\pi\ell}(E, x)$	photonuclear reaction cross section for production of a particular species x due to nuclear excitation from a particular multipole $\pi\ell$, mb

THE INVARIANCE OF CLASSICAL ELECTROMAGNETISM UNDER CHARGE-CONJUGATION, PARITY AND TIME-REVERSAL (CPT) TRANSFORMATIONS

by

John W. Norbury
Physics Department
Washington State University
Pullman, WA 99164

Abstract

The invariance of Classical Electromagnetism under CPT is studied by considering the motion of a charged particle in electric and magnetic fields. Upon applying CPT transformations to various physical quantities and noting that the motion still behaves physically demonstrates invariance.

1. Introduction

In teaching a recent course in electromagnetism I discussed the transformation properties of the electric $\vec{E}$, and magnetic fields $\vec{B}$ under parity (P) time reversal (T) and charge conjugation (C) transformations. I was amazed to find that a unified discussion of CPT transformations in classical electromagnetism does not exist in any of the standard text books. The best I could find was a discussion of time-reversal and axial and polar vectors in (Jackson 1975). The aim of the present paper is purely pedagogical. I wish to discuss CPT transformations, not from a mathematical point of view (Rosen 1973) but from a completely physical point of view by considering how the transformations affect the motion of a charged particle in an electromagnetic field. This approach was very successful with the students; they came away with an excellent physical understanding of these transformations.

Our procedure will be as follows: we shall look at the motion of a charged particle in either $\vec{E}$ or $\vec{B}$ fields and then apply one of the C, P or T transformations to the whole situation. Each quantity, such as force, charge, etc. will transform in their own particular way. Because Maxwell's equations are invariant however we know that our transformed situation shouldn't be any different. In particular, by looking simply at trajectory of the particle, we shouldn't be able to tell that a transformation has taken place. Examining these "pictorial" transformations will give us a very clear physical understanding of the corresponding mathematical transformations.

Before proceeding we note the transformation properties of some of the quantities we shall need. Details can be found in (Jackson 1975, Perkins 1987, Rosen 1973). Electric charge q is a scalar under P and T, but a pseudoscalar under C. ($Pq = q$, $Tq = q$, $Cq = -q$) Velocity $\vec{v}$ changes sign (vector) under T because of its form as $d\vec{x}/dt$. Otherwise it is a vector under P and a pseudovector under C. ($P\vec{v} = -\vec{v}$, $T\vec{v} = -\vec{v}$, $C\vec{v} = \vec{v}$) Force $\vec{F}$ or acceleration is a pseudovector under T because of the form $d^2\vec{x}/dt^2$. Otherwise it transforms the same as $\vec{v}$. ($P\vec{F} = -\vec{F}$, $T\vec{F} = \vec{F}$, $C\vec{F} = \vec{F}$).

2. Electric Field

The transformation properties of the electric field are $P\vec{E} = -\vec{E}$ (vector), $T\vec{E} = \vec{E}$ (pseudo-vector), $C\vec{E} = -\vec{E}$ (vector). Let us study these in turn by considering the motion of a positively charged particle in an electric field, as shown in Fig. 1.

2.1 Parity

Parity transformations are most easily visualized by reflection in a mirror. Imagine that the charge in Fig. 1 is moving to the right at right angles toward a mirror. Let us now reflect this whole situation in the mirror. Under reflection charge q is a scalar and electric field $\vec{E}$, force $\vec{F}$ and velocity $\vec{v}$ are vectors and so reverse sign as shown in Fig. 2. Thus the relative orientation of $\vec{F}$ and $\vec{E}$ are still the same. Thus we still have acceleration towards the mirror: we cannot tell that we are now in a reflected world.

2.2 Charge Conjugation

Under charge conjugation $\vec{F}$ and $\vec{v}$ remains the same, but $\vec{E}$ and q change sign, as shown in Figure 3. Thus we still have acceleration of the charge to the right, so we can't tell that a C transformation has been made.

2.3 Time-Reversal

Now q and $\vec{E}$ remain the same but $\vec{v}$ $(d\vec{x}/dt)$ changes direction, and $\vec{a}$ $(d^2\vec{x}/dt^2)$ or $\vec{F}$ remains the same also. This time $\vec{F}$ and $\vec{v}$ become <u>opposite</u> to each other. As depicted in Fig. 4, the motion is like a movie of Fig. 1 being run backwards. Thus the particle starts at the far right hand side with velocity $-\vec{v}$ but slows down because the force is to the right, as it travels into the past. The motion still makes physical sense and we cannot distinguish travel into the future from travel into the past. (The position of the particle in Fig. 4 can be superposed directly onto Fig. 1)

3. Magnetic Field

The magnetic field $\vec{B}$ transforms as $P\vec{B} = \vec{B}$ (pseudovector), $T\vec{B} = -\vec{B}$ (vector), $C\vec{B} = -\vec{B}$ (vector). We consider a positive charge moving counterclockwise in a magnetic field as shown in Fig. 5.

3.1 Parity

We now imagine a mirror parallel to the plane of the paper. Because $\vec{F}$ and $\vec{v}$ are in the same plane they will not be affected this time by a parity transformation. Any vector perpendicular to the plane of the paper will change sign. However, $\vec{B}$ (which is perpendicular) is a pseudo-vector under P and will not change sign. Thus the mirror-reflected version of Fig. 5 is identical to that figure. Obviously then the motion is invariant under reflection.

3.2 Charge Conjugation

Figure 6 represents a charge conjugated version of Fig. 5. As can be seen the motion is still counterclockwise, so we couldn't tell that a transformation has been made.

3.3 Time-Reversal

The time-reversed situation of Fig. 5 is shown in Fig. 7. The motion here is identical to what we would see if we took a movie of the motion of Fig. 5 and then ran it backwards.

Summary

Note the importance of what has been done in the 6 transformations presented above. We have transformed each quantity separately, thus making it quite possible to obtain a resultant unphysical trajectory, ie. a trajectory violating Maxwell's equations and the Lorentz force law. (An example of an unphysical trajectory is a positive charged particle moving clockwise in a magnetic field directed into the page.) However, none of our transformed trajectories have been unphysical indicating invariance of Classical Electromagnetism and thus preventing us from assigning an absolute value to C, P, or T. That is, by examining the physical motion we cannot tell if a C, P or T transformation has been made. It is hoped that the ideas presented in this paper will provide a useful physical supplement to the study of classical electromagnetism.

Acknowledgements

This work was supported, in part, by NASA research grant NAG-1-797

References

Jackson, J. D., Classical Electrodynamics, 1975, 2nd ed., John Wiley & Sons.

Perkins, D. H., 1987, Introduction to High Energy Physics, 3rd ed., Addison-Wesley, (section 3.7)

Rosen, J., 1973, American J. Phys. 41 586.

Figure Captions

Fig. 1. Motion of a Positive Charge moving towards a mirror with an initial velocity $\vec{v}$ in a Uniform Electric Field. The position of the charge at various times is indicated with a symbol $\oplus$, at time t_i.

Fig. 2 Motion of Fig. 1 reflected in a mirror

$(P\vec{E} = -\vec{E},\ Pq = q,\ P\vec{v} = -\vec{v},\ P\vec{F} = -\vec{F})$

Fig. 3 Charge - conjugated version of Fig. 1. The positive charge becomes a negative charge indicated with a symbol .

$(C\vec{E} = -\vec{E},\ Cq = -q,\ C\vec{v} = \vec{v},\ C\vec{F} = \vec{F}$

Fig. 4 The charge of Fig. 1 travelling into the past.

$(T\vec{E} = +\vec{E},\ Tq = q,\ T\vec{v} = -\vec{v},\ T\vec{F} = \vec{F})$

Fig. 5 Motion of a Positive Charge with a velocity $\vec{v}$ moving counterclockwise in a Uniform Magnetic Field directed into the page.

Fig. 6 Charge-conjugated version of Fig. 5 ($\vec{B}$ points out of the page) $(C\vec{B} = -\vec{B})$

Fig. 7 The charge of Fig. 5 travelling into the past.

$(T\vec{B} = -\vec{B})$

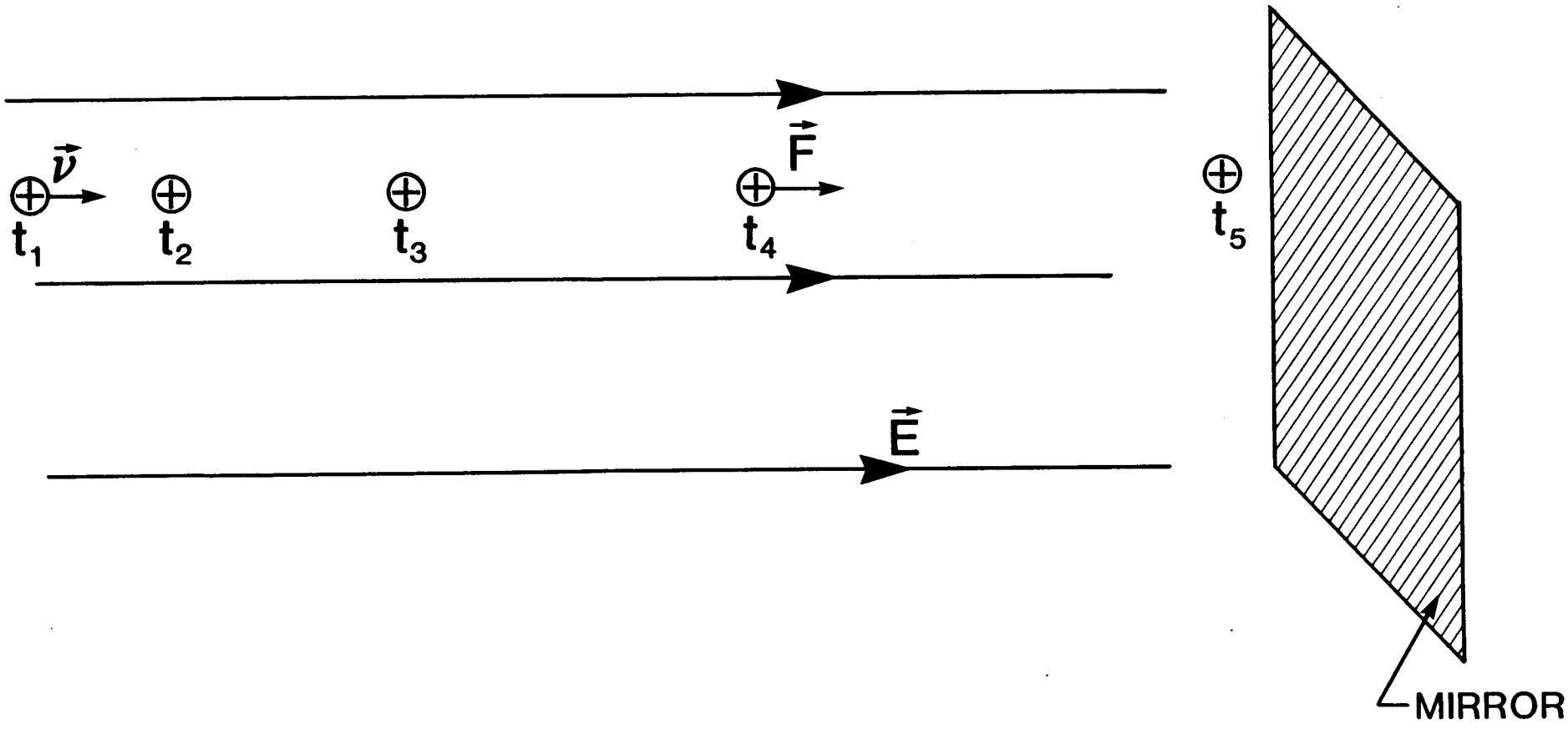

Fig. 1

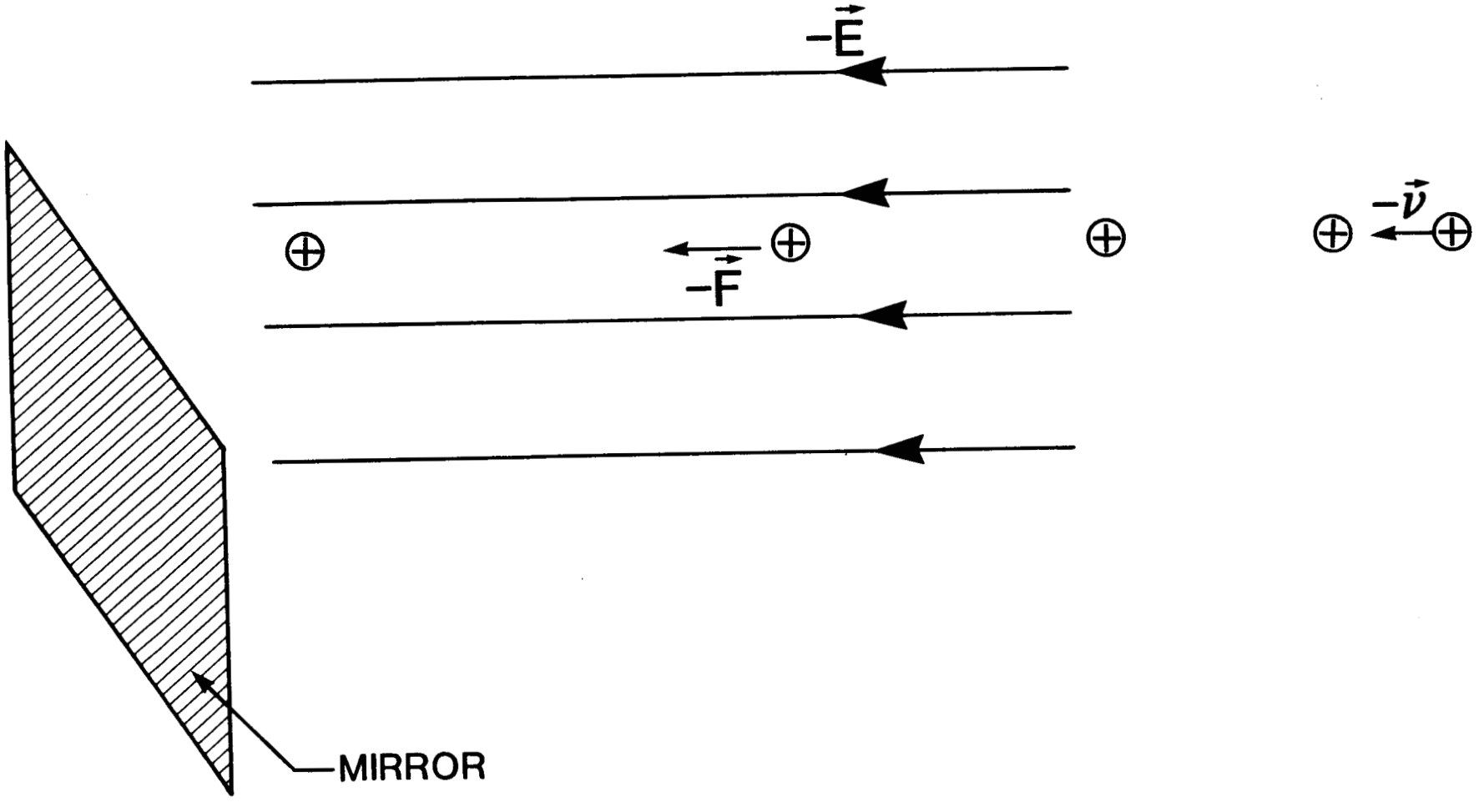

Fig. 2

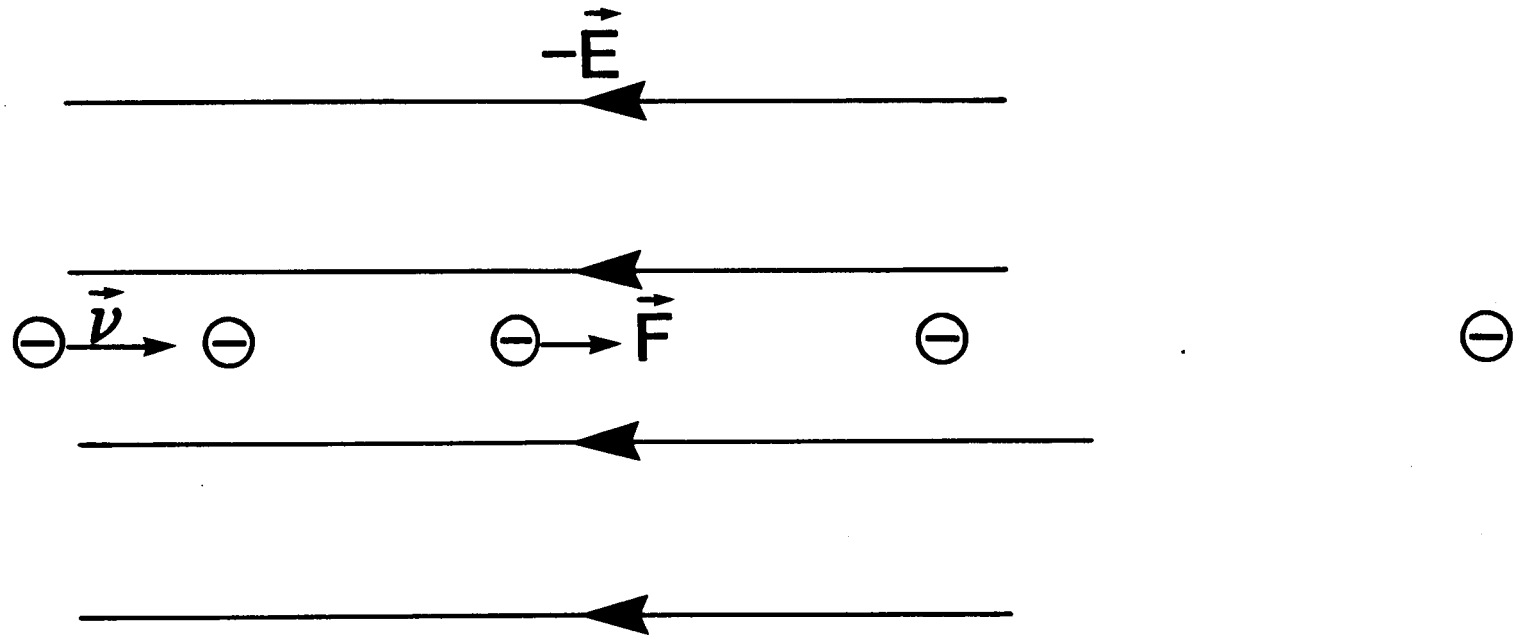

Fig. 3

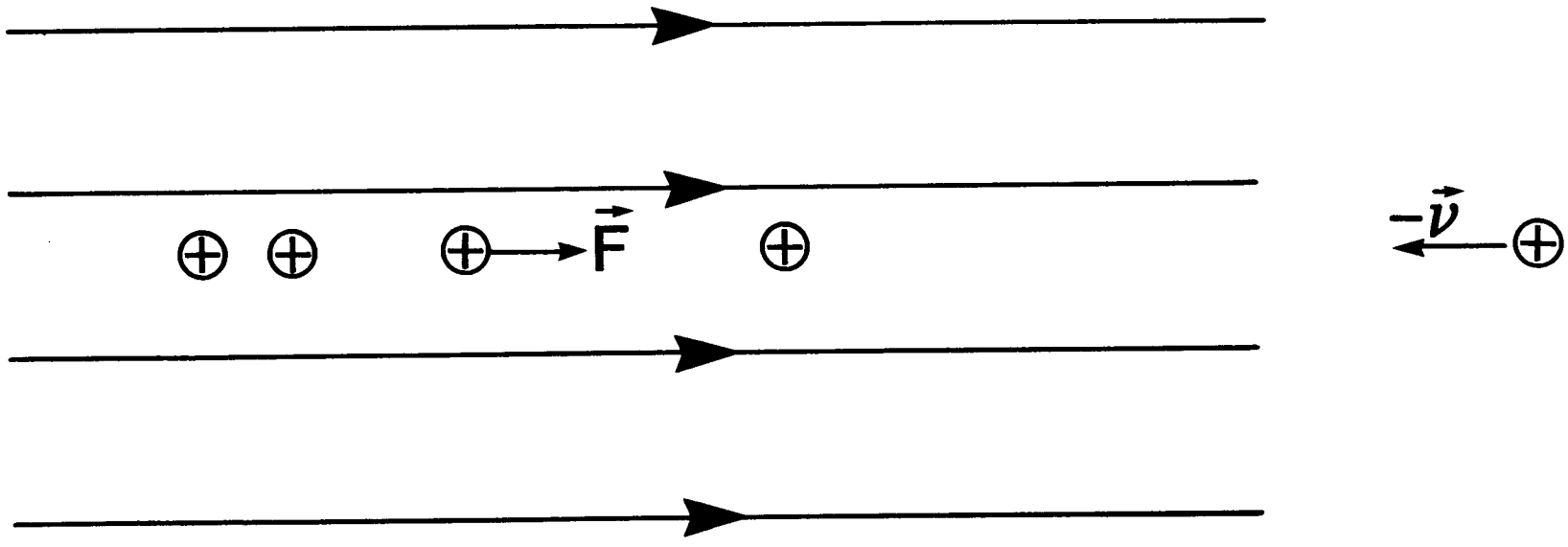

Fig 4

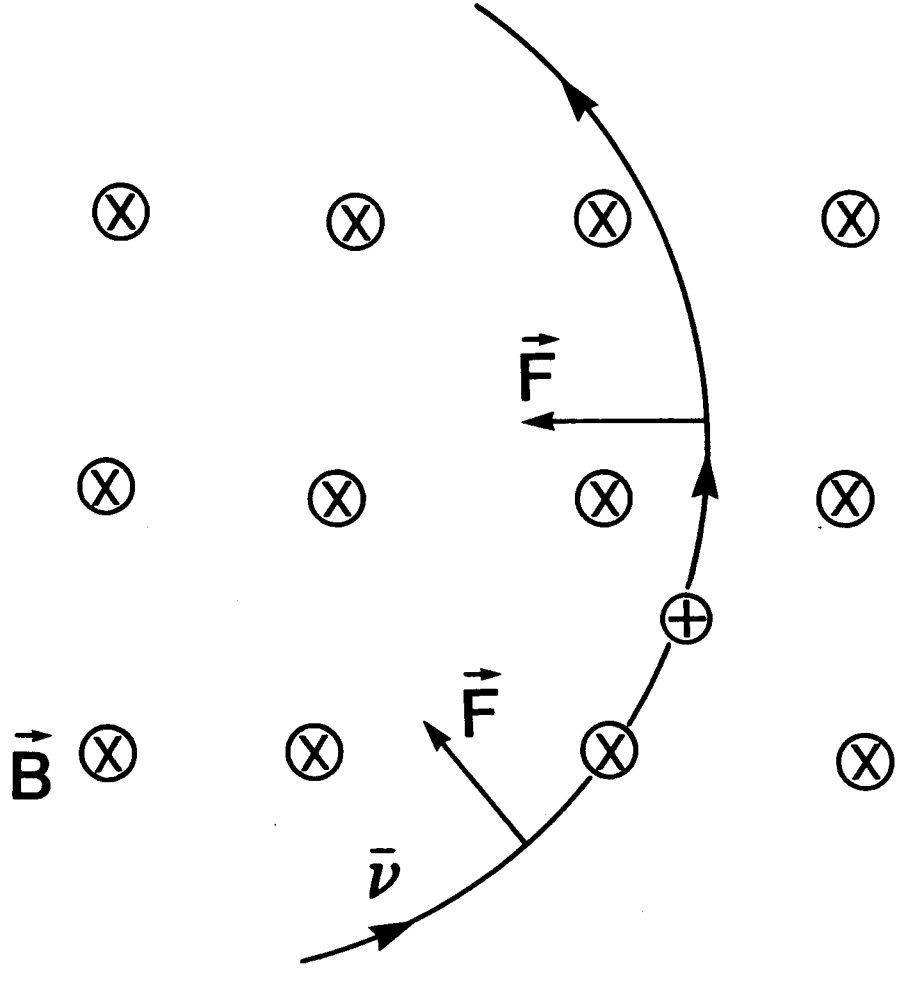

Fig 5

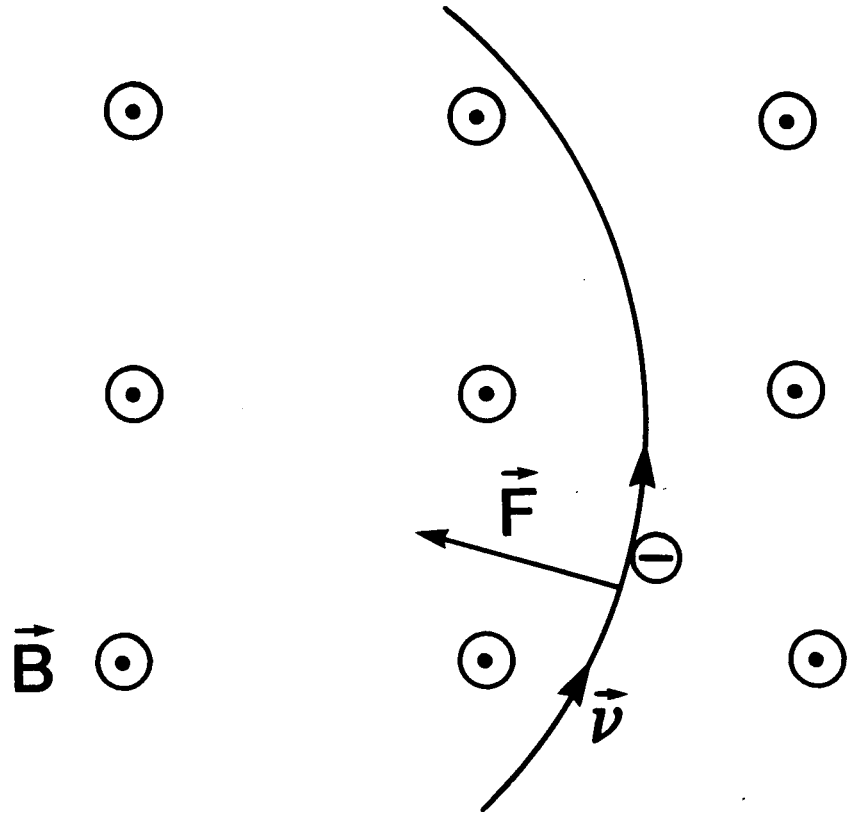

Fig. 6

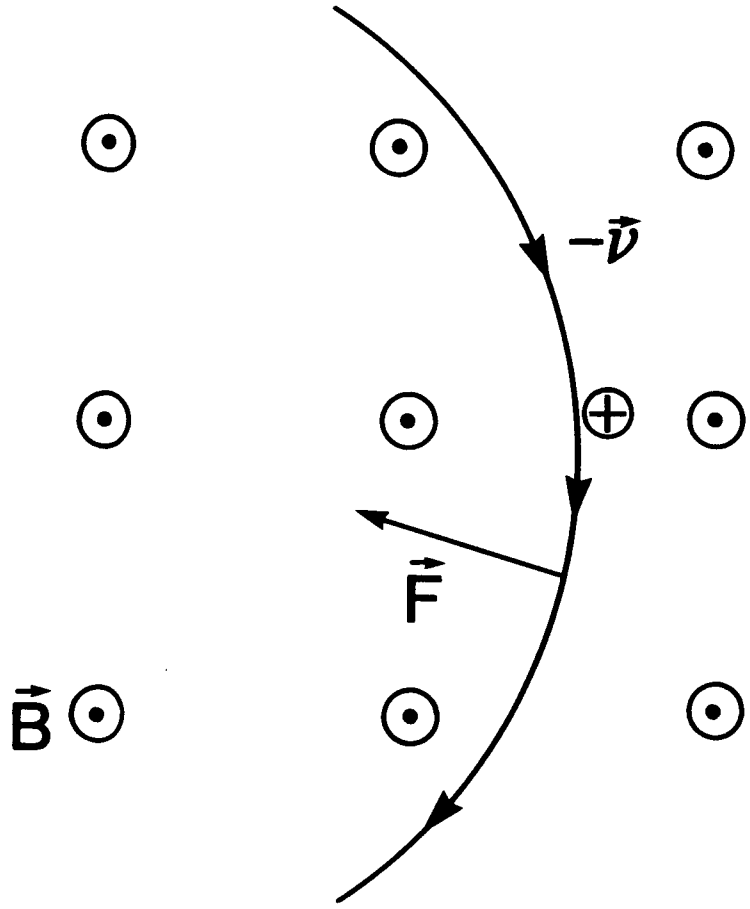

Fig. 7

AN OPTICAL MODEL DESCRIPTION OF MOMENTUM TRANSFER IN HEAVY ION COLLISIONS

F. Khan and G. S. Khandelwal
Physics Department
Old Dominion University
Norfolk, VA 23529-0116 USA

and

L. W. Townsend and J. W. Wilson
NASA Langley Research Center
Hampton, VA 23665-5225 USA

and

J. W. Norbury
Department of Mathematics & Physics
Rider College
Lawrenceville, NJ 08648 USA

PACS Numbers: 24.10.Ht, 25.70.Np

ABSTRACT

An optical model description of momentum transfer in relativistic heavy ion collisions, based upon composite particle multiple scattering theory, is presented. The imaginary component of the complex momentum transfer, which comes from the absorptive part of the optical potential, is identified as the longitudinal momentum downshift of the projectile. Predictions of fragment momentum distribution observables are made and compared with experimental data. Use of the model as a tool for estimating collision impact parameters is discussed.

1. INTRODUCTION

Since the pioneering experiments on relativistic heavy ion fragmentation using carbon and oxygen beams,[1, 2] attention has been directed toward understanding the underlying mechanisms of fragmentation processes. Over the past two decades, a substantial body of literature has resulted from studies of these phenomena, and several excellent reviews have been written.[3-6] Perhaps the most significant findings of the early experiments were the observations that the fragment momentum distributions were Gaussian in the projectile rest frame, and that the isotopic production cross sections factored into a product of target and beam-fragment terms. Initial attempts to explain these phenomena utilized a statistical model to describe the reactions.[7-9] This later evolved into a two-step model called

abrasion-ablation[10] where the abrasion stage can be formulated using geometric[10,11] or quantum mechanical arguments.[12, 13] In the present work, we use the impulsive excitation energy ideas of Fricke,[14] within the context of composite particle multiple scattering theory, to derive a method for predicting momentum transfers occurring in relativistic heavy ion collisions. This momentum transfer is a function of impact parameter. A new feature of this work is that the momentum transfer is a complex quantity. The real component is the usual transverse momentum transfer resulting from elastic scattering. The imaginary component is explicitly shown to be the longitudinal momentum transfer, or downshift, arising from the absorptive part of the complex optical potential. Using this formalism, projectile nucleus fragment momentum "downshifts" resulting from the dynamics of the nuclear collision can be calculated and compared with laboratory beam measurements. In addition, modifications to the widths of the momentum distributions can be estimated using the formalism.

The outline of the paper is as follows. In section 2 the dynamical momentum transfer expression is derived, and representative calculations of momentum transfer as a function of impact parameter are presented. In section 3 the connections between collisional momentum transfer and fragment momentum downshifts/widths are made. A method of choosing appropriate impact parameters

for each fragmentation channel is then described. Next, calculations of momentum downshifts for fragments produced by oxygen nuclei colliding with various targets are made and compared with experimental data.[2] We also compute widths of momentum distributions for ^{139}La fragments and compare with recent experimental measurements.[16] In section 4 we propose a method for using the momentum transfer model to estimate collision impact parameters. Finally, in section 5 we conclude by summarizing the current status of model development and discuss future directions for research.

2. METHOD OF CALCULATION

In reference 17, a coupled-channels Schrödinger equation for composite particle scattering, which relates the entrance channel to all of the excited states of the target and projectile, was derived by assuming large incident projectile kinetic energies and closure of the accessible eigenstates. The equation is written as

$$\left(\nabla^2 + k^2\right) \psi_{n\mu}(\vec{x}) = 2m\, A_p\, A_T\, (A_p + A_T)^{-1} \sum_{n'\mu'} V_{n\mu,\, n'\mu'}(\vec{x})\, \psi_{n'\mu'}(\vec{x}) \tag{1}$$

where the subscripts n and μ (primed and unprimed) label the projectile and target eigenstates; m is the nucleon mass; A_p and A_T are the mass numbers of the projectile and target; $\vec{k}$ is the projectile momentum relative to the center of mass; and $\vec{x}$ is the projectile position vector relative to the target. In terms of the nucleon-

nucleon scattering t-matrix $t_{\alpha j}$, and the internal state vectors of the projectile $g_n^P(\vec{\xi}_p)$ and target $g_\mu^T(\vec{\xi}_T)$, it was also demonstrated that the potential matrix is expressible as

$$V_{n\mu,\, n'\mu'}(\vec{x}) = \left\langle g_n^P\, g_\mu^T \middle| V_{opt}\left(\vec{\xi}_P, \vec{\xi}_T, \vec{x}\right) \middle| g_{n'}^P, g_{\mu'}^T \right\rangle \tag{2}$$

where

$$V_{opt}\left(\vec{\xi}_P, \vec{\xi}_T, \vec{x}\right) = \sum_{\alpha j} t_{\alpha j} \tag{3}$$

This same formalism can be used to investigate heavy ion collision momentum transfers. Within the context of eikonal scattering theory, the solution to the Schrödinger equation

$$H\,\Psi\left(\vec{x}, \vec{\xi}_P, \vec{\xi}_T\right) = E\,\Psi\left(\vec{x}, \vec{\xi}_P, \vec{\xi}_T\right) \tag{4}$$

is

$$\Psi\left(\vec{x}, \vec{\xi}_P, \vec{\xi}_T\right) = (2\pi)^{-3/2} \exp\left[-\frac{i}{v} \int_{-\infty}^{z} V_{opt}\left(\vec{x}, \vec{\xi}_P, \vec{\xi}_T\right) dz' \right] g_n^P(\vec{\xi}_P)\, g_\mu^T(\vec{\xi}_T)\, e^{i\vec{k}\,\cdot\,\vec{x}} \tag{5}$$

where v is the velocity. The total momentum of the projectile is then given by the matrix element involving the sum of the projectile single-nucleon momentum operators as

$$\vec{P}_{tot} = \left\langle \Psi \middle| -i \sum_{\alpha=1}^{A_P} \vec{\nabla}_{P,\,\alpha} \middle| \Psi \right\rangle \tag{6}$$

where the subscript P on the gradient operator denotes that the gradient is to be

taken with respect to the projectile internal coordinates. Equation (6) actually denotes a potential matrix $\vec{P}_{n\mu,\, n'\mu'}$ in analogy with (2). Therefore, substituting (5) into (6) yields

$$\vec{P}_{n\mu,\, n'\mu'} = \left\langle g_n^P(\vec{\xi}_P)\, g_\mu^T(\vec{\xi}_T) \left| e^{-iS} \left(-i \sum_{\alpha=1}^{A_P} \vec{\nabla}_{P,\alpha} \right) e^{iS} \right| g_{n'}^P(\vec{\xi}_P)\, g_{\mu'}^T(\vec{\xi}_T) \right| \right\rangle \tag{7}$$

where

$$S = \frac{1}{v} \int_{-\infty}^{z} V_{opt}\left(\vec{x}', \vec{\xi}_P, \vec{\xi}_T\right) dz'. \tag{8}$$

Equation (7) can be further expressed as

$$\vec{P}_{n\mu,\, n'\mu'} = \vec{P}_o + \left\langle g_n^P\, g_\mu^T \left| \left(-\sum_{\alpha}^{A_P} \vec{\nabla}_{P,\alpha} S \right) \right| g_{n'}^P\, g_{\mu'}^T \right\rangle \tag{9}$$

where the momentum before the collision is

$$\vec{P}_o = \left\langle g_n^P\, g_\mu^T \left| \left(-i \sum_{\alpha=1}^{A_P} \vec{\nabla}_{P,\alpha} \right) \right| g_{n'}^P\, g_{\mu'}^T \right\rangle. \tag{10}$$

The total momentum transfer to the projectile is then given by

$$\vec{Q} = \vec{P}_{n\mu,\, n'\mu'} - \vec{P}_o = \left\langle g_n^P\, g_\mu^T \left| \left(-\sum_{\alpha} \vec{\nabla}_{P,\alpha} S \right) \right| g_{n'}^P\, g_{\mu'}^T \right\rangle \tag{11}$$

For scattering near the forward directions, the couplings between various excited states is small and the off-diagonal elements in Eq. (11) can be neglected; hence, the

momentum transfer can be approximated by

$$\vec{Q} \approx \vec{P}_{el} - \vec{P}_o = \left\langle g_o^P\, g_o^T \left| \left(-\sum_\alpha \vec{\nabla}_{P,\alpha}\, S \right) \right| g_o^P\, g_o^T \right\rangle. \tag{12}$$

In terms of projectile and target number densities, and the constituent-averaged two-nucleon transition amplitude,[18] $\tilde{t}$, Eq. (12) becomes

$$\vec{Q}(\vec{b}) = -A_P A_T \int d^3\xi_P\, \rho_P(\vec{\xi}_P) \int d^3\xi_T\, \rho_T(\vec{\xi}_T) \left[\vec{\nabla}_P \int_{-\infty}^{\infty} \tilde{t}\,(\vec{b} + \vec{z}' + \vec{\xi}_P - \vec{\xi}_T)\, \frac{dz'}{v} \right] \tag{13}$$

where the integration limit in the longitudinal direction has been extended to infinity. The momentum transfer in (13) is therefore only a function of the impact parameter of the collision. The projectile and target number densities (ρ_P and ρ_T) are normalized to unity as

$$\int \rho(\vec{x})\, d^3x = 1. \tag{14}$$

The constituent-averaged two-nucleon transition amplitude is obtained from the first-order t-matrix used in our previous studies[13] of nucleus-nucleus collisions as

$$\tilde{t}(e, \vec{x}) = -(e/m)^{1/2}\, \sigma(e)[\alpha(e) + i][2\pi B(e)]^{-1/2} \exp\left[-x^2/2B(e) \right] \tag{15}$$

where e is the two-nucleon kinetic energy in their center-of-mass frame, $\sigma(e)$ is the nucleon-nucleon total cross section, $\alpha(e)$ is the ratio of the real-to-imaginary part of

the forward scattering amplitude, and B(e) is the nucleon-nucleon slope parameter. Values for these parameters taken from various compilations are listed in reference 18.

The dynamical momentum transfer to the projectile, given by Eq. (13), results from interactions with the target. A new feature, unique to this work, is that it is a complex quantity. The real part of the momentum transfer, which comes from the real part of the complex optical potential, is the contribution arising from elastic scattering. It is purely transverse. The imaginary component, which comes from the absorptive part of the complex optical potential, is the longitudinal kinetic momentum downshift. To demonstrate this last assertion, we rewrite Eq. (13) symbolically as

$$\vec{Q} = (Q_R + iQ_I)\,\hat{b} \tag{16}$$

where i is $\sqrt{-1}$ and $\hat{b}$ is the unit vector transverse to the beam direction. If $\hat{z}$ denotes the unit vector in the incident beam direction, then from elementary complex analysis[19] we know that

$$i\hat{b} = -\hat{z} \tag{17}$$

since i is an operator which rotates a unit vector counterclockwise through $\pi/2$ radians. Therefore, the momentum transfer is

$$\vec{Q} = Q_R\,\hat{b} - Q_I\,\hat{z} \tag{18}$$

which we relabel for clarity as

$$\vec{Q} = Q_{\perp}\,\hat{b} - Q_{||}\,\hat{z}. \tag{19}$$

Note the similarity of this argument to that of complex indices of refraction in electromagnetic wave propagation. From Eq. (13), the transverse component is

$$\vec{Q}_{\perp} = -A_P A_T \int d^3\xi_P\, \rho_P(\vec{\xi}_P) \int d^3\xi_T\, \rho_T(\vec{\xi}_T)\, \vec{\nabla}_P \int_{-\infty}^{\infty} \mathrm{Re}\,\tilde{t}\left(\vec{b} + \vec{z}' + \vec{\xi}_P - \vec{\xi}_T\right) \frac{dz'}{v} \tag{20}$$

and the longitudinal component is

$$Q_{||} = -A_P A_T \int d^3\xi_P\, \rho_P(\vec{\xi}_P) \int d^3\xi_T\, \rho_T(\vec{\xi}_T)\, \vec{\nabla}_P \int_{-\infty}^{\infty} \mathrm{Im}\,\tilde{t}\left(\vec{b} + \vec{z}' + \vec{\xi}_P - \vec{\xi}_T\right) \frac{dz'}{v} \tag{21}$$

Calculated momentum transfers obtained using equations (20) and (21) are displayed in Figure 1 for ^{16}O at 2.1 AGeV colliding with a beryllium target. These calculations utilize the harmonic well nuclear densities from our previous work.[13, 18] From the figure, two features are readily apparent. First, the longitudinal momentum transfer is larger than the transverse indicating the primarily absorptive nature of the nuclear collision at this energy. Second, the predicted momentum transfers decrease rapidly with increasing impact parameter. This will be a subject of further discussion in subsequent sections of this paper.

3. RESULTS

The collisional momentum transfers computed using the model described in the previous section can be related to experimentally-measured, heavy-ion fragment momentum downshifts/widths through considerations of energy and momentum conservation. As has been pointed out elsewhere,[8, 20] a momentum transfer in any direction Q_j modifies the width h_j of the momentum distribution in that direction by

$$(h_j')^2 = h_j^2 + \frac{F^2 Q_j^2}{A^2} \tag{22}$$

and the mean by

$$\vec{P}_j' = \vec{P}_j + \frac{F}{A}\vec{Q}_j. \tag{23}$$

From the latter, the longitudinal momentum downshift is given by

$$\Delta P_{||} = P_{||}' - P_{||} = \frac{F}{A} Q_{||} \tag{24}$$

where $Q_{||}$ is the magnitude of the longitudinal momentum transfer [obtained from eq. (21)], F is the fragment mass number, and A is the initial mass number of the fragmenting nucleus. Recalling that $Q_{||}$ is a function of impact parameter, an appropriate method for choosing it for each fragmentation channel is necessary. Recently a semiempirical abrasion-ablation fragmentation model, NUCFRAG, was proposed.[21] Although it assumes simple uniform density distributions for the

colliding ions, and a zero-range (delta function) interaction, it does include frictional-spectator-interactions (FSI) and agrees with experimental cross section data to the extent that they agree among themselves. Also, and most importantly for this work, it is easily modified to yield the impact parameters for each fragmentation channel. Hence, the procedure for evaluating equations (22) and (24) is to extract impact parameters from NUCFRAG for each nucleon removal corresponding to $\Delta A = 1, 2, 3, \ldots$. These impact parameters are then inserted into Eqs. (20) and (21) to obtain the corresponding momentum transfers for use in evaluating Eqs. (22) and (24). Because NUCFRAG uses uniform densities, uniform densities are also used in evaluating (20) and (21). In addition, the zero-range interaction in NUCFRAG is simulated for numerical integration purposes in (20) and (21) through the use of a very narrow Gaussian form for the t-matrix given by eq. (15). This narrow Gaussian is the same width for all collision pairs and therefore is not an arbitrarily adjusted parameter.

Representative calculations for momentum downshifts as a function of fragment mass number are displayed in Figure 2 for ^{16}O projectiles at 2.1 AGeV colliding with targets of Be, C, Al, Cu, Ag, and Pb. These momentum downshifts are target-averaged using simple arithmetic averaging. For comparison, the target-averaged experimental data from reference 2 are also also displayed. For display and

comparison purposes, the latter are also averaged over all isotopes contributing to each fragment mass number using

$$(\Delta P_{||})_{ave} = \frac{\sum_i \sigma_i \left(\Delta P_{||}^i\right)_{expt}}{\sum_i \sigma_i} \tag{25}$$

where σ_i is the experimental production cross section for the ith fragment isotope. Comparing the theoretical estimates to the experimental data, reasonable agreement is obtained considering the simplified form of the nuclear fragmentation model used in the calculations and the overall sensitivity of the calculated momentum transfer to the choice of impact parameter. Improved agreement is expected if impact parameters from a fragmentation model using realistic nuclear densities and interactions were available. This is especially true for collisions involving lighter ions, such as carbon, oxygen, and beryllium, which are poorly represented by simple uniform nuclear distributions.

Figure 3 displays transverse momentum widths as a function of fragment mass number for 1.2 AGeV ^{139}La fragmenting in carbon targets. The experimental data are taken from reference 16. Again, impact parameters from NUCFRAG are used as inputs into the momentum transfer expressions [Eqs. (20) and (21)]. For consistency with the use of these impact parameters, a narrow Gaussian t-matrix and uniform nuclear densities were again utilized in the momentum transfer

calculations. From Figure 3, it is clear that the agreement is much better than in Figure 2 and probably reflects the fact that a uniform nuclear density distribution is a more reasonable aproximation for a heavy nucleus-like lanthanum than for light nuclei such as oxygen.

4. ESTIMATING COLLISION IMPACT PARAMETERS

Thus far in this work, we have used collision impact parameters as inputs into a momentum transfer computational model which in turn has yielded estimates of heavy ion fragment momentum downshifts/widths for comparison with experimental data. However, this procedure can be reversed and the model used to estimate collision impact parameters from measured momentum downshifts for relativistic collisions. Let F be the fragment mass number with measured longitudinal momentum downshift $\Delta P_{||}$ produced in a relativistic collision between a projectile nucleus (mass number A) and some target. Then, from eq. (24), the longitudinal momentum transfer to the projectile from the target is

$$Q_{||} = \frac{A}{F} \Delta P_{||}. \tag{26}$$

The collision impact parameter can then be estimated from eq. (21) by computing $Q_{||}$ as a function of impact parameter (e.g., in Figure 1) and using $Q_{||}$ from eq. (26) as the entry. To illustrate, consider a collision involving 2.1 AGeV oxygen colliding

with a beryllium target. The calculated momentum transfer using realistic nuclear densities are displayed in Figure 1. If the measured (hypothetical) momentum downshift for the ^{14}N fragment is 35 ± 7 MeV/c, then eq. (26) yields a longitudinal momentum downshift of 40 ± 8 MeV/c. From Figure 1, the corresponding range of impact parameters is 6.1 - 6.4 fm. A similar procedure incorporating measured momentum distribution widths and Eqs. (22) and (20) or (21) could also be used to estimate collision impact parameters.

5. CONCLUDING REMARKS

Beginning with composite particle multiple scattering theory, an optical model description of collision momentum transfer in relativistic heavy ion collisions was derived. General expressions for transverse and longitudinal momentum transfer, which utilize a finite-range two-nucleon interaction and relativistic nuclear densities, were presented. The theory was used to estimate heavy ion fragment momentum downshifts for relativistic oxygen and transverse momentum widths for relativistic lanthanum projectiles. The main new feature of this work was the identification of the imaginary component of the momentum transfer as the longitudinal collision momentum transfer. Finally, the use of the model as a mechanism for estimating collision impact parameters was described.

The present theory is mainly applicable at intermediate or high energies because of the use of eikonal wavefunctions and the impulse approximation. At lower energies (below several hundred MeV/nucleon), the validity of straight line

trajectories and the assumption of a constant projectile velocity is questionable. Therefore, to compare theory with experiment at lower energies[22] revisions to the model are necessary. In particular, deceleration corrections to the constant velocity assumption are being developed. For incident energies greater than 1 AGeV, first-order deceleration corrections are small (< 1 percent). As the incident energy decreases, however, the first-order corrections increase significantly (over 50 percent at 100 A MeV), indicating that higher-order terms must be included. Work on this is in progress and will be reported when completed.

The authors wish to thank Hank Crawford and Peter Lindstrom of Lawrence Berkeley Laboratory, and Frank Cucinotta of the Environmental Measurements Laboratory (USDOE) for useful comments and suggestions. This work was supported by NASA Grant Nos. NCCI-42 (F. K. and G. S. K.) and NAG-1-797 (J. W. N.)

REFERENCES

1 P. J. Lindstrom, D. E. Greiner, H. H. Heckman, Bruce Cork, and F. S. Bieser, Lawrence Berkeley Laboratory Report No. LBL-3650, 1975 (unpublished).

2 D. E. Greiner, P. J. Lindstrom, H. H. Heckman, Bruce Cork, and F. S. Bieser, Phys. Rev. Lett. 35 (1975) 152.

3 A. S. Goldhaber and H. H. Heckman, Ann. Rev. Nucl. Part. Sci. 28 (1978) 161.

4 S. Nagamiya, J. Randrup, and T. J. M. Symons, Ann. Rev. Nucl. Part. Sci. 34 (1984) 155.

5 J. Hufner, Phys. Rep. 125 (1985) 129.

6 G. Baur, F. Rösel, D. Trautmann, and R. Shyam, Phys. Rep. 111 (1984) 333.

7 H. Feshbach and K. Huang, Phys. Lett. 47B (1973) 300.

8 A. S. Goldhaber, Phys. Lett. 53B (1974) 306.

9 R. K. Bhaduri, Phys. Lett. 50B (1974) 211.

10 J. D. Bowman, W. J. Swiatecki, and C. F. Tsang, Lawrence Berkeley Laboratory Report No. LBL-2908, 1973 (unpublished).

11 J. Gosset et al., Phys. Rev. C 16, (1977) 629; L. F. Oliveira, R. Donangelo, and J. O. Rasmussen, Phys. Rev. C 19 (1979) 826.

12 J. Hufner, K. Schafer, and B. Schurmann, Phys. Rev. C 12 (1975) 1888; M. Bleszynski and C. Sander, Nucl. Phys. A326 (1979) 525.

13 L. W. Townsend, Can. J. Phys. 61 (1983) 93; L. W. Townsend, J. W. Wilson, and J. W. Norbury, ibid. 63 (1985) 135; L. W. Townsend, J. W. Wilson, F. A. Cucinotta, and J. W. Norbury, Phys. Rev. C 34 (1986) 1491.

14 S. H. Fricke, Ph.D. Thesis, University of Minnesota, 1985 (unpublished); B. F. Bayman, P. J. Ellis, S. Fricke, and Y. C. Tang, Phys. Rev. Lett. 53 (1984) 1322.

15 L. W. Townsend and J. W. Wilson, Health Phys. 54 (1988) 409.

16 F. P. Brady et al., Phys. Rev. Lett. 60 (1988) 1699.

17 J. W. Wilson and L. W. Townsend, Can. J. Phys. 59 (1981) 1569.

18 L. W. Townsend and J. W. Wilson, NASA Reference Publication No. RP-1134, May 1985.

19 P. M. Morse and H. Feshbach, Methods of Theoretical Physics, (Mc-Graw Hill, New York, 1953) Part I, pp. 349-356.

20 C. Y. Wong, in Proceedings of the 5th High Energy Heavy Ion Study, Lawrence Berkeley Laboratory, Report No. LBL-12652, 1981 (unpublished).

21 J. W. Wilson, L. W. Townsend, and F. F. Badavi, Nucl. Inst. & Meth. B18 (1987) 225.

22 J. P. Wefel et al., Bull. Am. Phys. Soc. 34 (1989) 1137.

Figure 1: Momentum transfer to the ^{16}O projectile, as a function of impact parameter, for 2.1 AGeV oxygen colliding with a beryllium target.

Figure 2: Target-averaged longitudinal momentum downshifts as a function of projectile fragment mass number for 2.1 AGeV ^{16}O colliding with Be, C, Al, Cu, Ag, and Pb targets. The experimental data, taken from reference 2, are averaged over isotopes for each fragment mass.

Figure 3: Transverse momentum widths as a function of fragment mass number for 1.2 AGeV ^{139}La colliding with a carbon target. The experimental data are taken from reference 16.

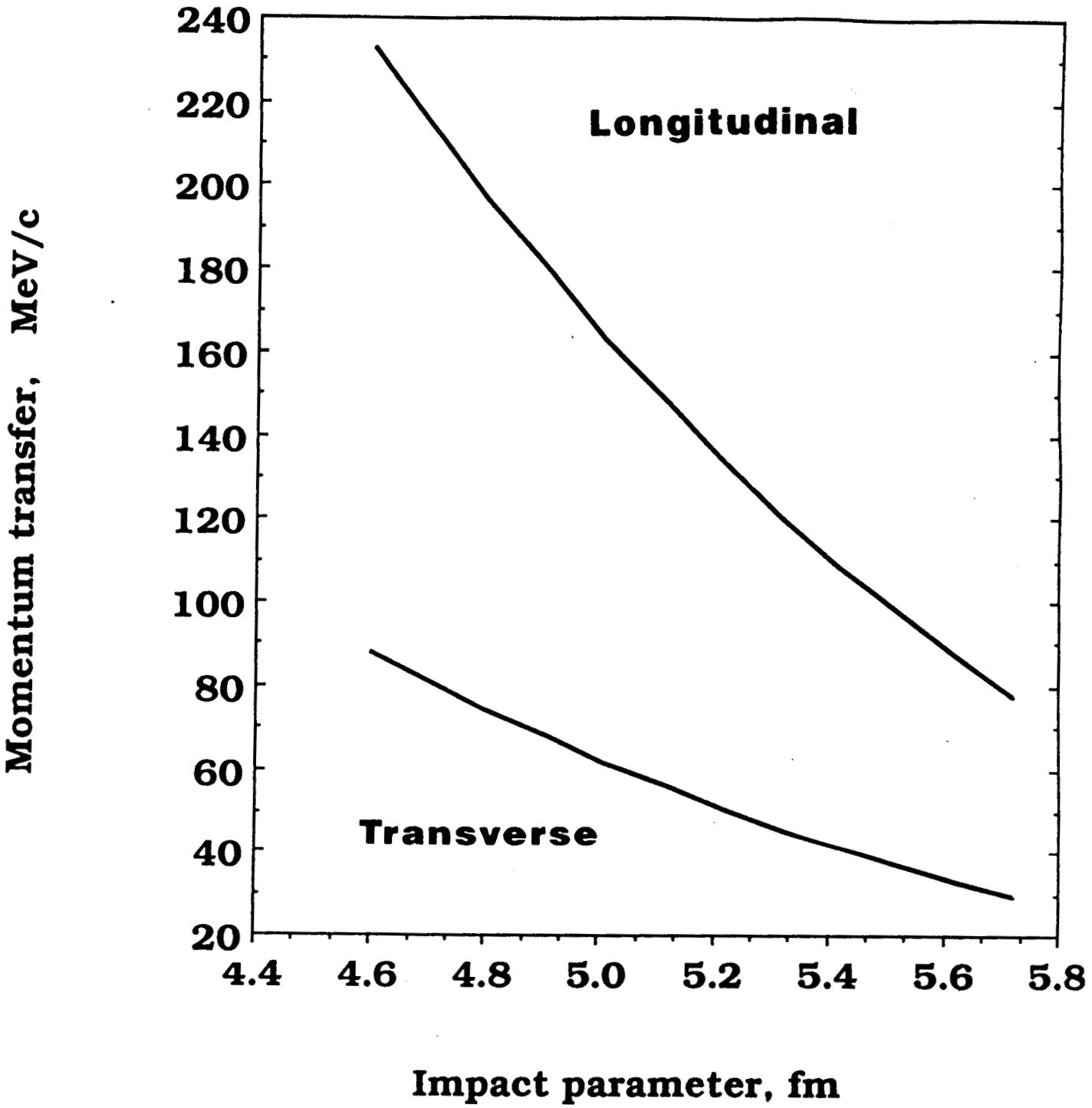

Khan/Khandelwal/Townsend/Wilson/Norbury

"An Optical Model Description of Momentum..

Figure 1.

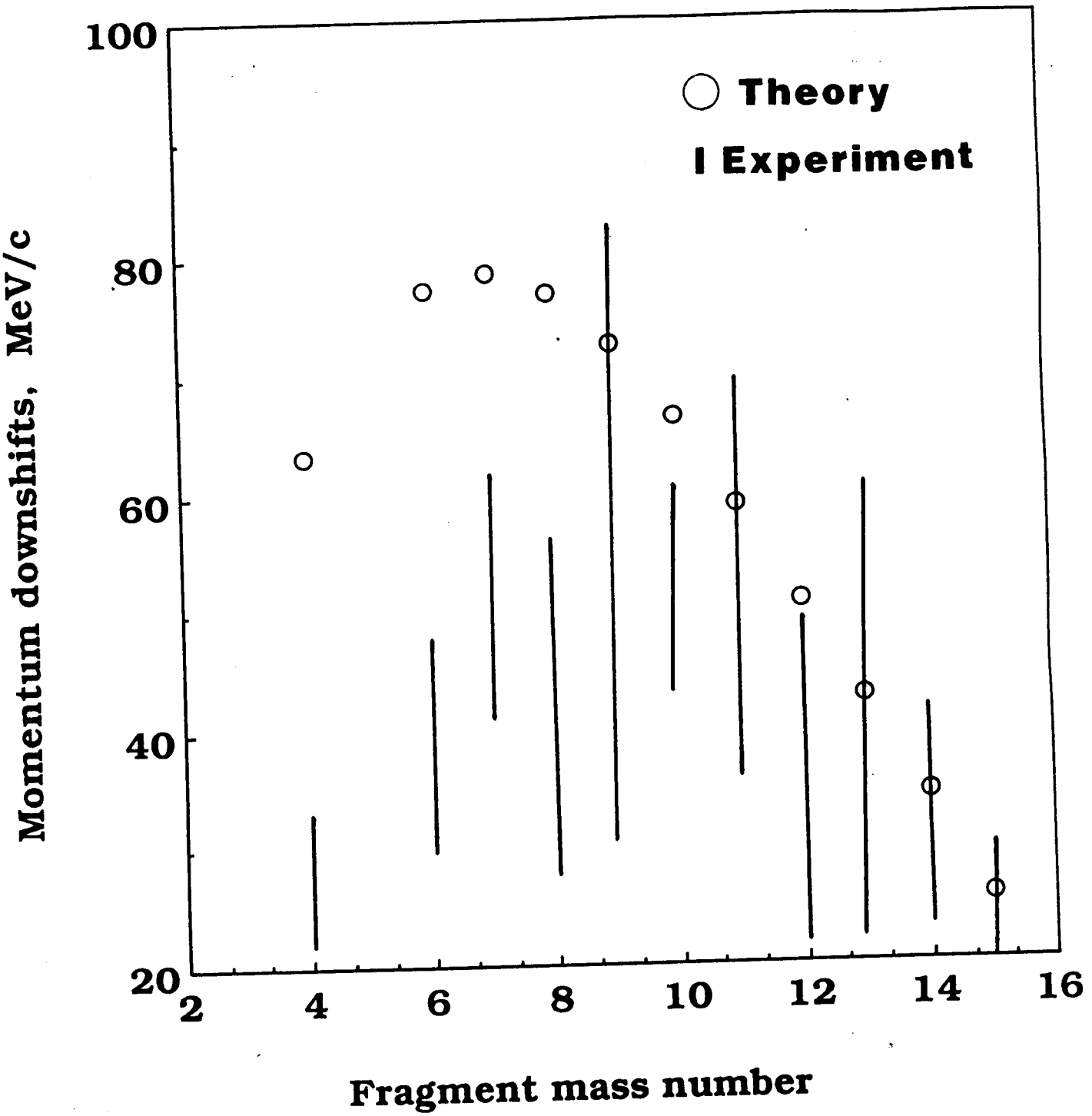

Khan/Khandelwal/Townsend/Wilson/Norbury

"An Optical Model Description of Momentum..."

Figure 2.

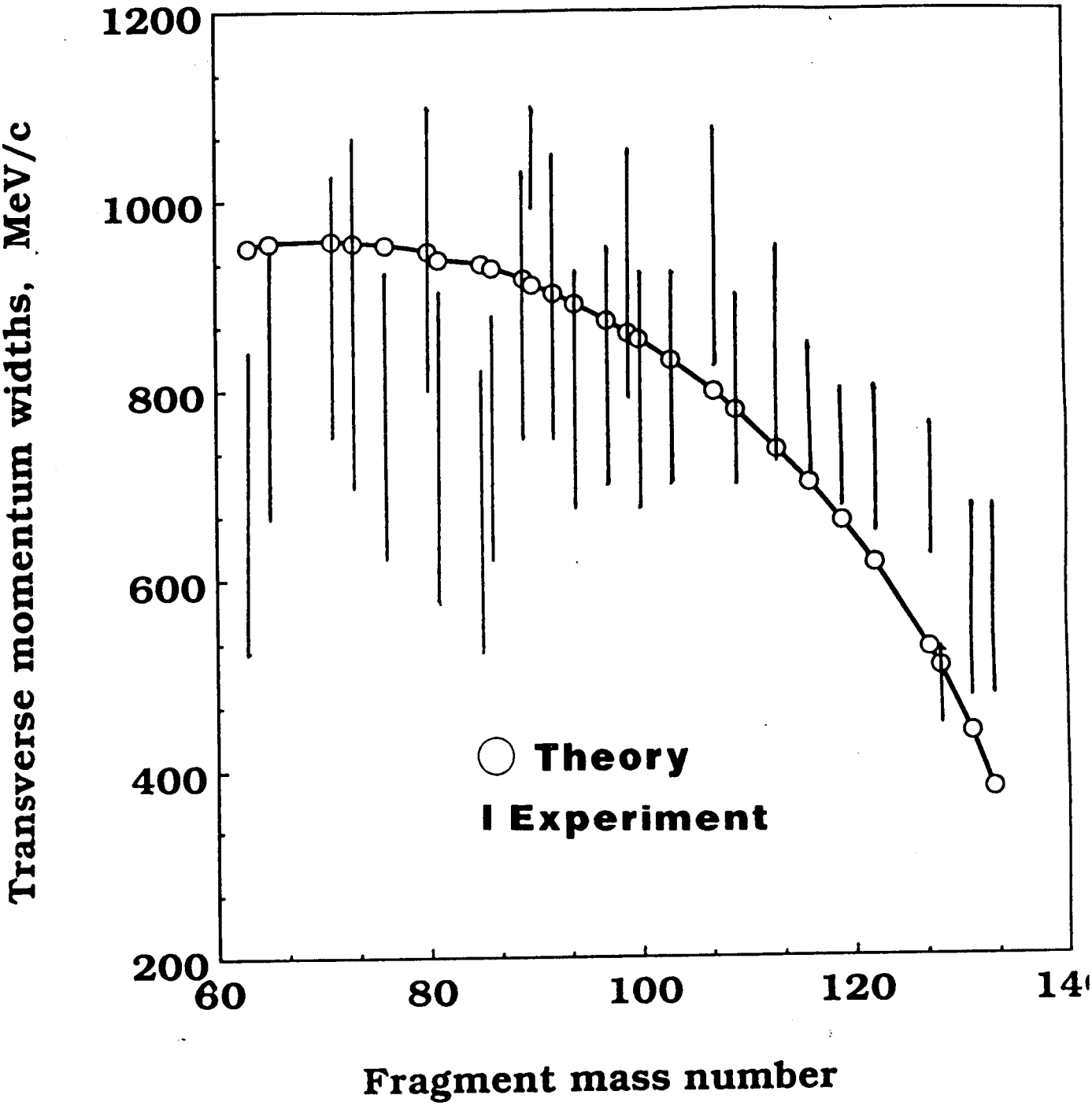

Khan/Khandelwal/Townsend/Wilson/Norbury

"An Optical Model Description of Momentum...

Figure 3.

ELECTROMAGNETIC INTERACTIONS OF COSMIC RAYS WITH NUCLEI

by

John W. Norbury†
Department of Physics
Washington State University
Pullman, WA 99164-2814

Subject Headings: cosmic rays

†This work was supported in part by NASA grant NAG-1-797

ABSTRACT

Parameterizations of single nucleon emission from the electromagnetic interactions of cosmic rays with nuclei are presented. These parameterizations are based upon the most accurate theoretical calculations available today. When coupled with Strong interaction parameterizations, they should be very suitable for use in cosmic ray propagation through interstellar space, the Earth's atmosphere, lunar samples, meteorites and spacecraft walls.

Introduction

Galactic cosmic rays are very high energy particles confined to the region of our Milky Way galaxy. They consist of about 98% bare nuclei (stripped of all electrons) and about 2% electrons and protons (Simpson 1983). Of the nuclear component about 87% is hydrogen, about 12% is helium and the other 1% consists of heavier nuclei. Fe is the most abundant of these nuclei with a typical energy of about 1 GeV/N. Even though these heavy nuclei are not very abundant, they are very penetrating due to their large mass and high speed.

An understanding of the interactions of galactic cosmic ray nuclei is important for several reasons:

1) Knowledge of the cosmic ray spectrum at the top of the Earth's atmosphere and knowledge of the composition of the interstellar medium enables us to determine the cosmic ray spectrum at the source (Simpson 1983).

2) Knowledge of the spectrum at the surface of the Earth and knowledge of the composition of the Earth's atmosphere enables us to determine the cosmic ray spectrum at the top of the atmosphere (Wilson, Townsend and Badavi 1987).

3) The radiation environment inside a spacecraft, due to solar and galactic cosmic rays may be determined (Wilson and Townsend 1988).

4) Studies of the history of extraterrestrial matter (such as lunar samples, meteorites and cosmic spherules and dust found in deep sea sediments) and also of the history of cosmic rays themselves can be made with knowledge of the production rate of various nuclides (Reedy 1987; Reedy, Arnold and Lal 1983).

The basic nucleus-nucleus interaction that a cosmic ray undergoes can occur mainly via the Strong or Electromagnetic force. Strong interaction processes (Gyulassy 1981) have been studied extensively and quite recently the study of Electromagnetic processes in high energy nuclear collisions has begun (Bertulani and Baur 1988).

In order to study the propagation of cosmic rays through interstellar space, the Earth's atmosphere or a spacecraft wall it is not enough to have only a good understanding of the nucleus-

nucleus interaction mechanism. One must have an accurate theory of transport as well. Generally one uses a nucleus-nucleus interaction cross section as input to a transport computer code. These codes however can be very complex and therefore require simple expressions for the cross sections rather than the use of data bases or complicated theoretical expressions (Wilson and Townsend 1988). Thus there has been a considerable effort to parameterize the cross section expressions so that the only required inputs are the nuclear energies and charge and mass numbers (Letaw, Silberberg and Tsao 1983; Silberberg and Tsao 1973; Townsend and Wilson 1986; Norbury, Cucinotta, Townsend and Wilson 1988; Wilson, Townsend and Badavi 1987).

One approach to the parameterization of cross sections is to simply take all the available experimental data and fit a curve through it (Letaw, Silberberg and Tsao 1983; Silberberg and Tsao 1973). Such an approach has certainly been useful and successful, but a much more satisfying parameterization would be one tied more directly to theory. It is the aim of the present work to obtain such a parameterization for the Electromagnetic (EM) part of the nucleus-nucleus interaction. One can then couple this with a similar theoretical parameterization of the Strong interaction process (Wilson, Townsend and Badavi 1987) to obtain a complete theoretical parameterization of the complete cross section.

A preliminary parameterization of the EM process has already been presented (Norbury, Cucinotta, Townsend and Badavi 1988), which utilizes the Weizsäcker-Williams (WW) method of virtual quanta (Bertulani and Baur 1988; Jackson 1975). However, since then the theory has been improved to include the effects of both electric dipole (E1) and electric quadrupole (E2) interactions (Bertulani and Baur 1988; Norbury 1989a), which will henceforth be referred to as multipole theory in contrast to WW theory. These E1 and E2 effects modify the parameterization considerably. Also in the present work several different parameterizations are presented differing in degree of complexity. In addition much more data has become available with which to compare the parameterizations (Heckman and Lindstrom 1976; Olson, Berman, Greiner, Heckman, Lindstrom, Westfall and Crawford 1981; Mercier, Hill, Wohn, McCullough, Nieland, Winger, Howard, Renwick, Matheis and Smith 1986; Hill, Wohn, Winger and Smith 1988; Smith, Hill,

Winger and Karol 1988; Hill, Wohn, Winger, Khayat, Leininger and Smith 1988; Hill, Wohn, Winger, Khayat, Mercier and Smith 1989; Norbury 1989b; Hill and Wohn 1989). The parameterizations to be presented below can then be combined with Strong interaction parameterizations such as the excellent parameterization by Wilson, Townsend and Badavi (1987). This combination should provide for much more accurate models of cosmic ray propagation through interstellar space, the Earth's atmosphere and spacecraft walls.

The present work will only consider single nucleon emission from cosmic ray nuclei. This has been shown to be the dominant electromagnetic process. Other particle emission processes such as two-neutron emission have much smaller probability (Hill, Wohn, Winger, Khayat, Mercier and Smith 1989), and will be studied in future work.

ELECTROMAGNETIC THEORY

The EM theory has already been discussed extensively (Bertulani and Baur 1988; Norbury 1989a) and only a few relevant details will be given here. The total nucleus-nucleus EM cross section is written as

$$\sigma = \sigma_{E1} + \sigma_{E2}$$
$$= \int [N_{E1}(E)\,\sigma_{E1}(E) + N_{E2}(E)\,\sigma_{E2}(E)]\,dE \quad (1)$$

where $N_{E1}(E)$ is the virtual photon spectrum (of energy E) of a particular multipolarity due to the projectile nucleus and $\sigma_{E1}(E) + \sigma_{E2}(E)$ is the photonuclear reaction cross section of the target nucleus. (In principle the above equation should include other EM multipoles, but their effect is much less important.) A less exact expression is given by WW theory as

$$\sigma_{WW}(E) = \int N_{WW}(E)\,[\sigma_{E1}(E) + \sigma_{E2}(E)]\,dE \quad (2)$$

where $N_{WW}(E)$ is the WW virtual photon spectrum. Bertulani and Baur (1988) have shown that

$$N_{WW}(E) = N_{E1}(E) = \frac{1}{E}\frac{2}{\pi} Z^2 \alpha \frac{1}{\beta^2}\left[\xi K_0 K_1 - \frac{1}{2}\xi^2 \beta^2 (K_1^2 - K_0^2)\right] \quad (3a)$$

$$N_{E2}(E) = \frac{1}{E}\frac{2}{\pi} Z^2 \alpha \frac{1}{\beta^4}\left[2(1-\beta^2)K_1^2 + \xi(2-\beta^2)^2 K_0 K_1 - \frac{1}{2}\xi^2 \beta^4 (K_1^2 - K_0^2)\right] \quad (3b)$$

with

$$\xi = \frac{E b_{min}}{\gamma \beta (\hbar c)} \quad (4)$$

where all of the Bessel functions K are functions of ξ. In the above equation E is the virtual photon energy, Z is the nuclear charge, α is the EM fine structure content, and b_{min} is the minimum impact parameter, below which the collision occurs via the Strong interaction. Also

$\beta = \frac{v}{c}$ and $\gamma = \frac{1}{\sqrt{1-\beta^2}}$ where c is the speed of light and v is the speed of the cosmic ray.

The minimum impact parameter is given by

$$b_{min} = R_{0\cdot1}(T) + R_{0\cdot1}(P) - d \tag{5a}$$

where $R_{0\cdot1}$ are the 10 per cent charge density radii of the projectile and target and d is an adjustable overlap parameter. An excellent approximation to $R_{0\cdot1}$ is (Norbury, Cucinotta, Townsend and Badavi 1988).

$$R_{0\cdot1} = (1.18\, A^{1/3} + 0.75)\ \text{fm} \tag{5b}$$

where A is the nuclear mass number.

Jackson has provided high and low virtual photon energy approximations as

$$N_{WW}(E) \approx \frac{1}{E}\frac{2}{\pi} Z^2 \alpha \frac{1}{\beta^2}\left[\ln\left(\frac{1.123}{\xi}\right) - \frac{1}{2}\beta^2\right] \tag{6a}$$

for small ξ, and

$$N_{WW}(E) \approx \frac{1}{E} Z^2 \alpha \frac{1}{\beta^2}\left(1 - \frac{1}{2}\beta^2\right)\exp(-2\xi) \tag{6b}$$

for large ξ.

In equation (1) the E1 photonuclear cross section can be written in terms of the electric giant dipole resonance (GDR) cross section as

$$\sigma_{E1}(E) = \frac{\sigma_m}{1 + [(E^2 - E_{GDR}^2)^2/E^2\Gamma_{GDR}^2]} \tag{7}$$

where E_{GDR} is the energy of the peak in the GDR cross section, Γ_{GDR} is the width of GDR, and

$$\sigma_m = \frac{\sigma_{TRK}}{\pi\Gamma_{GDR}/2} \tag{8}$$

with the Thomas-Reiche-Kuhn cross section (Levinger 1960) given by

$$\sigma_{TRK} = \frac{60NZ}{A}\ \text{MeV mb} \tag{9}$$

where N and A are the neutron and mass numbers. The GDR energy is given by (Westfall, Wilson, Lindstrom, Crawford, Greiner and Heckman 1979)

$$E_{GDR} = \hbar c\left[\frac{m^* c^2 R_0^2}{8J}\left(1 + u - \frac{1 + \varepsilon + 3u}{1 + \varepsilon + u}\varepsilon\right)\right]^{-1/2} \tag{10}$$

with

$$u = \frac{3J}{Q'} A^{-1/3} \tag{11}$$

and

$$R_0 = r_0 A^{1/3} \tag{12}$$

where $\varepsilon = 0.0768$, $Q' = 17$ MeV, $J = 36.8$ MeV, $r_0 = 1.18$ fm, and m^* is 7/10 of the nucleon mass. Note that other expressions for E_{GDR} such as $80A^{-1/3}$ (Bertulani and Baur 1988) provide very inaccurate results for light nuclei. Equation (10) is accurate for all mass regions.

The E2 cross section is dominated by the giant quadrupole resonance (GQR). The main contribution to single nucleon emission (Bertulani and Baur 1988) comes from the isoscalar component given by (Bertrand 1976)

$$\sigma_{E2}(E) = \frac{\sigma_{EWSR} E^2}{1 + (E^2 - E_{GQR}^2)^2 / E^2 \Gamma^2_{GQR}} \tag{13a}$$

with the energy-weighted sum rule (EWSR) cross section

$$\sigma_{EWSR} = f \frac{0.22\ ZA^{2/3}\ \mu b\ MeV^{-1}}{\pi\ \Gamma_{GQR}/2} \tag{13b}$$

where f is the fractional exhaustion of the EWSR (Bertrand 1976) and

$$E_{GQR} = \frac{63}{A^{1/3}} \tag{14}$$

Finally, all of the above cross sections refer to total absorption cross sections. To obtain the reaction for proton or neutron emission they must be multiplied by the proton or neutron branching ratios. The proton branching ratio has been parameterized by Westfall et al (Westfall, Wilson, Lindstrom, Crawford, Greiner and Heckman 1979) as

$$g_p = \text{Min}\,[Z/A,\ 1.95 \exp(-0.075\ Z)] \tag{15a}$$

where Z is the number of protons and the minimum value of the two quantities in square brackets is to be taken. Assuming that only single nucleon emission occurs, the neutron branching ratio is

$$g_n = 1 - g_p \tag{15b}$$

Comparison Between Theory and Experiment

In the above paragraphs I have provided the basic equations to be used in the present work. However in analyzing the validity of the basic EM theory one uses only equations (3) - (5) and instead of equations (7) - (15) one uses actual experimental data for the photonuclear cross sections. A detailed study of the validity of this EM theory has been made (Norbury 1989a, b, c, d) and the results from this work are presented in Table 1, both for the WW theory and the separate E1 and E2 multipole theory calculations, and are compared to experimental data. A detailed discussion is to be found in Norbury 1989a, b, c, d, but the following features are to be noticed. Both WW and multipole theory give reasonably good results although multipole theory is somewhat better. It is found that electric quadrupole (E2) effects are not significant for proton and neutron emission from ^{12}C, ^{16}O or ^{18}O. However, E2 contributions are substantial for neutron emission from ^{59}Co, ^{89}Y and ^{197}Au, generally leading to improved agreement between theory and experiment. Notable disagreements occur for ^{139}La projectiles (1.26 GeV/N) where the theoretical $\sigma_{E1} + \sigma_{E2}$ are too big. Quadrupole effects improve the theoretical results for ^{16}O projectiles at 60 and 200 GeV/N, although the theoretical cross sections are still too small. In general it has been found (Norbury 1989a, d) that electric quadrupole effects are an important component in nucleus-nucleus collisions and that these effects can be calculated accurately.

Parameterizations

As mentioned above in testing the basic WW and multipole EM theory one uses experimental data for the photonuclear cross sections. However this is not a practical procedure for use in cosmic ray transport codes and instead my approach will be to use expressions (7) - (15).

In the present work I shall discuss three separate parameterizations of the above EM theory for use in cosmic ray transport codes. These will be presented in decreasing order of accuracy, but the aim is to provide parameterizations that will be useful in different contexts.

Parameterization #1 of Multipole Theory

This is the most accurate parameterization and uses the following equations:

1) Equation (1) is used for the total nucleus-nucleus EM cross section. The integration is done numerically using the Trapezoidal Rule.

2) Equations (3) are used for the virtual photon spectra N_{E1} (E) and N_{E2} (E).

3) Equations (5) are used for the minimum impact parameter with the overlap parameter adjusted to give the best fit to data at d = -1.5 fm.

4) Equations (7) - (14) are used for the photonuclear cross sections.

5) The width Γ_{GDR} in equations (7) and (8) is set at

$$\begin{aligned} \Gamma_{GDR} &= 10 \text{ MeV} \quad \text{for} \quad A < 50 \\ &= 4.5 \text{ MeV} \quad \text{for} \quad A \geq 50 \end{aligned} \tag{16}$$

and Γ_{GQR} in equations (13) is set at

$$\begin{aligned} \Gamma_{GQR} &= 2.5 \text{ MeV} \quad \text{for} \quad A > 180 \\ &= 4.5 \text{ MeV} \quad \text{for} \quad 70 < A \leq 180 \\ &= 5.5 \text{ MeV} \quad \text{for} \quad 19 < A \leq 70 \\ &= 3.0 \text{ MeV} \quad \text{for} \quad A \leq 19 \end{aligned} \tag{17}$$

These values for Γ_{GRD} are discussed in Norbury, Cucinotta, Townsend and Badavi (1988) and for Γ_{GQR} in Bertrand (1976).

6) The fractional exhaustion of the Energy-Weighted Sum Rule in equation (13b) is given by (Bertrand 1976)

$$\begin{aligned} f &= 0.9 \quad \text{for} \quad A > 100 \\ &= 0.6 \quad \text{for} \quad 40 < A \leq 100 \\ &= 0.3 \quad \text{for} \quad 40 \leq A \end{aligned} \tag{18}$$

7) The proton and neutron branching ratios are given by equations (15).

The results of the above parameterizations are given in Table 1. It can be seen that it agrees extremely well with the multipole theory. Thus I regard this parameterization #1 of the multipole theory as describing very accurately the most advanced state-of-the-art EM theory. Agreement between this parameterization and experiment is, of course, of the same quality as between the multipole theory and experiment.

Parameterization #1 of WW Theory

WW theory gives a simpler treatment of the virtual photon field and is included here for the sake of completeness. The only difference between parameterization #1 of WW theory and parameterization #1 of multipole theory is that equation (2) is used for the total cross section instead of equation (1). Results are listed in Table 1 and are fairly comparable to the parameterization #1 of the multipole theory.

Parameterization #2 of Multipole Theory

A difficulty that might occur in some cosmic ray transport theories is the necessity of having to do a numerical integration in equation (1) every time σ is to be evaluated. To get around this, parameterization #2 is based on the technique of Bertulani and Baur (1988). This involves taking $N_{Ei}(E)$ outside of the integral in equation (1) and evaluating $N_{E1}(E)$ at E_{GDR} (see equation 10) and $N_{E2}(E)$ at E_{GQR} (equation 14). The remaining integral is evaluated from sum rules. That is (Bertulani and Baur 1988), equation (1) becomes

$$\sigma \approx N_{E1}(E_{GDR}) \int \sigma_{E1}(E)\, dE + N_{E2}(E_{GQR})\, E_{GQR}^2 \int \frac{\sigma_{E2}(E)}{E^2} dE \qquad (19)$$

with the sum rules

$$\int \sigma_{E1}(E)\, dE \approx \frac{60\, NZ}{A} \text{ mb MeV} \qquad (20a)$$

and

$$\int \frac{\sigma_{E2}(E)}{E^2} dE \approx f \frac{0.22\, ZA^{2/3}}{1000} \text{ mb MeV}^{-1} \qquad (20b)$$

Bertulani and Baur (1988) claim that this is an accurate procedure. However, I found it necessary to change d to d = -2.4 fm (see equation 5a) in order to give good comparison to experiment.

In the present parameterization #2 of multipole theory items 1) - 3) of parameterization #1 were changed to those discussed in the preceding paragraph. Note especially that a numerical integration is no longer necessary. Items 4) - 5) are no longer relevant. Items 6) - 7) remained the same. Results are again listed in Table 1. With the new value of d = -2.4 fm parameterization #2 agrees well with parameterization #1 (which used d = -1.5 fm).

Parameterization #2 of WW Theory

WW theory is again included for completeness. In this case equation (2) was replaced with

$$\sigma_{WW} \approx N_{WW}(E_{GDR}) \int \sigma_{E1}(E)\, dE + N_{WW}(E_{GQR})\, E_{GQR}^2 \int \frac{\sigma_{E2}(E)}{E^2} dE \qquad (21)$$

with the same sum rules in equations (20). Results are listed in Table 1.

Parameterization #3

Parameterizations #1 and #2 require the evaluation of Bessel functions as indicated in equations (3) for the virtual photon spectra. In the interest of providing an even simpler parameterization that could be used on a pocket calculator for rough estimates of the cross section, a third parameterization is presented. The E2 cross section was ignored and equations (1) or (2) were replaced with

$$\sigma \approx N_{WW}(E_{GDR}) \int \sigma_{E1}(E)\, dE \qquad (22)$$

Note that this is identical to neglecting the GQR in equation (1). The sum rule in equation (20a) was used for the integral. $N_{WW}(E_{GDR})$ was evaluated using equations (6), with (6a) used for $\xi \leq 0.5$ and (6b) for $\xi > 0.5$. This prescription avoids the evaluation of Bessel functions and almost allows one to calculate σ in one's head. In this case the value of d was d = +1.0 fm. Items 4) - 6) are not relevant and item 7) was again used. The results are presented in Table 1 and are seen to give surprisingly similar results to the other parameterizations.

Conclusion and Recommendations

As discussed in previous work (Norbury 1989a, d) the multipole theory is generally more accurate than WW theory. This is also true for the above parametrizations as can be seen from Table 1.

However, WW theory and multipole theory do not describe ^{18}O very well, and the parameterizations are even worse. I trace this to the fact that the branching ratio equations (15) do not work well for nuclei off the stability curve.

Both WW theory and multipole theory do not describe ^{197}Au very well either, but the parameterizations do a somewhat better job due to the choice of the overlap parameter d. There seems to be a problem also for very high energies especially 200 GeV/N.

Apart from these problems the multipole theory and multipole parameterizations (#1, #2 and #3) seem to describe the data quite accurately.

As regards which parameterization to use, they all seem to do an equivalent job in describing the data. This of course is because a different value for d was chosen for each. Even the parameterization #3 does quite well, although it is a little high for nucleon emission from the lighter nuclei.

Given the above problems with ^{18}O, ^{197}Au and 200 GeV/N I recommend that the above parameterizations be used [i] only with nuclei on the stability curve, [ii] for nuclei lighter than ^{197}Au and [iii] for energies less than 10 GeV/N. These requirements should not be too restrictive in Cosmic Ray work because most nuclei have energies of around 1 GeV/N and the most abundant nuclei are not much heavier that ^{56}Fe (Simpson 1983). Having to deal only with nuclei on the stability curve is probably the most severe restriction.

Parameterizations #1, #2, #3 decrease in order of accuracy, but, as discussed above, not by very much. I would recommend using the most accurate parameterization (#1), but if one's computer codes are such that it would save CPU time by using either #2 or #3, then I would recommend their use. However, one should perhaps be careful about using parameterization #3

for light nuclei. I recommend the multipole parameterizations, but I do not recommend the use of the WW parameterizations.

Finally, by combining the above EM parameterizations with the Strong Interaction parameterization of Wilson, Townsend and Badavi (1987), which is not subject to the same restrictions as above, transport of cosmic rays through matter can be described very accurately. Future work will involve parameterization of both multiple nucleon emission (a much smaller effect) and also neutron branching ratios for nuclei off the stability curve.

Acknowledgements

I wish to thank Frank Cucinotta, Larry Townsend and John Wilson for reviewing the paper and Gayle Norbury for checking the computer programs.

References

Bertrand, F. E. 1976, Ann. Rev. Nucl. Sci., 26, 457.

Bertulani, C. A., and Baur, G. 1988, Phys. Rep., 163, 299.

Gyulassy, M. 1981, Nucl. Phys. A 354, 395.

Heckman, H. H., and Lindstrom, P. J. 1976, Phys. Rev. Lett. 37, 56.

Hill, J. C., Wohn, F. K., Winger, J. A., and Smith, A. R. 1988, Phys. Rev. Lett., 60, 999.

Hill, J. C., Wohn, F. K., Winger, J. A., Khayat, M., Leininger, K., and Smith, A. R. 1988, Phys. Rev. C 38, 1722.

Hill, J. C., and Wohn, F. K. 1989, Phys. Rev. C 39, 2474.

Hill, J. C., Wohn, F. K., Winger, J. A., Khayat, M., Mercier, M. T., and Smith, A. R. 1989, Phys. Rev. C 39, 524.

Jackson, J. D. 1975, *Classical Electrodynamics*, Wiley, New York.

Letaw, J. R., Silberberg, R., and Tsao, C. H. 1983, Astrophys. J. Suppl., 51, 271.

Levinger, J. S. 1960, *Nuclear Photo-Disintegration*, Oxford University Press, London.

Mercier, M. T., Hill, J. C., Wohn, F. K., McCullough, C. M., Nieland, M. E., Winger, J. A., Howard, C. B., Renwick, S., Matheis, D. K., and Smith, A. R. 1986, Phys. Rev. C 33, 1655.

Norbury, J. W. 1989a, *Electric Quadrupole Excitations in the Interactions of ^{89}Y with Relativistic Nuclei*, Phys. Rev. C (in press).

Norbury, J. W. 1989b, Phys. Rev. C 39, 2472.

Norbury, J. W. 1989c, *Nucleon Emission via Electromagnetic Excitation in Relativistic Nucleus-Nucleus Collisions: Re-Analysis of the Weizsäcker-Williams Method*, Phys. Rev. C (in press).

Norbury, J. W. 1989d, *Electric Quadrupole Excitations in Relativistic Nucleus-Nucleus Collisions*, submitted to Phys. Rev. C.

Norbury, J. W., Cucinotta, F. A., Townsend, L. W., and Badavi, F. F. 1988, Nucl. Inst. Meth. Phys. Res. B 31, 535.

Olson, D. L., Berman, B. L., Greiner, D. E., Heckman, H. H., Lindstrom, P. J., Westfall, G. D., and Crawford, H. J. 1981, Phys. Rev. C 24, 1529.

Reedy, R.C. 1987, Nucl. Inst. Meth. Phys. Res. B 29, 251.

Reedy, R.C., Arnold, J.R., and Lal, D. 1983, Ann. Rev. Nucl. Part. Sci. 33, 503.

Silberberg, R., and Tsao, C. H. 1973, Astrophys. J., 25, 315, 335.

Simpson, J. A. 1983, Ann. Rev. Nucl. Part. Sci., 33, 323.

Smith, A. R., Hill, J. C., Winger, J. A., and Karol, P. J. 1988, Phys. Rev. C 38, 210.

Townsend, L. W., and Wilson, J. W. 1986, Radiation Research, 106, 283.

Westfall, G. D., Wilson, L. W., Lindstrom, P. J., Crawford, H. J., Greiner, D. E., and Heckman, H. H. 1979, Phys. Rev. C 19, 1309.

Wilson, J. W., and Townsend, L. W. 1988, Radiation Research, 114, 201.

Wilson, J. W., Townsend, L. W. , and Badavi, F. F. 1987, Radiation Research, 109, 173.

Wilson, J.W., Townsend, L.W., and Badavi, F.F. 1987, Nucl. Inst. Meth. Phys. Res. B 18, 225.

Table 1 Theoretical (Norbury 1989 a, c, d), Parameterized (this work) and Experimental (Heckman and Lindstrom 1976, Olson et al. 1981, Mercier et al. 1986, Smith et al. 1988, Hill et al. 1988, 1989) EM Cross Sections, all in units of milli-barn (mb).

Projectile	Target	Energy (GeV/N)	Final State	σ_{expt}	σ_{WW} (theory)	σ_{E1} (theory)	σ_{E2} (theory)	$\sigma_{E1} + \sigma_{E2}$ (theory)	Parameterization #1 d = - 1.5 fm		Parameterization #2 d = - 2.4 fm		Parameterization #3 d = +1.0 fm
									σ_{WW}	$\sigma_{E1} + \sigma_{E2}$	σ_{WW}	$\sigma_{E1} + \sigma_{E2}$	σ
^{12}C	Pb	2.1	^{11}C	51±18	47	46	2	48	59	59	56	57	62
"	"	"	^{11}B	50±25	68	68	2	70	59	59	56	57	62
"	"	1.05	^{11}C	39±24	28	28	1	29	35	36	29	30	33
"	"	"	^{11}B	50±25	42	42	1	43	35	36	29	30	33
^{16}O	"	2.1	^{15}O	50±24	59	58	2	60	87	88	84	85	93
"	"	"	^{15}N	96±26	111	110	4	114	87	88	84	85	93
^{12}C	Ag	"	^{11}C	21±10	18	18	0	18	22	22	21	22	26
"	"	"	^{11}B	18±13	26	26	1	27	22	22	21	22	26
"	"	1.05	^{11}C	21±10	12	11	1	12	14	14	12	12	13
"	"	"	^{11}B	25±19	17	17	1	18	14	14	12	12	13
^{16}O	"	2.1	^{15}O	26±13	23	22	1	23	32	32	32	32	39
"	"	"	^{15}N	30±16	42	42	1	43	32	32	32	32	39

Table 1 (cont.)

Projectile	Target	Energy (GeV/N)	Final State	σ_{expt}	σ_{WW} (theory)	σ_{E1} (theory)	σ_{E2} (theory)	$\sigma_{E1} + \sigma_{E2}$ (theory)	Parameterization #1 d = - 1.5 fm		Parameterization #2 d = - 2.4 fm		Parameterization #3 d = +1.0 fm
									σ_{WW}	$\sigma_{E1} + \sigma_{E2}$	σ_{WW}	$\sigma_{E1} + \sigma_{E2}$	σ
^{12}C	Cu	2.1	^{11}C	10±7	8	8	0	8	9	9	9	9	12
"	"	"	^{11}B	4±8	11	11	0	11	9	9	9	9	12
"	"	1.05	^{11}C	9±8	5	5	0	5	6	6	5	5	6
"	"	"	^{11}B	5±8	8	8	0	8	6	6	5	5	6
^{16}O	"	2.1	^{15}O	9±8	10	10	0	10	13	14	13	13	17
"	"	"	^{15}N	15±8	18	17	1	18	13	14	13	13	17
^{12}C	Al	"	^{11}C	0±5	2	2	0	2	2	2	2	2	3
"	"	"	^{11}B	0±5	3	3	0	3	2	2	2	2	3
"	"	1.05	^{11}C	1±6	1	1	0	1	1	1	1	1	2
"	"	"	^{11}B	1±7	2	2	0	2	1	1	1	1	2
^{16}O	"	2.1	^{15}O	0±5	2	2	0	2	3	3	3	3	4
"	"	"	^{15}N	-1±9	4	4	0	4	3	3	3	3	4
^{12}C	C	"	^{11}C	-2±5	0.4	0.4	0	0.4	0.5	0.5	0.5	0.5	0.7
"	"	"	^{11}B	-1±4	0.6	0.6	0	0.6	0.5	0.5	0.5	0.5	0.7
"	"	1.05	^{11}C	-2±5	0.3	0.3	0	0.3	0.3	0.4	0.3	0.3	0.5
"	"	"	^{11}B	-2±5	0.5	0.5	0	0.5	0.3	0.4	0.3	0.3	0.5

Table 1 (cont.)

Projectile	Target	Energy (GeV/N)	Final State	σ_{expt}	σ_{WW} (theory)	σ_{E1} (theory)	σ_{E2} (theory)	$\sigma_{E1} + \sigma_{E2}$ (theory)	Parameterization #1 d = - 1.5 fm		Parameterization #2 d = - 2.4 fm		Parameterization #3 d = +1.0 fm
									σ_{WW}	$\sigma_{E1} + \sigma_{E2}$	σ_{WW}	$\sigma_{E1} + \sigma_{E2}$	σ
^{16}O	C	2.1	^{15}O	-1±4	0.5	0.5	0	0.5	0.7	0.7	0.7	0.7	1
"	"	"	^{15}N	-1±4	1	1	0	1	0.7	0.7	0.7	0.7	1
^{18}O	Ti	1.7	^{17}O	8.7±2.7	15	15	0	15	9	9	9	9	11
"	"	"	^{17}N	-0.5±1.0	3	3	0	3	7	7	7	7	9
"	Pb	"	^{17}O	136±2.9	155	154	4	158	96	98	91	92	93
"	"	"	^{17}N	20.2±1.8	28	27	2	29	77	78	73	74	74
"	U	"	^{17}O	140.8±4.1	191	189	5	194	117	119	110	112	108
"	"	"	^{17}N	25.1±1.6	34	33	3	36	94	95	88	89	87

Table 1 (cont.)

Projectile	Target	Energy (GeV/N)	Final State	σ_{expt}	σ_{WW} (theory)	σ_{E1} (theory)	σ_{E2} (theory)	$\sigma_{E1} + \sigma_{E2}$ (theory)	Parameterization #1 d = - 1.5 fm		Parameterization #2 d = - 2.4 fm		Parameterization #3 d = +1.0 fm
									σ_{WW}	$\sigma_{E1} + \sigma_{E2}$	σ_{WW}	$\sigma_{E1} + \sigma_{E2}$	σ
^{12}C	^{197}Au	2.1	^{196}Au	75±14	38	37	6	43	36	41	37	41	43
^{20}Ne	"	"	"	153±18	100	97	16	113	98	108	99	110	116
^{40}Ar	"	1.8	"	348±34	289	278	48	326	279	310	281	311	321
^{56}Fe	"	1.7	"	601±54	565	545	93	638	547	609	549	609	617
^{139}La	"	1.26	"	1970±130	2076	2001	367	2368	2018	2272	1966	2213	1979
^{16}O	"	60	"	280±30	215	207	15	222	223	229	241	247	252
"	"	200	"	440±40	278	268	17	285	291	297	316	322	325

Table 1 (cont.)

Projectile	Target	Energy (GeV/N)	Final State	σ_{expt} (mb)	σ_{WW} (theory)	σ_{E1} (theory)	σ_{E2} (theory)	$\sigma_{E1} + \sigma_{E2}$ (theory)	Parameterization #1 d = - 1.5 fm		Parameterization #2 d = - 2.4 fm		Parameterization #3 d = +1.0 fm
									σ_{WW}	$\sigma_{E1} + \sigma_{E2}$	σ_{WW}	$\sigma_{E1} + \sigma_{E2}$	σ
^{12}C	^{89}Y†	2.1	^{88}Y	9±12	12	12	1	13	12	13	12	13	15
^{20}Ne	"	"	"	43±12	32	31	3	34	32	34	32	34	39
^{40}Ar	"	1.8	"	132±17	90	88	9	97	90	95	89	94	106
^{56}Fe	"	1.7	"	217±20	175	171	16	187	175	186	172	182	202

Table 1 (cont.)

Projectile	Target	Energy (GeV/N)	Final State	σ_{expt} (mb)	σ_{WW} (theory)	σ_{E1} (theory)	σ_{E2} (theory)	$\sigma_{E1} + \sigma_{E2}$ (theory)	Parameterization #1 d = - 1.5 fm		Parameterization #2 d = - 2.4 fm		Parameterization #3 d = +1.0 fm
									σ_{WW}	$\sigma_{E1} + \sigma_{E2}$	σ_{WW}	$\sigma_{E1} + \sigma_{E2}$	σ
^{12}C	^{59}Co	2.1	^{58}Co	6±9	7	7	0	7	6	6	6	6	7
^{20}Ne	"	"	"	32±11	18	18	1	19	16	17	15	16	19
^{56}Fe	"	1.7	"	88±14	98	96	7	103	85	89	82	87	99
^{139}La	"	1.26	"	280±40	339	333	24	357	297	313	277	294	281

ELECTRIC QUADRUPOLE EXCITATIONS IN RELATIVISTIC NUCLEUS-NUCLEUS COLLISIONS

by

John W. Norbury †
Physics Department
Washington State University
Pullman, WA

PACS: 25.70. Np

† This work was supported in part by NASA grant NAG-1-797.

Abstract

Calculations are presented for electric quadrupole excitations in relativistic nucleus-nucleus collisions. The theoretical results are compared to an extensive data set and it is found that electric quadrupole effects provide substantial corrections to cross sections, especially for heavier nuclei.

1. INTRODUCTION

The search for a fundamentally new state of matter in the form of a Quark-Gluon Plasma [1] has stimulated the production of very high energy nuclear beams. The hope is to observe the Quark-Gluon Plasma in a relativistic nucleus-nucleus collision. At the Berkeley Bevalac a variety of light nuclei such as ^{12}C, ^{16}O and ^{20}Ne can be accelerated up to energies of 2.1 GeV/N and heavier nuclei such as ^{139}La and ^{238}U can be accelerated to 1.26 and 0.96 GeV/N respectively. At Brookhaven, New York, ^{16}O beams are available at 14.6 GeV/N and at the CERN SPS, in Geneva, beams of ^{16}O and ^{32}S are both produced at 60 and 200 GeV/N. The Relativistic Heavy Ion Collider (RHIC) is expected to produce two colliding beams at 100 GeV/N to give a total center-of-mass energy of 200 GeV/N, which corresponds to a single beam energy of 21 TeV/N. Grabiak [2] has pointed out that nuclear beams of 3.5 TeV/N and 8 TeV/N may be possible at the CERN Large Hadron Collider (LHC) or the Superconducting Super Collider (SSC). By way of comparison, the majority of Galactic Cosmic Rays have energies [3] of about 1 GeV/N, with a range [3] typically from 10 MeV/N to 1 TeV/N. However, the JACEE collaboration [4] has made observations as high as 1000 TeV/N.

Nucleus-nucleus reactions proceed mainly through either the Strong or Electromagnetic (EM) interactions. Historically, Strong interaction processes have been the main object of study [5], however with the availability of the above high energy nuclear beams there has been a resurgence of interest in EM interactions in relativistic nucleus-nucleus collisions. [6]

The primary theoretical tool for studying these relativistic EM processes has been via the Weizsäcker-Williams (WW) method [6-7] of virtual quanta. The nucleus-nucleus total EM reaction cross section is

$$\sigma = \int N_{WW}(E_\gamma)\, \sigma(E_\gamma)\, dE_\gamma \qquad (1)$$

where E_γ is the virtual photon energy, $N_{WW}(E\gamma)$ is the WW virtual photon spectrum and $\sigma(E_\gamma)$ is the photonuclear reaction cross section. For high accuracy it is important to use experimental photonuclear data for $\sigma(E_\gamma)$. (For an excellent compilation of photoneutron

data see reference 8.) However, a more exact formulation of σ involves a breakdown into the various EM multipolarities such as electric dipole (E1), electric quadrupole (E2), magnetic dipole (M1) etc. The most important contributions to σ are from E1 and E2 so that

$$\sigma = \sigma_{E1} + \sigma_{E2}$$
$$= \int [N_{E1}(E_\gamma)\sigma_{E1}(E_\gamma) + N_{E2}(E_\gamma)\sigma_{E2}(E_\gamma)]\, dE_\gamma \qquad (2)$$

where $N_{Ei}(E_\gamma)$ is the virtual photon spectrum of a particular multipolarity due to the projectile nucleus and $\sigma_{Ei}(E_\gamma)$ is the photonuclear reaction cross section of the target nucleus. Bertulani and Baur [6] have derived expressions for $N_{Ei}(E_\gamma)$ and found that the electric dipole spectrum is the same as the WW spectrum, i.e. $N_{E1}(E_\gamma) = N_{ww}(E_\gamma)$. Furthermore at very high projectile energies <u>all</u> $N_{Ei}(E_\gamma)$ and $N_{Mi}(E_\gamma)$ are equal so that equation (1) is seen to be a very high energy approximation to all multipolarities included in equation (2). Bertulani and Baur [6] have made a crude estimate of the EM cross section using equation (2) but they pulled $N_{E1}(E_\gamma)$ and $N_{E2}(E_\gamma)$ outside the integral and evaluated them at a single energy and used sum rules to evaluate $\int \sigma_{Ei}(E_\gamma)\, dE_\gamma$. However, this procedure did not yield very accurate results. Thus I undertook a more exact study [9] leaving equation (2) as it stands, and using experimental data for the photonuclear cross sections by defining

$$\sigma_{E1}(E_\gamma) \equiv \sigma_{expt.}(E_\gamma) - \sigma_{E2}(E_\gamma) \qquad (3)$$

where $\sigma_{expt.}(E_\gamma)$ is the <u>experimentally</u> measured photonuclear cross section and $\sigma_{E2}(E_\gamma)$ is a <u>theoretical</u> calculation based on a Lorentzian shape for the Electric Giant Quadrupole Resonance (GQR). Details for this procedure can be found in reference 9. As was noted in that reference, the above procedure yields very accurate values for the sum $\sigma_{E1} + \sigma_{E2}$ (which is to be compared to nucleus-nucleus reaction experiments) even though the GQR parameters are uncertain. The basic reason for this, as can be seen from equation (3), is

that an under (over) estimate in σ_{E2} (E_γ) will give an over (under) estimate in σ_{E1} ($E\gamma$), so that the combined $\sigma_{E1} + \sigma_{E2}$ in equation (2) will not change very much.

In reference 9 a detailed study of E1 and E2 was undertaken for the reaction ^{89}Y (RHI, X) ^{88}Y where RHI refers to various Relativistic Heavy Ions and X is anything. It was found that E2 effects account for a considerable fraction of the cross section, and that inclusion of E2 (via equation 2) provides improved agreement with experiment over the WW method. Given this situation, it was decided to compare this theoretical approach to as much experimental data as possible. Thus the present work involves a comparison to neutron emission from ^{89}Y, ^{197}Au, ^{59}Co and neutron and proton emission from ^{12}C, ^{16}O and ^{18}O which includes both electric dipole and quadrupole effects. This complements earlier work [7] which involved an extensive comparison of WW theory to experiment.

CALCULATIONAL METHOD

The basic calculational method is outlined in reference 9 and the discussion will not be repeated here. Also reference 7 includes a very detailed summary of which photonuclear data were used for $\sigma_{expt.}$ ($E\gamma$) in equation (3). The same data is used in the present work. All isoscalar GQR parameters were taken from the compilation of Bertrand [10] and are listed in Table 1. As mentioned in the Introduction, even though these parameters are somewhat uncertain the total EM cross section $\sigma_{E1} + \sigma_{E2}$ is expected to be very accurate [9] due to the subtraction procedure of equation (3). The most inaccurate results would be expected for the ^{12}C, ^{16}O, ^{18}O GQR parameters where the isoscalar GQR is fragmented into several components [10]. Only a single Lorentzian [9] was

Table 1: Isoscalar Giant Quadrupole Resonance (GQR) Parameters taken from the compilation of Bertrand [10]. E is the GQR resonance excitation energy, Γ is the full-width at half maximum and f is the fractional depletion of the Energy Weighted Sum Rule. (The GQR of light nuclei are fragmented into several peaks, so that the parameters below represent an estimated average value.)

Nucleus	E (MeV)	Γ (MeV)	f
^{12}C	27.5[a]	3.0[b]	0.4[d]
^{16}O	22.0[b]	3.0[c]	0.4[d]
^{18}O	24.0[a]	3.0[c]	0.4[c]
^{59}Co	16.3[b]	5.6[b]	0.61[b]
^{89}Y	13.8[b]	3.2[b]	0.55[d]
^{197}Au	10.8[a]	2.9[b]	0.95[d]

[a] E is calculated from 63 $A^{-1/3}$

[b] best value taken from Table 4 of ref. 10

[c] estimate

[d] from Fig 23 of ref. 10

used in the present work. However σ_{E2} is found to be quite small for these nuclei (see below) so that my conclusion that the calculated $\sigma_{E1} + \sigma_{E2}$ is accurate remains valid.

For the nuclei ^{12}C, ^{16}O and ^{18}O, proton (p) emission occurs as well as neutron (n) emission. Thus equation (3) needs to be modified to incorporate the branching ratio. I assume that the excited nucleus decays only by proton or neutron emission and that the (photon) energy dependent neutron branching ratio is defined as

$$f_n(E_\gamma) \equiv \frac{\sigma_{expt.}(E_\gamma,n)}{\sigma_{expt.}(E_\gamma,n) + \sigma_{expt.}(E_\gamma,p)} \qquad (4)$$

so that

$$\sigma_{E2}(E_\gamma, n) = f_n(E_\gamma)\,\sigma_{E2}(E_\gamma) \quad (5)$$

where $\sigma_{E2}(E_\gamma)$ is the photonuclear GQR cross section. Thus for proton and neutron emission equation (3) becomes

$$\sigma_{E1}(E_\gamma, n) = \sigma_{expt.}(E\gamma, n) - f_n(E_\gamma)\,\sigma_{E2}(E_\gamma) \quad (6a)$$

and

$$\sigma_{E1}(E_\gamma, p) = \sigma_{expt.}(E\gamma, p) - [1 - f_n(E_\gamma)]\,\sigma_{E2}(E_\gamma) \quad (6b)$$

Equations (4) - (6) were used for nucleon emission from ^{12}C, ^{16}O and ^{18}O. For ^{59}Co, the (γ, p) cross section is not available and so a constant value of $f_n = 0.7$ (suggested from reference 11) was used. For ^{89}Y and ^{197}Au I used $f_n = 1.0$.

RESULTS AND DISCUSSION

The calculated results are listed in Table 2, along with the experimental results of various groups. [12-16] $\sigma_{E1} + \sigma_{E2}$ is the calculated result to be compared with the data $\sigma_{expt.}$ Also listed are the results of WW calculations.[7] In all cases two theoretical cross sections are listed. The first is calculated using an expression for the minimum impact parameter as

$$b_{min} = R_{0\cdot1}(T) + R_{0\cdot1}(P) \quad (7)$$

where $R_{0\cdot1}$ represents the 10-percent charge density radius [7] of the target or projectile. The second theoretical cross section listed in parentheses in Table 2 uses b_{min} given by Hill et al. [14-16] as

$$b_{min} = r_o\,[A_p^{1/3} + A_T^{1/3} - X(A_p^{-1/3} + A_T^{-1/3}] \quad (8)$$

where $r_o = 1.34$ fm and $X = 0.75$. (Note that my WW calculations disagree with earlier results of Hill et al. [14-16] due to an error in their calculations. [19-20])

There are several features readily apparent from Table 2;

(i) $\sigma_{E1} + \sigma_{E2}$ is <u>always</u> larger than σ_{WW}. However, for nucleon emission from ^{12}C, ^{16}O and ^{18}O this difference is never larger than about 4%, but for neutron emission from ^{59}Co, ^{89}Y and ^{197}Au the difference is much larger varying between about 7% - 15%.

ii) For nucleon emission from ^{12}C and ^{16}O both $\sigma_{E1} + \sigma_{E2}$ and σ_{WW} agree with experiment for both choices of b_{min}.

iii) For nucleon emission from ^{18}O both $\sigma_{E1} + \sigma_{E2}$ and σ_{WW} disagree with experiment for both choices of bmin. σ_{WW} actually gives slightly better agreement but not by a significant amount.

iv) For neutron emission from ^{197}Au, $\sigma_{E1} + \sigma_{E2}$ is significantly closer to experimental values than is σ_{WW}, although for most cases it still lies outside the error bars. An exception however is a much poorer agreement for ^{139}La (see also references 19 and 20). Significant discrepancies with ^{197}Au data have been noted previously for WW theory.[7]

v) For neutron emission from ^{89}Y, $\sigma_{E1} + \sigma_{E2}$ is in much better agreement with experiment than is σ_{WW}. This is especially true for the ^{40}Ar and ^{56}Fe projectiles.

vi) For ^{59}Co, $\sigma_{E1} + \sigma_{E2}$ is again better for ^{20}Ne, although slightly worse for ^{56}Fe. As above the agreement for the ^{139}La projectile is significantly poorer.

SUMMARY AND CONCLUSIONS

Calculations have been made for nucleon emission via EM dissociation in relativistic nucleus-nucleus collisions. Results are presented for Weizsäcker-Williams theory and also for separate electric dipole and quadrupole components. The theories have been compared to an extensive data set. It is found that electric quadrupole (E2) effects are not significant for proton and neutron emission from ^{12}C, ^{16}O or ^{18}O. However, E2 contributions are substantial for neutron emission from ^{59}Co, ^{89}Y and ^{197}Au, generally leading to improved agreement between theory and experiment. Notable disagreements occur for ^{139}La projectiles (1.26 GeV/N) where the theoretical $\sigma_{E1} + \sigma_{E2}$ are too big. Quadrupole effects improve the theoretical results for ^{16}O projectiles at 60 and 200 GeV/N, although the theoretical cross sections are still too small.

In general it has been found that electric quadrupole effects are an important component in nucleus-nucleus collisions and that these effects can be calculated accurately.

ACKNOWLEDGEMENTS

I wish to thank Larry Townsend for useful discussions and Gayle Norbury for help with the photonuclear data.

REFERENCES

1. K. Kajantie and L. McLerran, Ann. Rev. Nucl. Part. Sci. 37 293 (1987).
2. M. Grabiak, B. Muller, W. Greiner, G. Soff and P. Koch, J. Phys. G 15 L25 (1989).
3. J. A. Simpson, Ann. Rev. Nucl. Part. Sci. 33 323 (1983).
4. W. V. Jones, Y. Takahashi, B. Wosiek and O. Miyamura, Ann. Rev. Nucl. Part. Sci. 37 71 (1987).
5. W. G. Lynch, Ann. Rev. Nucl. Part. Sci. 37 493 (1987).
6. C. A. Bertulani and G. Baur, Phys. Rep. 163 299 (1988).
7. J. W. Norbury, "Nucleon Emission via Electromagnetic Excitation in Relativistic Nucleus-Nucleus Collisions: Re-analysis of the Weizsäcker-Williams Method" Phys. Rev. C (in press).
8. S. S. Dietrich and B. L. Berman, Atomic Data and Nuclear Data Tables 38 199 (1988).
9. J. W. Norbury, "Electric Quadrupole Excitations in the Interactions of ^{89}Y with Relativistic Nuclei," Phys. Rev. C (in press).
10. F. E. Bertrand, Ann. Rev. Nucl. Sci. 26 457 (1976).
11. J. W. Norbury, F. A. Cucinotta, L. W. Townsend and F. F. Badavi, Nucl. Inst. Meth. Phys. Res. B 31 535 (1988).
12. H. H. Heckman, and P. J. Lindstrom, Phys. Rev. Lett. 37, 56 (1976).
13. D. L. Olson, B. L. Berman, D. E. Greiner, H. H. Heckman, P. J. Lindstrom, G. D. Westfall, and H. J. Crawford, Phys. Rev. C 24, 1529 (1981).
14. M. T. Mercier, J. C. Hill, F. K. Wohn, C. M. McCullough, M. E. Nieland J. A. Winger, C. B. Howard, S. Renwick, D. K. Matheis and A. R. Smith, Phys. Rev. C 33 1655 (1986).
15. J. C. Hill, F. K. Wohn, J. A. Winger, and A. R. Smith, Phys. Rev. Lett. 60 999 (1988).
16. J. C. Hill, F. K. Wohn, J. A. Winger, M. Khayat, K. Leininger, and A. R. Smith, Phys. Rev. C 38 1722 (1988).
17. A Lepretre, H. Beil, R. Bergere, P. Carlos, A. Veyssiere and M. Sugawara, Nucl. Phys. A 175 609 (1971).
18. B. L. Berman, R. E. Pywell, S. S. Dietrich, M. N. Thompson, K. G. McNeill and J. W. Jury, Phys. Rev. C 36 1286 (1987).
19. J. W. Norbury, Phys. Rev. C 39 2472 (1989).
20. J. C. Hill and F. K. Wohn, Phys. Rev. C 39 2474 (1989).

Table 2 Calculated results, $\sigma_{E1} + \sigma_{E2}$ and σ_{WW}, compared to experiment. [12-16] Two theoretical cross sections are listed. The first set uses b_{min} given by equation (7) and the second set (in parentheses) uses b_{min} given by equation (8).

Projectile	$R_{0\text{-}1}$(P) (fm)	Target	$R_{0\text{-}1}$ (T) (fm)	Energy (GeV/N)	Final State	σ_{expt} (mb)	σ_{WW} (mb)	σ_{E1} (mb)	σ_{E2} (mb)	$\sigma_{E1} + \sigma_{E2}$ (mb)
^{12}C	3.30	Pb	7.83	2.1	^{11}C	51±18	47 (51)	46 (50)	2 (2)	48 (52)
"	"	"	"	"	^{11}B	50±25	68 (74)	68 (73)	2 (2)	70 (75)
"	"	"	"	1.05	^{11}C	39±24	28 (31)	28 (31)	1 (1)	29 (32)
"	"	"	"	"	^{11}B	50±25	42 (47)	42 (46)	1 (2)	43 (48)
^{16}O	3.68	"	"	2.1	^{15}O	50±24	59 (64)	58 (63)	2 (2)	60 (65)
"	"	"	"	"	^{15}N	96±26	111 (120)	110 (119)	4 (4)	114 (123)
^{12}C	3.30	Ag	6.37	"	^{11}C	21±10	18 (20)	18 (19)	0 (1)	18 (20)
"	"	"	"	"	^{11}B	18±13	26 (29)	26 (29)	1 (1)	27 (30)
"	"	"	"	1.05	^{11}C	21±10	12 (13)	11 (13)	1 (1)	12 (14)
"	"	"	"	"	^{11}B	25±19	17 (20)	17 (19)	1 (1)	18 (20)
^{16}O	3.68	"	"	2.1	^{15}O	26±13	23 (25)	22 (25)	1 (1)	23 (26)
"	"	"	"	"	^{15}N	30±16	42 (46)	42 (46)	1 (2)	43 (48)

Table 2 (cont.)

Projectile	$R_{0\cdot1}$(P) (fm)	Target	$R_{0\cdot1}$ (T) (fm)	Energy (GeV/N)	Final State	σ_{expt} (mb)	σ_{WW} (mb)	σ_{E1} (mb)	σ_{E2} (mb)	$\sigma_{E1} + \sigma_{E2}$ (mb)
^{12}C	3.30	Cu	5.45	2.1	^{11}C	10±7	8 (9)	8 (9)	0 (0)	8 (9)
"	"	"	"	"	^{11}B	4±8	11 (12)	11 (12)	0 (0)	11 (12)
"	"	"	"	1.05	^{11}C	9±8	5 (6)	5 (6)	0 (0)	5 (6)
"	"	"	"	"	^{11}B	5±8	8 (9)	8 (9)	0 (0)	8 (9)
^{16}O	3.68	"	"	2.1	^{15}O	9±8	10 (11)	10 (11)	0 (0)	10 (11)
"	"	"	"	"	^{15}N	15±8	18 (20)	17 (20)	1 (1)	18 (21)
^{12}C	3.30	Al	4.09	"	^{11}C	0±5	2 (2)	2 (2)	0 (0)	2 (2)
"	"	"	"	"	^{11}B	0±5	3 (3)	3 (3)	0 (0)	3 (3)
"	"	"	"	1.05	^{11}C	1±6	1 (2)	1 (2)	0 (0)	1 (2)
"	"	"	"	"	^{11}B	1±7	2 (2)	2 (2)	0 (0)	2 (2)
^{16}O	3.68	"	"	2.1	^{15}O	0±5	2 (3)	2 (3)	0 (0)	2 (3)
"	"	"	"	"	^{15}N	-1±9	4 (5)	4 (5)	0 (0)	4 (5)
^{12}C	3.30	C	3.30	"	^{11}C	-2±5	0.4 (0.5)	0.4 (0.5)	0 (0)	0.4 (0.5)
"	"	"	"	"	^{11}B	-1±4	0.6 (0.7)	0.6 (0.7)	0 (0)	0.6 (0.7)
"	"	"	"	1.05	^{11}C	-2±5	0.3 (0.4)	0.3 (0.4)	0 (0)	0.3 (0.4)
"	"	"	"	"	^{11}B	-2±5	0.5 (0.6)	0.5 (0.6)	0 (0)	0.5 (0.6)

Table 2 (cont.)

Projectile	$R_{0.1}$(P) (fm)	Target	$R_{0.1}$ (T) (fm)	Energy (GeV/N)	Final State	σ_{expt} (mb)	σ_{WW} (mb)	σ_{E1} (mb)	σ_{E2} (mb)	$\sigma_{E1} + \sigma_{E2}$ (mb)
^{16}O	3.68	C	3.30	2.1	^{15}O	-1±4	0.5 (0.6)	0.5 (0.6)	0 (0)	0.5 (0.6)
"	"	"	"	"	^{15}N	-1±4	1 (1)	1 (1)	0 (0)	1 (1)
^{18}O	3.78	Ti	5.00	1.7	^{17}O	8.7±2.7	15 (16)	15 (16)	0 (1)	15 (17)
"	"	"	"	"	^{17}N	-0.5±1.0	3 (3)	3 (3)	0 (0)	3 (3)
"	"	Pb	7.83	"	^{17}O	136±2.9	155 (165)	154 (164)	4 (4)	158 (168)
"	"	"	"	"	^{17}N	20.2±1.8	28 (31)	27 (30)	2 (2)	29 (32)
"	"	U	8.09	"	^{17}O	140.8±4.1	191 (202)	189 (200)	5 (5)	194 (205)
"	"	"	"	"	^{17}N	25.1±1.6	34 (37)	33 (36)	3 (3)	36 (39)

Table 2 (cont.)

Projectile	$R_{0\text{-}1}$(P) (fm)	Target	$R_{0\text{-}1}$ (T) (fm)	Energy (GeV/N)	Final State	σ_{expt} (mb)	σ_{WW} (mb)	σ_{E1} (mb)	σ_{E2} (mb)	$\sigma_{E1} + \sigma_{E2}$ (mb)
^{12}C	3.30	^{89}Y†	6.02	2.1	^{88}Y	9±12	12 (13)	12 (13)	1 (1)	13 (14)
^{20}Ne	4.00	"	"	"	"	43±12	32 (35)	31 (34)	3 (4)	34 (38)
^{40}Ar	4.72	"	"	1.8	"	132±17	90 (96)	88 (94)	9 (10)	97 (104)
^{56}Fe	5.24	"	"	1.7	"	217±20	175 (185)	171 (181)	16 (18)	187 (199)

Table 2 (cont.)

Projectile	$R_{0\cdot1}$(P) (fm)	Target	$R_{0\cdot1}$ (T) (fm)	Energy (GeV/N)	Final State	σ_{expt} (mb)	σ_{WW} (mb)	σ_{E1} (mb)	σ_{E2} (mb)	$\sigma_{E1} + \sigma_{E2}$ (mb)
^{12}C	3.30	^{59}Co	5.33	2.1	^{58}Co	6±9	7 (8)	7 (7)	0 (1)	7 (8)
^{20}Ne	4.00	"	"	"	"	32±11	18 (20)	18 (20)	1 (1)	19 (21)
^{56}Fe	5.24	"	"	1.7	"	88±14	98 (105)	96 (104)	7 (7)	103 (111)
^{139}La	6.89	"	"	1.26	"	280±40	339 (358)	333 (352)	24 (26)	357 (378)

† for ^{89}Y calculations are presented using the photonuclear data of Lepretre [16], multiplied by 0.82, as suggested, by Berman et al. [17]

Electric Quadrupole Excitations in the Interactions of ^{89}Y with Relativistic Nuclei

by

John W. Norbury
Department of Mathematics & Physics
Rider College
Lawrenceville, NJ 08648

and

Physics Department
Washington State University
Pullman, WA 99164

Abstract

The first complete calculations of electric quadrupole excitations in relativistic nucleus-nucleus collisions are presented herein. Neutron emission from ^{89}Y is studied and quadrupole effects are found to be a significant fraction of the cross section.

PACS 25.70.Np

Nucleus-nucleus collisions proceed predominantly via the Strong and Electromagnetic (EM) forces, both of which have been studied extensively.[1,2] The EM interaction consists of many multipoles such as electric dipole (E1), electric quadrupole (E2), magnetic dipole (M1) etc. The electric dipole is the most important of these and this has been the only EM multipole for which calculations have been made and compared to experiment in relativistic nucleus-nucleus collisions. In this paper I present the very first accurate calculations of the electric quadrupole effect.

In nucleus-nucleus collisions the Strong interaction dominates the cross section at impact parameters approximately less than the sum of the nuclear radii, ie. for impact parameters smaller than

$$b_{min} = R_{0.1}(T) + R_{0.1}(P) \qquad (1)$$

where $R_{0.1}$ represents the 10-percent charge density radius [3,4] of the target or projectile. (Other expressions for b_{min} are possible, [2,5] but for the sake of simplicity they are not discussed here. For impact parameters larger than b_{min}, the interaction occurs via the EM force and the EM cross section is calculated via

$$\sigma = \sigma_{E1} + \sigma_{E2}$$

$$= \int \left[N_{E1}(E)\, \sigma_{E1}(E) + N_{E2}(E)\, \sigma_{E2}(E) \right] dE \qquad (2)$$

where N_{Ei} (E) is the virtual photon spectrum (of energy E) of a particular multipolarity due to the projectile nucleus and σ_{Ei} (E) is the photonuclear reaction cross section of the target nucleus. (In principle the above equation should include other EM multipoles, but their effect is much less important.)

All previous comparisons between theory and experiment [5-9] have only included the electric dipole effect using $N_{E1}(E)$ calculated from Weizsacker-

Williams (WW) theory [2, 10] where

$$\sigma_{WW} = \int N_{WW}(E)\,\sigma(E)\,dE \qquad (3)$$

where $\sigma(E)$ is the experimentally measured photonuclear reaction cross section. $N_{WW}(E)$ is equal to $N_{E1}(E)$ [2] so that WW theory does not include the quadrupole component.

There are difficulties in evaluating σ in equation (2). To be as accurate as possible, one should use experimental values for $\sigma_{E1}(E)$ and $\sigma_{E2}(E)$, fold them into the energy dependent spectra $N_{E1}(E)$ and $N_{E2}(E)$ and integrate the whole expression numerically. Bertulani and Baur [2] have made a crude estimate of the EM cross section using equation (2). However they pulled N_{E1} and N_{E2} outside of the integral and evaluated them only at a single energy corresponding to a theortical estimate of the peak in the E1 and E2 cross section. The remaining $\int \sigma(E)\,dE$ for E1 and E2 were evaluated using theoretical sum rules. This procedure led, for example, to a total cross section σ of 839 mb and 266 mb for the reactions ^{197}Au (^{56}Fe, X) ^{196}Au and ^{89}Y (^{56}Fe, X) ^{88}Y respectively (at 1.7 GeV/N), whereas the measured cross sections are 601 ± 54 mb and 217 ± 20 mb respectively [5]. Given such a discrepancy, I decided to retain the energy dependence in N(E) by doing a numerical integration, as described above, using, where possible experimental photonuclear cross sections, as detailed below.

In the present work, results are presented for the reaction ^{89}Y (Projectile, X) ^{88}Y only; the major point being simply to illustrate the importance of E2 effects using an accurate calculation. Results for other nuclei such as ^{12}C, ^{16}O, ^{18}O, ^{59}Co and ^{197}Au and detailed comparisons to data will be presented elsewhere.

For best accuracy I have followed the suggestions of Berman et al. [11] concerning which photonuetron reaction data to use for ^{89}Y. Following their suggestion I have used the Saclay [12] data but multiplied by a factor of 0.82. (The data actually stops at 27 MeV and a smooth extrapolation was used to estimate the small amount of remaining data beyond this energy.) However, all experimental photoneutron data consists of $\sigma_{E1}(E)$

plus σ_{E2} (E) and a way must be found to separate out these components so that they can be inserted into equation (2) and numerically integrated. This separation was achieved by using a theoretical calculation [13] of the isoscalar component of the electric giant quadrupole resonance (GQR)

$$\sigma_{E2}(E) = \frac{\sigma_{EWSR}\, E^2}{1 + (E^2 - E_{GQR}^2)^2 / E^2 \Gamma^2} \qquad (4)$$

with the energy-weighted sum rule cross section

$$\sigma_{EWSR} = f \frac{0.22\, Z\, A^{2/3} \mu b\ MeV^{-1}}{\pi\, \Gamma/2} \qquad (5)$$

The parameters in the above expressions were taken from Bertrand. [14] For ^{89}Y the width Γ is 3.2 MeV, the energy of the giant quadrupole resonance E_{GQR} is 13.8 MeV and the fractional exhaustion of the EWSR f is 55%. (Note that the ^{89}Y nucleus is approximately spherical, thus justifying the use of a single Lorentzian in equation (4).) The expressions for σ_{E2} (E) in equations (4) and (5) were used in equation (2). The dipole cross section was determined by subtracting σ_{E2} (E), as given above, from the experimental cross section $\sigma_{expt.}$ (E) of Lepretre [12] as in

$$\sigma_{E1}(E) = \sigma_{expt.}(E) - \sigma_{E2}(E) \qquad (6)$$

where $\sigma_{expt.}$ is 0.82 times the Lepretre [12] cross section. Then σ_{E2} (E) and σ_{E1} (E) were inserted into equation (2) and N_{E1} (E) and N_{E2} (E) were taken from expressions derived by Bertulani and Baur.[2] The integrals in equation (2) were performed numerically to give the EM nucleus-nucleus cross sections. Because of the use of equation (6) , uncertainties in the GQR parameters (even if they were as large as $\pm$ 2MeV in Γ and E_{GQR} and $\pm$ 20% in f) do not change the total calculated EM cross section $\sigma_{E1} + \sigma_{E2}$ (which is compared to data in Table 1) by more than 4%. Thus the calculations presented herein are expected to be very accurate even if the quadrupole parameters are uncertain.

Results for the reaction ^{89} Y (projectile, X) ^{88} Y are presented in Table 1 and compared to the experimental measurements of Mercier et al. [5] Both individual dipole σ_{E1} and quadrupole σ_{E2} cross sections are presented as well as their sum σ which is to be compared to the data. Also presented are results obtained using WW theory. (Note that the EM calculations using WW theory in reference 5 are not correct. [15, 16]) In all calculations b_{min} from equation (1) are used. The 10-percent charge radii [3, 4] are also listed in Table 1.

One can see that WW theory agrees with experiment for the ^{12}C and ^{20}Ne projectiles and is reasonably close for the ^{40}Ar and ^{56}Fe projectiles. Agreement could be reached by using a different expression for b_{min}. However a detailed study of treating b_{min} as an adjustable parameter will be reported elsewhere [17]. The quadrupole cross sections σ_{E2} are all seen to be about 10% of the dipole cross sections σ_{E1}, and for all reactions $\sigma_{E1} + \sigma_{E2}$, is about 7% bigger than σ_{WW}. This is because N_{E2} (E) is always larger than N_{E1}(E) so that the quadrupole photonuclear component σ_{E2} (E) is enhanced over the dipole. Adding the quadrupole now gives improved agreement between theory and experiment.

In summary, the first accurate calculations of electric quadrupole effects in relativistic nucleus-nucleus collisions are reported. For the reaction ^{89}Y (Projectile, X) ^{88}Y the quadrupole cross section is about 10% of the dipole cross section, and thus I conclude that electric quadrupole effects are an important consideration in the analysis of nucleus-nucleus collisions.

Acknowledgements

I wish to thank Gayle Norbury for extensive help with the photonuclear data. This work was supported in part by NASA grant NAG-1-797.

Table 1 EM Cross Sections for the Reaction ^{89}Y (Projectile, X) ^{88}Y

The Photoneutron Cross Section measured by Lepretre et al [12] (but multiplied [11] by 0.82) was used in the analysis described in the text. The 10 percent charge radius used for ^{89}Y is 6.02 fm and the GQR parameters (see text) are f = 0.55, Γ = 3.2 MeV, E_{GQR} = 13.8 MeV. The ^{89}Y (γ, n) threshold is at 11.0 MeV. Calculations are made for Weizacker-Williams theory (σ_{WW}) and also individual E1 & E2 multipole cross sections are calculated. The total cross section $\sigma_{E1} + \sigma_{E2}$ is to be compared to experiment. All calculations use the minimum impact parameter given by $b_{min} = R_{0\cdot1}$ (P) + $R_{0\cdot1}$ (T).

Projectile	$R_{0\cdot1}$ (P) (fm)	Energy (GeV/N)	$\sigma_{expt.}$ (mb) (ref. 5)	σ_{WW} (mb)	σ_{E1} (mb)	σ_{E2} (mb)	$\sigma_{E1} + \sigma_{E2}$ (mb)
^{12}C	3.30	2.1	9 ± 12	12	12	1	13
^{20}Ne	4.00	2.1	43 ± 12	32	31	3	34
^{40}Ar	4.72	1.8	132 ± 17	90	88	9	97
^{56}Fe	5.24	1.7	217 ± 20	175	171	16	187

References

1. M. Gyulassy, Nucl. Phys. A 354, 395 (1981).

2. C. A. Bertulani and G. Baur, Phys. Rep. 163 299 (1988).

3. C. W. DeJager, H. DeVries and C. DeVries, Atomic Data and Nuclear Data Tables, 14 479 (1974).

4. H. DeVries, C. W. DeJager and C. DeVries, Atomic Data and Nuclear Data Tables, 36 495 (1987).

5. M. T. Mercier, J. C. Hill, F. K. Wohn, C. M. McCullough, M. E. Nieland, J. A. Winger, C. B. Howard, S. Renwick, D. K. Matheis and A. R. Smith, Phys. Rev. C 33 1655 (1986).

6. J. C. Hill, F. K. Wohn, J. A. Winger, and A. R. Smith, Phys. Rev. Lett. 60 999 (1988).

7. J. C. Hill, F. K. Wohn. J. A. Winger, M. Khayat, K. Leininger, and A. R. Smith, Phys. Rev. C 38 1722 (1988).

8. H. H. Heckman, and P. J. Lindstrom, Phys. Rev. Lett. 37, 56 (1976).

9. D. L. Olson, B. L. Berman, D. E. Greiner, H. H. Heckman, P. J. Lindstrom, G. D. Westfall, and H. J. Crawford, Phys. Rev. C 24, 1529 (1981).

10. J. D. Jackson, Classical Electrodynamics (Wiley, New York, 1975), 2nd ed.

11. B. L. Berman, R. E. Pywell, S. S. Dietrich, M. N. Thompson, K. G. McNeill and J. W. Jury, Phys. Rev. C 36 1286 (1987).

12. A. Lepretre, H. Beil, R. Bergere, P. Carlos, A. Veyssiere and M. Sugawara, Nucl. Phys. A 175 609 (1971).

13. R. Ligensa, W. Greiner and M. Danos, Phys. Rev. Lett. 16 364 (1966).

14. F. E. Bertrand, Ann. Rev. Nucl. Sci. 26 457 (1976).

15. J. W. Norbury, Comment Paper on References 5, 6 and 7 Physical Review C (in press).

16. J. C. Hill and F. K. Wohn, Reply to Reference 15, Physical Review C (in press).

17. J. W. Norbury, submitted to Physical Review C.

NUCLEON EMISSION VIA ELECTROMAGNETIC EXCITATION IN RELATIVISTIC NUCLEUS-NUCLEUS COLLISIONS: RE-ANALYSIS OF THE WEIZSÄCKER-WILLIAMS METHOD

John W. Norbury
Physics Department
Washington State University
Pullman, WA 99164

Abstract

Previous analyses of the comparison of Weizsäcker-Williams (WW) theory to experiment for nucleon emission via electromagnetic (EM) excitations in nucleus-nucleus collisions have not been definitive because of different assumptions concerning the value of the minimum impact parameter. This situation is corrected by providing criteria that allow one to make definitive statements concerning agreement or disagreement between WW theory and experiment.

PACS: 25.70. N_p

1. INTRODUCTION

Collisions between relativistic nuclei can occur via the Strong or Electromagnetic interaction. There is an enormous literature on processes induced by the Strong force[1], but relatively few studies have been carried out on the Electromagnetic (EM) aspects of relativistic nucleus-nucleus collisions.[2-25] This situation is surprising given the richness of applications of EM effects. These effects are of importance for the following reasons: i) EM interactions between relativistic nuclei are interesting in their own right; ii) they will form a significant background to the formation of a quark-gluon plasma at ultrarelativistic energies; iii) other applications in physics such as subthreshold pion production [3] iv) astrophysical applications [4]; v) interference effects between Strong and EM amplitudes [5]; vi) studies of virtual photon theory [4, 6-10] and vii) applications in space radiation effects [11] Bertulani and Baur [25] have written an outstanding review article on EM effects in nucleus-nucleus collisions to which the reader is referred.

The present paper is concerned with nucleon emission via electromagnetic dissociation in relativistic nucleus-nucleus collisions. The first experiment of this kind was performed by Heckman and Lindstrom[15] looking at excitations in ^{12}C and ^{16}O projectiles at energies of 1.05 and 2.1 GeV/N on a variety of targets (^{12}C, ^{27}Al, ^{64}Cu, ^{108}Ag, ^{208}Pb). Measured EM cross sections for nucleon emission ranged from 0 to 50 mb. Olson et al [13] later measured excitation of ^{18}O projectiles at 1.7 GeV/N on ^{48}Ti, ^{208}Pb and ^{238}U with cross sections up to 140 mb. Studies of ^{197}Au and ^{59}Co target excitation [14, 20-22] were later reported with cross sections all the way up to 1970 mb for ^{139}La projectiles at 1.26 GeV/N. Lighter projectiles were also used [14, 20-23] with smaller cross sections. All studies mentioned so far have been for projectile energies less than or equal to 2.1 GeV/N. The measurements were made at the Berkeley Bevalac. However, some very interesting measurements have also been made for ^{197}Au target excitation at the CERN SPS using ^{16}O projectiles at 60 and 200 GeV/N with cross sections of 820 and 440 mb respectively. All the above data is summarized in Tables 1 and 3.

The authors of the above experiments have generally made a comparison of their data to theoretical predictions based on the Weizäcker-Williams (WW) method of virtual quanta.[6, 12, 15, 25] The basic idea is that the vertical photon spectrum N(E) of one nucleus is calculated from WW theory.[6] This is folded into the photonuclear cross section $\sigma_V(E)$ for processes induced in the excited nucleus and then numerically integrated over energy to give the total EM nucleus-nucleus cross section

$$\sigma_{EM} = \int \sigma_V(E)\, N(E)\, dE \qquad (1)$$

Expressions for N(E) are given by Jackson[6] for the WW theory. These expressions include a minimum impact parameter b, below which EM interactions are supposed not to take place; the interaction proceeding via the much stronger nuclear force. One might naively expect b to be just the sum of the two nuclear radii. Note also that in WW theory N(E) is the same for all EM multipoles[25] and so $\sigma_V(E)$ does not need to be divided into its constituent multipoles. It is partly for this reason that the present paper concerns itself exclusively with WW theory. Alternative theories for N(E) [7, 8, 25] require that $\sigma_V(E)$ be divided into its constituent multipoles which is very involved and beyond the scope of the present paper, although work is proceeding in this direction. Here I wish to analyze WW theory only.

Agreement between WW theory and experiment has generally been claimed to be good[13-15, 20-23, 25] and upon reading the literature on the subject one is left with the impression that WW theory is an accurate theoretical tool. However, if one examines the calculations and data more carefully one is lead into some serious doubts. The following concerns arise.

1) Table 1 provides a list of some experimental cross sections versus the theoretical calculations presented by various authors. As can be seen there is, in fact, very noticeable disagreement between experiment and WW theory, which might lead one to conclude that WW theory is no good at all.

2) Each research group[13-15, 20-23] uses a different procedure for determining the minimum impact parameter, and hence agreement between theory and experiment depends to some extent on whose impact parameter one chooses. The differences in this parameter are in fact large enough to change agreement between theory and experiment.

3) The calculation of the EM nucleus-nucleus cross section depends heavily on the photonuclear cross section $\sigma_V(E)$ used in equation (1). These authors have always used experimental data for the photonuclear cross section $\sigma_V(E)$. The trouble is that various experimental data for $\sigma_V(E)$ for a particular nucleus are often in disagreement [26] and this can lead to significant differences in the calculated nucleus-nucleus EM cross section depending on whose data one chooses for $\sigma_V(E)$.

For the above reasons it was decided to re-analyze the WW method applying a single method to all existing data paying particular attention to the following points.

A) Some recent articles have made a detailed study of the conflicting experimental photonuclear data [27, 28] and have made recommendations concerning what is the correct data. The $\sigma_V(E)$ used in the present work is that recommended by these studies [27, 28] for ^{12}C, ^{16}O and ^{197}Au. For ^{18}O and ^{59}Co the data of references 33 and 32 are expected to be very accurate. The two sets of conflicting data [30, 31] for ^{89}Y are both used herein for two separate nucleus-nucleus calculations.

B) Some incorrect calculations have been presented in the literature.[20-22] They are listed correctly herein. (See references 37, 38 for a discussion of these corrections).

C) To get around the problem of different possible choices of the minimum impact parameter b, it was decided to use it simply as an adjustable parameter fitted so that the theoretical WW cross section is equal to the experimental one. If b is a reasonable (unreasonable) value then one can definitely say that WW theory does (does not) agree with experiment. A reasonable value would be the sum of the two nuclear radii, whereas an

Table 1 Selected Data and Theoretical Calculations Showing Marked Disagreement between Theory and Experiment

Projectile	Target	Energy (GeV/N)	Final State	$\sigma_{expt.}$ (mb) from Reference	Reference	σ_{theory} (mb) from Reference
^{18}O	Ti	1.7	^{17}O	8.7 ± 2.7	13	12.5
"	"	"	^{17}N	-0.5 ± 1.0	"	2.4
"	Pb	"	^{16}O	65.2 ± 2.3	"	55.2
"	U	"	^{17}O	140.8 ± 4.1	"	167
"	"	"	^{17}N	25.1 ± 1.6	"	29.2
"	"	"	^{16}O	74.3 ± 1.7	"	68.1
^{12}C	^{197}Au	2.1	^{196}Au	75 ± 14	20	45
^{20}Ne	"	"	"	153 ± 18	"	121
^{139}La	"	1.26	"	1970 ± 130	22	2340
^{56}Fe	^{89}Y	1.7	^{88}Y	217 ± 20	20	248
^{56}Fe	^{59}Co	"	^{58}Co	88 ± 14	"	122
^{139}La	"	"	"	280 ± 40	22	430
^{16}O	^{197}Au	60	^{196}Au	280 ± 30	21	220
"	"	200	"	440 ± 40	"	300
^{20}Ne	"	2.1	^{195}Au	49 ± 15	23	14
^{40}Ar	"	1.8	"	76 ± 18	"	38
^{139}La	"	1.26	"	73 ± 13	"	238

unreasonable value might be close to 0 or very much larger than the sum of the radii. Note that there will be cases where one cannot make a definite statement concerning agreement between theory and experiment. However, the advantage of the above criterion is that it does provide for an unambiguous comparison between theory and experiment. One will not be left wondering whether the agreement or disagreement with experiment is due to a choice of parameters. The value of the fitted parameter b will provide either a definitive conclusion regarding agreement or disagreement and in the cases in which such a conclusion is not possible it will be clear why such a conclusion is, in fact, not possible.

In summary, the present work goes beyond other studies [13-15, 20-23, 25] in 4 respects. First, it provides a comprehensive comparison to all existing nucleon emission data. Second, problems due to inaccurate photonuclear input data are avoided. Third, previous incorrect calculations are corrected. Fourth, obtaining the value of b needed to fit the data enables one to make definitive statements concerning the agreement with WW theory, thus sidestepping the problem of comparing the calculations of various authors using various values of b to calculate the cross section.

2. SELECTION OF PHOTONUCLEAR REACTION CROSS SECTION DATA

Following references 1 and 2, $\sigma(\gamma, jn)_a$ is defined as the cross section in which j and only j neutrons are emitted and

$$\sigma(\gamma, n) \equiv \sigma(\gamma, 1n)_a \tag{2}$$

by definition.

Also

$$\sigma(\gamma, 1n) = \sigma(\gamma, n) + \sigma(\gamma, pn) + \cdots \tag{3}$$

$$\sigma(\gamma, 2n) = \sigma(\gamma, 2n)_a + \sigma(\gamma, p2n) + \cdots \tag{4}$$

where the $+ \cdots$ indicate unimportant additional contributions (for present purposes). The total photoneutron cross section is

$$\sigma(\gamma, n_t) = \sigma(\gamma, 1n) + \sigma(\gamma, 2n) + \cdots \tag{5}$$

In nucleus-nucleus collisions what is typically measured is ^{197}Au (RHI, X) ^{196}Au for example, implying that $\sigma(\gamma, n)$ only is needed. Unfortunately what photonuclear experimentalist usually measure is $\sigma(\gamma, 1n)$ or $\sigma(\gamma, n_t)$. Thus we must discuss how to arrive at $\sigma(\gamma, n)$ alone. Furthermore, many photonuclear experiments provide contradictory data. For this reason I have relied heavily on references 26-28 and have followed their recommendations in the selection of data which is summarized in Table 2.

How to obtain individual (γ, n) and (γ, p) data for various nuclei is now discussed

^{197}Au(γ, n)

Following the suggestion of Berman et al [27] I have used the data of reference 29 but multiplied it by a factor of 0.93 (the data was actually extrapolated out to where the cross section is zero). The data actually used (Fig. 2, ref. 29) represents $\sigma(\gamma, 1n)$, but because of the large Coulomb barrier, $\sigma(\gamma, 1n)$ will equal $\sigma(\gamma, n)$.

^{89}Y(γ, n)

The data of references 30 and 31 for ^{89}Y are somewhat different requiring separate calculations for each set of data. The data is taken from Fig. 8b of reference 30 and Fig. 3 of reference 31, both of which represent $\sigma(\gamma, 1n)$. As for ^{197} Au, $\sigma(\gamma, 1n)$ is equal to $\sigma(\gamma, n)$ for ^{89}Y. Following the suggestion of Berman et al [27], the data of reference 31 has been multiplied by 0.82.

^{59}Co(γ, n)

The data of Fig. 3b, reference 32 is used and again $\sigma(\gamma, 1n)$ is measured but is very nearly equal $\sigma(\gamma, n)$ for ^{59}Co.

^{16}O(γ, n)

The normalized data presented by Fuller [28] represents $\sigma(\gamma, n_{tot})$. However this is very close to $\sigma(\gamma, 1n)$ because $\sigma(\gamma, 2n)$ is only about 2% of $\sigma(\gamma, 1n)$ beyond 30 MeV. (This can be seen from Fig. 19A (d) of reference 26). The data of Fuller [28] extends out to 37 MeV and, in principle there is data beyond this that should be estimated and included. However various measurements of this higher energy data are not in agreement with the

normalized data of Fuller, so it was decided to simply only use Fuller's data up to 37 MeV. The neglect of the higher energy photonuclear cross section is compensated by the fact that $\sigma(\gamma, 1n)$ includes not only $\sigma(\gamma, n)$ but also a small component of $\sigma(\gamma, pn)$ which we have not subtracted. Further, N(E) is quite small in this energy region and so the error in the resulting EM nucleus-nucleus cross section will not be more than a few percent.

$^{18}O(\gamma, n)$

Here the data of reference 33, Fig 3b, is used which is for $\sigma(\gamma, 1n)$. This cross section is used for $\sigma(\gamma, n)$ in the present work with no correction. However, based on the above discussion for ^{16}O, the (γ, np) correction is expected to be very small. Furthermore, the nucleus-nucleus calculation for ^{18}O presented herein is only done at 1.7 GeV/N where the photon spectrum dominates at low energy, so that a small uncertainty at higher energy, in the region of $\sigma(\gamma, np)$ will again not affect the results.

$^{12}C(\gamma, n)$

The data of Fig. 2.1 reference 28 is used here which represents $\sigma(\gamma, n_{tot})$. This normalized data represents the original data of Fultz et al [34] multiplied by 1.17 which has been used to get the data from 30 MeV to 37.5 MeV. Dietrich and Berman [26] point out that $\sigma(\gamma, 2n)$ is measured to be consistent with zero so that $\sigma(\gamma, n_{tot}) \approx \sigma(\gamma, 1n)$. Again I have no way of subtracting $\sigma(\gamma, np)$ but this will not affect the results presented herein for the same reason as discussed for $^{18}O(\gamma, n)$ and $^{16}O(\gamma, n)$ above.

$^{16}O(\gamma, p)$

I have used $\sigma(\gamma, p_t)$ from Fig. 4.4 reference 28 up to 30 MeV. The data missing beyond 30 MeV affects the results of the present work by only a few percent. Following the discussion above comparing $\sigma(\gamma, 2n)$ to $\sigma(\gamma, n_t)$ for ^{16}O, the contribution of $\sigma(\gamma, 2p)$ to $\sigma(\gamma, p_t)$ is expected to be negligible, as is the contribution of $\sigma(\gamma, np)$.

$^{18}O(\gamma, p)$

This is given directly in Fig. 3a of reference 33.

$^{12}C(\gamma, p)$

Fig. 2.1 of reference 28 gives $\sigma(\gamma, Pt)$ up to 30 MeV. The same considerations for $^{16}O(\gamma, p)$ were followed for $^{12}C(\gamma, p)$.

$^{18}O(\gamma, 2n)$

This is given directly in Fig. 3c of reference 33.

$^{197}Au\ (\gamma, 2n)$

As for $^{197}Au\ (\gamma, n)$ (see above) the data of reference 29, multiplied by a factor of 0.93, was used.

$^{59}Co\ (\gamma, 2n)$

This data was taken from reference 32.

Table 2 Choice of Photonuclear Reaction Cross Sections

(see text for details)

Nucleus	Data	Remarks
^{197}Au	ref. 27, 29	Data of ref. 29 are multiplied by 0.93 following suggestions of ref. 27.
^{89}Y	ref. 30, 31	Data for these two references differ. Thus two sets of calculations for both data sets is performed. Data of ref. 31 are multiplied by 0.82 following suggestions of ref. 27.
^{59}Co	ref. 32	The only existing data.
^{18}O	ref. 33	The most accurate data that exists.
^{16}O	ref. 28	The normalized data presented in ref. 28 is used.
^{12}C	ref. 28, 34	The normalized data presented in ref. 28 is used.

3. CRITERIA FOR EVALUATING THEORETICAL ANALYSES

The only adjustable parameter that appears in the present theory is the minimum impact parameter b, below which the reaction proceeds via the Strong Interaction. This has been the subject of much discussion and every author chooses their own form. For instance Heckman and Lindstrom [15] and Olson et al [13] choose a form

$$b = R_{o\cdot1}\,(p) + R_{o\cdot1}\,(T) - d \qquad (6)$$

where $R_{o\cdot1}$ is the 10 percent charge density radii of the projectile and target and d is a parameter measuring the amount of overlap. These authors choose values of d ranging from 0 up to 3 fm. Hill et al [14, 20-23] choose

$$b = r_o[Ap^{1/3} + A_T^{1/3} - X(A_p^{-1/3} + A_T^{-1/3})] \qquad (7)$$

where X = 0.75 and r_o = 1.34 fm. Further, Bertulani and Baur [25] use the form

$$b = R(p) + R(T) + \pi/2\ a \qquad (8)$$

where a is given by $\dfrac{Z_1 Z_2 e^2}{m_o v^2}$ with m_o the reduced mass and v the relative speed. The above authors variously suggest that a particular form of b accounts for Rutherford bending of the orbit (derivation from a straight line) and the effect of a finite charge distribution.

The problem with choosing a particular form of b and then comparing a resultant theoretical cross section to experiment is that the theory incorporates (perhaps unjustified) assumptions concerning b. Then, when one compares theory to experiment and makes claims about the WW method's validity, it is not only the WW method that one is testing but also mixed in is a test of one's assumption for b. I believe that this approach which has been taken in the literature leads to ambiguity concerning whether the WW method agrees with experiment.

Let us now formulate a model-independent criterion that will enable us to firmly establish whether or not WW theory agrees with experiment. The simplest possible assumption that one can make concerning b is that it is the sum of the projectile and target

charge radii equivalent to choosing d = 0 in equation 6 or X = 0 in equation 17 or a = 0 in equation 8. All cross section calculations listed in Table 3 are calculated using this naive assumption for b. If theory agrees within experimental error, then this is taken as indicating that WW theory agrees with experiment. However, what is also calculated is the value of d from equation 6 needed to make theory agree with experiment. In this case d simply determines the difference of b from our naive assumption of the sum of the radii. Remember that the theoretical cross section σ is calculated for d = 0. If agreement between theory and experiment is found it simply means that the value of b_{min} (or d) needed to fit experiment is the sum of the radii (or d = 0). In this case d has a reasonable value and it can be claimed that WW theory agrees with experiment. If the theoretical cross section (for d = 0) does not fit experiment, but <u>does</u> fit it for another reasonable value of d (say 0.5 fm) then again agreement with WW theory and experiment is claimed given the inherent uncertainties in b. On the other hand if the calculated cross section (for d = 0) does not agree with experiment and if a ridiculously large value of d (say 10 fm) is needed for agreement then we conclude that WW theory does <u>not</u> agree with experiment. Finally if an intermediate value of d (say 3 fm) is needed for agreement then the validity of WW theory is uncertain. These criteria however are best expressed in terms of percentages. The percentages listed in Table 3 for d are the percentage of d relative to $R_{0\cdot1}(p) + R_{0\cdot1}(T)$. Thus the criteria are re-stated as follows:

a) Where a zero value of d is listed, then WW theory does agree with experiment.

b) Where d is say 30% or greater of $R_{0\cdot1}(p) + R_{0\cdot1}(T)$ then WW theory definitely does not agree with experiment.

c) Where d is between 0% and 30%, then a definitive statement concerning agreement or disagreement is not possible.

Note that this 30% criteria was chosen to be as pessimistic as possible. One could argue that it should in fact be lowered. However, its main use is to highlight any disagreement between theory and experiment. This 30% criterion is based on the assumption that

Rutherford bending or finite charge effects can not account for differences in d larger than 30%.

The advantage of the above criteria is that we can make a model independent definitive statement concerning whether WW theory is adequate. Further, we can also say where it is clearly inadequate. This latter point means that a clear delineation is possible of where any new physics may emerge. The adoption of the above criteria is suggested in all future analysis both for WW theory and other theories of N(E).

4. RESULTS AND DISCUSSION

The basic calculational method has been described and criteria established for evaluating theoretical comparisons. Ten percent charge radii are determined from the compilations of references 35 and 36 and are listed in Table 3. For the sake of comparison the theoretical cross section has been calculated using the sum of the projectile and target radii as the minimum impact parameter. However, as emphasized above, *one should not focus on the calculated versus experimental cross section, but rather on the minimum impact parameter b needed to fit the data* which is listed in the second-to-last column in Table 3. Also listed is the difference between the fitted b and the sum of the nuclear radii. This difference is denoted by d (last 2 columns Table 3) as given in equation 6. Note that the values of the fitted b and d are not unique because of the non-zero size of the experimental errors. However, where d is listed as zero, it means rather that the calculated σ based on b as the sum of the radii already agrees with the experimental σ (In this case no fitting of b or d took place). d is also listed as a percentage of $R_{0.1}$ (P) + $R_{0.1}$ (T).

Where a zero value of d is listed, I conclude that WW theory agrees with the data within the experimental uncertainty. It can be seen that this is the case with all the data on ^{12}C and ^{16}O projectile breakup. [15] This is in agreement with the original conclusions of Heckman and Lindstrom [15], although more accurate data could conceivably change this situation. With the data for ^{18}O projectile breakup and ^{197}Au, ^{89}Y and ^{59}Co target breakup the situation is more complicated. First of all, note that even though the experimental and

calculated cross section might only differ by a small amount, the value of the overlap parameter d required to fit the data may be enormous. This is another reason why one should concentrate on d and not σ in comparing WW theory to experiment.

Based on the above 30% criterion, I conclude from Table 3 that WW theory disagrees with experiment for the following reactions:

$^{18}O + Ti \rightarrow {}^{17}N + X$ (1.7 GeV/N)

$^{12}C + {}^{197}Au \rightarrow {}^{196}Au + X$ (2.1 GeV/N)

$^{20}Ne + {}^{197}Au \rightarrow {}^{196}Au + X$ (2.1 GeV/N)

$^{20}Ne + {}^{197}Au \rightarrow {}^{195}Au + X$ (2.1 GeV/N)

$^{40}Ar + {}^{197}Au \rightarrow {}^{195}Au + X$ (1.8 GeV/N)

$^{20}Ne + {}^{89}Y \rightarrow {}^{88}Y + X$ (2.1 GeV/N)

$^{40}Ar + {}^{89}Y \rightarrow {}^{88}Y + X$ (1.8 GeV/N)

$^{12}C + {}^{59}Co \rightarrow {}^{57}Co + X$ (2.1 GeV/N)

$^{16}O + {}^{197}Au \rightarrow {}^{196}Au + X$ (60 GeV/N)

$^{16}O + {}^{197}Au \rightarrow {}^{196}Au + X$ (200 GeV/N)

If one lowers the criterion to say 25% then WW theory disagrees with the following additional reactions:

$^{18}O + Ti \rightarrow {}^{17}O + X$ (1.7 GeV/N)

$^{18}O + {}^{238}U \rightarrow {}^{17}O + X$ (1.7 GeV/N)

It can be seen that there is serious disagreement between WW theory and experiment for ^{197}Au target fragmentation both at low (2.1 GeV/N) and high energies (60 and 200 GeV/N), for both single and double neutron emission. There is also disagreement

for two of the ^{89}Y data sets. (The disagreement for $^{18}O \rightarrow {}^{17}N$ and $^{59}Co \rightarrow {}^{57}Co$ is perhaps due to the fact that the measured and calculated cross sections are very small.) It is also likely (using 25% criterion) that WW theory does not account for some of the ^{18}O projectile fragmentation data at 1.7 GeV/N.

Summary and Conclusions

By considering the value of the overlap parameter d, needed to fit the data I have been able to clearly delineate the region where WW theory disagrees with experiment. My basic conclusion is that target fragmentation of ^{197}Au is not understood either at high or low energy. This is very important. The results of Hill et al [20-23] did indicate that WW theory failed for ^{197}Au at 60 and 200 GeV/N and thus one would naturally conclude that the failure is due to a high energy effect. (These authors plotted the cross section as a function of nuclear charge to see if it followed the trend of WW theory.) However, using the present criterion based on the 30% overlap parameter it is clear that the failure for ^{197}Au also occurs at low energy (2.1 GeV/N). Thus I conclude that the problem may be with the nature of ^{197}Au EM fragmentation and not necessarily due to high energy assumptions. (Note that the photonuclear data for ^{197}Au is extremely accurate. [27,29]) High energy data for lighter nuclei (say ^{59}Co) would refute or verify this conclusion.

A referee has pointed out that for heavy nuclei such as ^{197}Au and ^{238}U, the first order perturbation theory on which the WW theory is based is probably incorrect and that the WW formula is only the first approximation. This could explain why WW theory fails for ^{197}Au and suggests that it would be worthwhile to calculate higher order effects. Note that ^{197}Au is the heaviest nucleus considered in the present work.

Finally, the whole situation with respect to EM excitations could be very much clarified if we had a clear and precise way of calculating the overlap parameter d. Then one could use the actual cross section to compare theory and experiment.

Acknowledgements

I wish to thank Gayle Norbury for extensive help with the photonuclear data and John Hill (Iowa State University) for a useful conversation. This work was supported in part by NASA grant NAG-1-797.

Table 3 Overlap parameters d required to fit data. Zero overlap corresponds to a minimum impact parameter equal to the sum of the nuclear radii. Where d is listed as 0, it means that σ calculated for $b = R_{0\cdot1}(p) + R_{0\cdot1}(T)$, already agrees within error. Data are from references 13, 15, 20, 21, 22, 23.

Projectile	$R_{0\cdot1}(P)$ (fm)	Target	$R_{0\cdot1}(T)$ (fm)	Energy (GeV/N)	Final State	σ_{expt} (mb)	σ calculated for $b = R_{0\cdot1}(p) + R_{0\cdot1}(T)$ (i.e. d = 0)		d	
							σ(b) (mb)	$R_{0\cdot1}(P) + R_{0\cdot1}(T)$ (fm)	(fm)	Percentage of $R_{0\cdot1}(P) + R_{0\cdot1}(T)$
^{12}C	3.30	Pb	7.83	2.1	^{11}C	51±18	47	11.13	0	0
"	"	"	"	"	^{11}B	50±25	68	"	0	0
"	"	"	"	1.05	^{11}C	39±24	28	"	0	0
"	"	"	"	"	^{11}B	50±25	42	"	0	0
^{16}O	3.68	"	"	2.1	^{15}O	50±24	59	11.51	0	0
"	"	"	"	"	^{15}N	96±26	111	"	0	0
^{12}C	3.30	Ag	6.37	"	^{11}C	21±10	18	9.67	0	0
"	"	"	"	"	^{11}B	18±13	26	"	0	0
"	"	"	"	1.05	^{11}C	21±10	12	"	0	0
"	"	"	"	"	^{11}B	25±19	17	"	0	0
^{16}O	3.68	"	"	2.1	^{15}O	26±13	23	10.05	0	0
"	"	"	"	"	^{15}N	30±16	42	"	0	0

Table 3 (cont.)

Projectile	$R_{0.1}(p)$ (fm)	Target	$R_{0.1}$ (T) (fm)	Energy (GeV/N)	Final State	σ_{expt} (mb)	σ calculated for $b = R_{0.1}(p) + R_{0.1}$ (T) (i.e. d = 0)		d	
							$\sigma(b)$ (mb)	$R_{0.1}(P) + R_{0.1}(T)$ (fm)	(fm)	Percentage of $R_{0.1}(P) + R_{0.1}(T)$
^{12}C	3.30	Cu	5.45	2.1	^{11}C	10±7	8	8.75	0	0
"	"	"	"	"	^{11}B	4±8	11	"	0	0
"	"	"	"	1.05	^{11}C	9±8	5	"	0	0
"	"	"	"	"	^{11}B	5±8	8	"	0	0
^{16}O	3.68	"	"	2.1	^{15}O	9±8	10	9.13	0	0
"	"	"	"	"	^{15}N	15±8	18	"	0	0
^{12}C	3.30	Al	4.09	"	^{11}C	0±5	2	7.39	0	0
"	"	"	"	"	^{11}B	0±5	3	"	0	0
"	"	"	"	1.05	^{11}C	1±6	1	"	0	0
"	"	"	"	"	^{11}B	1±7	2	"	0	0
^{16}O	3.68	"	"	2.1	^{15}O	0±5	2	7.77	0	0
"	"	"	"	"	^{15}N	-1±9	4	"	0	0
^{12}C	3.30	C	3.30	"	^{11}C	-2±5	0.4	6.60	0	0
"	"	"	"	"	^{11}B	-1±4	0.6	"	0	0
"	"	"	"	1.05	^{11}C	-2±5	0.3	"	0	0
"	"	"	"	"	^{11}B	-2±5	0.5	"	0	0

Table 3 (cont.)

Projectile	$R_{0\cdot1}(p)$ (fm)	Target	$R_{0\cdot1}$ (T) (fm)	Energy (GeV/N)	Final State	σ_{expt} (mb)	σ calculated for $b = R_{0\cdot1}(p) + R_{0\cdot1}$ (T) (i.e. d = 0)		d	
							$\sigma(b)$ (mb)	$R_{0\cdot1}(P) + R_{0\cdot1}(T)$ (fm)	(fm)	Percentage of $R_{0\cdot1}(P) + R_{0\cdot1}(T)$
^{16}O	3.68	C	3.30	2.1	^{15}O	-1±4	0.5	6.98	0	0
"	"	"	"	"	^{15}N	-1±4	1	"	0	0
^{18}O	3.78	Ti	5.00	1.7	^{17}O	8.7±2.7	15	8.78	$-5.7^{+3.1}_{-4.8}$	-65^{+35}_{-55}
"	"	"	"	"	^{16}O	6.3±2.5	6	"	0	0
"	"	"	"	"	^{17}N	-0.5±1.0	3	"	-15.5†	-177†
"	"	Pb	7.83	"	^{17}O	136±2.9	155	11.61	$-1.5^{+0.2}_{-0.3}$	-13^{+2}_{-3}
"	"	"	"	"	^{16}O	65.2±2.3	63	"	0	0
"	"	"	"	"	^{17}N	20.2±1.8	28	"	-2.8±0.8	-24±7
"	"	U	8.09	"	^{17}O	140.8±4.1	191	11.87	-3.6±0.4	-30±3
"	"	"	"	"	^{16}O	74.3±1.7	77	"	$-0.3^{+0.2}_{-0.3}$	-3^{+2}_{-3}
"	"	"	"	"	^{17}N	25.1±1.6	34	"	$-2.6^{+0.5}_{-0.6}$	-22^{+4}_{-5}
"	"	Cu	5.45	"	^{16}O	9.0±3.5	10	9.23	0	0
"	"	Sn	6.58	"	"	27.5±4.0	27	10.36	0	0
"	"	W	7.69	"	"	50.0±4.3	52	11.47	0	0

Table 3 (cont.)

Projectile	$R_{0.1}$(p) (fm)	Target	$R_{0.1}$ (T) (fm)	Energy (GeV/N)	Final State	σ_{expt} (mb)	σ calculated for b = $R_{0.1}$(p) + $R_{0.1}$ (T) (i.e. d = 0)		d	
							σ(b) (mb)	$R_{0.1}$(P) + $R_{0.1}$(T) (fm)	(fm)	Percentage of $R_{0.1}$(P) + $R_{0.1}$(T)
^{12}C	3.30	^{197}Au	7.56	2.1	^{196}Au	75±14	38	10.86	$7.5^{+1.2}_{-1.8}$	69^{+11}_{-17}
"	"	"	"	"	^{195}Au	9±17	5	"	0	0
^{20}Ne	4.00	"	"	"	^{196}Au	153±18	100	11.56	$5.4^{+1.1}_{-1.5}$	47^{+10}_{-13}
"	"	"	"	"	^{195}Au	49±15	15	"	$10.1^{+0.8}_{-2.0}$	87^{+7}_{-17}
^{40}Ar	4.72	"	"	1.8	^{196}Au	348±34	289	12.28	$2.5^{+1.1}_{-1.4}$	20^{+9}_{-11}
"	"	"	"	"	^{195}Au	76±18	40	"	$6.2^{+1.7}_{-2.4}$	51^{+14}_{-20}
^{56}Fe	5.24	"	"	1.7	^{196}Au	601±54	565	12.80	0	0
"	"	"	"	"	^{195}Au	73±13	77	"	0	0
^{139}La	6.89	"	"	1.26	^{196}Au	1970±130	2076	14.45	0	0
"	"	"	"	"	^{195}Au	335±49	257	"	$2.4^{+1.3}_{-1.4}$	21^{+12}_{-13}
^{16}O	3.68	"	"	60	^{196}Au	280±30	215	11.24	$8.0^{+1.4}_{-2.5}$	71^{+13}_{-22}
"	"	"	"	200	"	440±40	278	"	$10.7^{+0.3}_{-0.6}$	95^{+3}_{-5}

Table 3 (cont.)

Projectile	$R_{0\cdot1}(p)$ (fm)	Target	$R_{0\cdot1}$ (T) (fm)	Energy (GeV/N)	Final State	σ_{expt} (mb)	σ calculated for $b = R_{0\cdot1}(p) + R_{0\cdot1}$ (T) (i.e. d = 0)			d			
							σ(b) (mb)		$R_{0\cdot1}(P) + R_{0\cdot1}(T)$ (fm)	(fm)		Percentage of $R_{0\cdot1}(P) + R_{0\cdot1}(T)$	
							B	L		B	L	B	L
^{12}C	3.30	^{89}Y*	6.02	2.1	^{88}Y	9±12	11	12	9.32	0	0	0	0
^{20}Ne	4.00	"	"	"	"	43±12	29	32	10.02	$4.2^{+2.0}_{-3.4}$	$3.2^{+2.2}_{-3.6}$	42^{+20}_{-34}	32^{+22}_{-36}
^{40}Ar	4.72	"	"	1.8	"	132±17	82	90	10.74	$4.8^{+1.0}_{-1.2}$	$3.9^{+1.1}_{-1.3}$	45^{+9}_{-11}	36^{+10}_{-12}
^{56}Fe	5.24	"	"	1.7	"	217±20	159	175	11.26	$3.3^{+0.8}_{-1.0}$	$2.3^{+0.9}_{-1.0}$	2.9^{+7}_{-9}	20^{+8}_{-9}

Table 3 (cont.)

Projectile	$R_{0\cdot1}(p)$ (fm)	Target	$R_{0\cdot1}$ (T) (fm)	Energy (GeV/N)	Final State	σ_{expt} (mb)	σ calculated for $b = R_{0\cdot1}(p) + R_{0\cdot1}$ (T) (i.e. d = 0)		d	
							$\sigma(b)$ (mb)	$R_{0\cdot1}(P) + R_{0\cdot1}(T)$ (fm)	(fm)	Percentage of $R_{0\cdot1}(P) + R_{0\cdot1}(T)$
^{12}C	3.30	^{59}Co	5.33	2.1	^{58}Co	6±9	7	8.63	0	0
"	"	"	"	"	^{57}Co	6±4	1	"	$8.5^{+0.1}_{-2.7}$	98^{+1}_{-31}
^{20}Ne	4.00	"	"	"	^{58}Co	32±11	18	9.33	$5.4^{+1.8}_{-3.7}$	58^{+19}_{-40}
"	"	"	"	"	^{57}Co	3±5	2	"	0	0
^{56}Fe	5.24	"	"	1.7	^{58}Co	88±14	98	10.57	0	0
"	"	"	"	"	^{57}Co	13±6	12	"	0	0
^{139}La	6.89	"	"	1.26	^{58}Co	280±40	339	12.22	$-1.8^{+1.3}_{-1.6}$	15^{+11}_{-13}
"	"	"	"	"	^{57}Co	32±16	36	"	0	0

* for ^{89}Y two calculations are presented using the photonuclear data of Lepretre [31] (L), multiplied by 0.82, and Berman [30] (B).

† fitted to $\sigma_{expt} = 0.5$ mb only

REFERENCES

1. M. Gyulassy, Nucl. Phys. A 354, 395 (1981).
2. J. Cleymans, R.V. Gavai, and E. Suhonen, Phys. Rep. 130, 217 (1986).
3. J. W. Norbury, and L. W. Townsend, Phys. Rev. C 33, 377 (1986).
4. G. Baur, C. A. Bertulani, and H. Rebel, Nucl,. Phys. A 458, 188 (1986).
5. G. Fäldt, Phys. Rev. D 2, 846 (1970).
6. J. D. Jackson, Classical Electrodynamics (Wiley, New York, 1975), 2nd ed.
7. H. Pilkuhn, Phys. Lett. B 38, 143 (1972).
8. R. Jäckle, and H. Pilkuhn, Nucl. Phys. A 247, 521 (1975).
9. W. R. Dodge, Nucl. Inst. Meth. in Phys. Res. B 10/11, 423 (1985).
10. A. Goldberg, Nucl. Phys. A 420, 636 (1984).
11. J. W. Norbury, and L. W. Townsend, NASA TP-2527 (1986).
12. G. D. Westfall, L. W. Wilson, P. J. Lindstrom, H. J. Crawford, D. E. Greiner, and H. H. Heckman, Phys. Rev. C 19, 1309 (1979).
13. D. L. Olson, B. L. Berman, D. E. Greiner, H. H. Heckman, P. J. Lindstrom, G. D. Westfall, and H. J. Crawford, Phys. Rev. C 24, 1529 (1981).
14. M. T. Mercier, J. C. Hill, F. K. Wohn, and A. R. Smith, Phys. Rev. Lett., 52, 898 (1984); erratum ibid, 2390 (1984).
15. H. H. Heckman, and P. J. Lindstrom, Phys. Rev. Lett. 37, 56 (1976).
16. B. M. Spicer, Adv. Nucl. Phys. 1, 1 (1969).
17. W. D. Myers, W. J. Swiatecki, T. Kodama, L. J. El-Jaick, and E. R. Hilf, Phys. Rev. C 15, 2032 (1977).
18. G. Fäldt, H. Pilkuhn, and H. G. Schlaile, Ann. Phys. 82, 326 (1974)
19. J. W. Norbury, F. A. Cucinotta, L. W. Townsend, and F. F. Badavi, Nucl. Inst. Meth. in Phys. Res. B 31 535 (1988).

20. M. T. Mercier, J. C. Hill, F. K. Wohn, C. M. McCullough, M. E. Nieland J. A. Winger, C. B. Howard, S. Renwick, D. K. Matheis and A. R. Smith, Phys. Rev. C 33 1655 (1986).

21. J. C. Hill, F. K. Wohn, J. A. Winger, and A. R. Smith, Phys. Rev. Lett. 60 999 (1988).

22. J. C. Hill, F. K. Wohn, J. A. Winger, M. Khayat, K. Leininger, and A. R. Smith, Phys. Rev. C 38 1722 (1988).

23. J. C. Hill, F. K. Wohn, J. A. Winger, M. Khayat, M. T. Mercier, and A. R. Smith, Phys. Rev. C 39 524 (1989).

24. C. Brechtmann and W. Heinrich, Z. Phys. A 330 407 (1988).

25. C. A. Bertulani and G. Baur, Phys. Rep. 163 299 (1988). See also references therein by the same authors.

26. S. S. Dietrich and B. L. Berman, Atomic Data and Nuclear Data Tables 38 199 (1988).

27. B. L. Berman, R. E. Pywell, S. S. Dietrich, M. N. Thompson, K. G. McNeill and J. W. Jury, Phys. Rev. C 36 1286 (1987)

28. E. G. Fuller, Phys. Rep 127 185 (1985).

29. A. Veyssiere, H. Beil, R. Bergere, P. Carlos and A. Lepretre, Nucl. Phys. A 159, 561 (1970).

30. B. L. Berman, J. T. Caldwell, R. R. Harvey, M. A. Kelly, R. L. Bramblett, and S. C. Fultz, Phys. Rev. 162 1098 (1967).

31. A. Lepretre, H. Beil, R. Bergere, P. Carlos, A. Veyssiere and M. Sugawara, Nucl. Phys. A 175 609 (1971).

32. R. A. Alvarez, B. L. Berman, D. D. Faul, F. H. Lewis and P. Meyer, Phys. Rev. C 20 128 (1979).

33. J. G. Woodworth, K. G. McNeill, J. W. Jury, R. A. Alvarez, B. L. Berman, D. D. Faul and P. Meyer, Phys. Rev. C 19 1667 (1979).

34. S. C. Fultz, J. T. Caldwell, B. L. Berman, R. L. Bramblett and R. R. Harvey, Phys. Rev. 143 790 (1966).

35. C. W. DeJager, H. DeVries and C. DeVries, Atomic Data and Nuclear Data Tables, 14 479 (1974).

36. H. DeVries, C. W. DeJager and C. DeVries, Atomic Data and Nuclear Data Tables, 36 495 (1987).

37. J. W. Norbury, Comment on Ref. 20-22, Phys. Rev. C 39 2472 (1989).

38. J. C. Hill and F. K. Wohn, Reply to Ref. 37, Phys. Rev. C 39 2474 (1989).